

**Aus dem Institut für Humangenetik
der Universität Würzburg**

Vorstand: Professor Dr. med. Thomas Haaf

**Paternal age effects on sperm DNA methylation and its
impact on the next generation**

Inaugural-Dissertation

zur Erlangung der Doktorwürde der

Medizinischen Fakultät

der

Julius-Maximilians-Universität Würzburg



vorgelegt von

Juliane Renate Reichenbach

aus München

Würzburg, Januar 2019

Aus dem Institut für Humangenetik der Universität Würzburg

Die Arbeit wurde angefertigt unter der Leitung von Prof. Dr. Thomas Haaf

Referent: Professor Dr. med. Thomas Haaf

Koreferent/in: Professor Dr. med. Manuel Mattheisen

Dekan: Professor Dr. med. Matthias Frosch

Tag der mündlichen Prüfung: 20. Januar 2020

Die Promovendin ist Ärztin.

Meiner Familie

Table of contents

I.	INTRODUCTION	1
1	Fundamental epigenetic principles	3
1.1	Epigenetic mechanisms.....	3
1.2	Epigenetic reprogramming.....	5
1.3	Genomic imprinting	6
2	Epigenetic impacts of aging.....	7
2.1	Epigenetic changes in the life span.....	8
2.2	Male aging	10
2.2.1	Genetics of male aging.....	10
2.2.2	Arising <i>de novo</i> mutations during spermatogenesis	11
2.2.3	Epigenetics of male aging.....	15
3	Intergenerational epigenetic inheritance	16
3.1	The influence of environmental changes on future generations.....	16
3.2	Impacts of aged gametes on the offspring	17
3.3	The “missing heritability” problem.....	18
3.4	The sperm cell as a carrier of epigenetic information.....	18
4	Aims of this thesis	19
5	Genes of interest	20
II.	MATERIAL AND METHODS.....	24
1	Material.....	24
1.1	Chemicals	24
1.2	Kits.....	25
1.3	Buffers	25
1.4	Equipment	26
1.5	Software	26
1.6	Primers	27
1.7	Samples	30
1.7.1	Samples for the age-associated methylation analysis by pyrosequencing	30
1.7.2	Samples for the age-associated methylation analysis by deep bisulfite sequencing	32

1.7.3	Samples for the FOXK1 study in patients with autism spectrum disorders.....	34
2	Methods	34
2.1	Sample preparation	34
2.1.1	Purification	34
2.1.2	DNA Isolation and quantification	35
2.1.2.1	Sperm-DNA Isolation	35
2.1.2.2	Fetal cord blood and peripheral blood leucocyte DNA Isolation....	36
2.1.2.3	DNA quantification	36
2.1.3	Bisulfite conversion.....	37
2.2	Pyrosequencing	38
2.2.1	Basic principles	38
2.2.2	Application fields	39
2.2.3	Sample amplification	40
2.2.4	Pyrosequencing-assays	41
2.2.5	Sequencing	41
2.2.6	Data processing and analysis	42
2.3	Deep Bisulfite Sequencing.....	44
2.3.1	Basic principles	44
2.3.2	Application fields	45
2.3.3	Library preparation	45
2.3.3.1	Sample Amplification.....	46
2.3.3.2	Library purification	47
2.3.3.3	Amplicon quantification and quality control	48
2.3.3.4	Pooling and dilution.....	49
2.3.4	Deep bisulfite sequencing assay.....	50
2.3.5	Emulsion based PCR amplification	50
2.3.6	Sequencing	51
2.3.7	Data processing and analysis	52
III.	RESULTS	54
1	Age-associated methylation analysis in fathers and their resulting offspring....	54
1.1	Age-associated methylation analysis in sperm-DNA	54

1.1.1	Pyrosequencing results for DMPK, FO XK1, GET4, PDE4C and TNXB in the sperm cohort 1	54
1.1.2	Pyrosequencing results for FO XK1 in the sperm cohort 2	57
1.1.3	Deep bisulfite sequencing results for FO XK1 in sperm-DNA	57
1.1.3.1	Correlation analysis methylation versus paternal age	57
1.1.3.2	Group comparison young versus aged group	58
1.1.3.3	Methylation analysis at the single read level	60
1.2	Paternal age effect on methylation in the offspring	60
2	Allele specific methylation analysis in the offspring	61
2.1	Genotyping fetal cord blood samples by pyrosequencing	62
2.1.1	Analyzed region	62
2.1.2	Genotypes for sperm and fetal cord blood samples	62
2.2	Allele-specific deep bisulfite sequencing results in fetal cord blood	64
2.3	Allele-specific pyrosequencing results in fetal cord blood	64
3	FO XK1 and Autism Spectrum Disorders.....	65
IV.	DISCUSSION.....	67
1	Age-associated methylation alterations in sperm of elder men.....	67
1.1	<i>FO XK1</i> -hypomethylation in the sperm of elder men.....	67
1.2	The inter-allelic sperm <i>FO XK1</i> methylation variability	67
1.3	Possible consequences of <i>FO XK1</i> hypomethylation in sperm of elder men	68
2	Intergenerational inheritance of age-associated methylation alterations.....	69
2.1	Transmission of paternal <i>FO XK1</i> -hypomethylation to the next generation	69
2.2	The influence of sperm methylation on early embryonal development processes	69
3	The impact of inherited methylation alterations on the offspring's disease susceptibility.....	70
3.1	Epigenetic processes and the development of autism spectrum disorders	70
3.2	<i>FO XK1</i> -methylation as a possible contributing factor to the development of complex neuropsychiatric diseases.....	71
V.	CONCLUSION.....	73
VI.	ABSTRACT.....	74
VII.	ZUSAMMENFASSUNG.....	76
VIII.	INDEX OF FIGURES.....	78

IX. INDEX OF TABLES.....	78
X. APPENDIX.....	80
XI. REFERENCES.....	93
XII. ACKNOWLEDGEMENT	104
XIII. CURRICULUM VITAE	105

INDEX OF ABBREVIATIONS

A	
A	Adenosine
APOBEC	Apolipoprotein B mRNA-editing enzyme catalytic polypeptide-like enzyme
APS	Adenosine 5' phosphosulfate
ART	Assisted reproductive technology
ASD	Autism spectrum disorder
ATP	Adenosine triphosphate
B	
BDD	Bead Deposition Device
bp	Basepairs
C	
°C	Degree Celsius
C	Cytosine
cAMP	Cyclic adenosine monophosphate
cGMP	Cyclic guanosine monophosphate
CCD	Charge couple device
CH ₃	Methyl group
CpG	Cytosine-phosphate-guanine dinucleotides
D	
DBS	Deep bisulfite sequencing
dH ₂ O	Distilled water
DNA	Deoxyribonucleic acid
DNMT	DNA methyltransferases
dNTP	Deoxynucleotide triphosphates
DMPK	Myotonic dystrophy protein kinase
E	
EDTA	Ethylenediaminetetraacetic acid
EDS	Ehlers-Danlos-syndrome
emPCR	Emulsion-based clonal amplification
EtOH	Ethanol
F	
F	Forward
FOXP1	Forkhead box protein K1
FCB	Fetal cord blood
FSH	Follicle-stimulating hormone
G	
G	Guanine
GET4	Golgi to ER traffic protein 4 homolog
GTP	Guanine triphosphate
GWAS	Genome-wide association studies

H	
H19	H19, imprinted maternally expressed transcript
HCl	Hydrochloride
I	
ICR	Imprinted control region
ICSI	Intracytoplasmic sperm injection
IGF2	Insulin-like growth factor 2
IVF	In-vitro fertilization
L	
LH	Luteinizing hormone
lncRNA	Long non-coding RNA
M	
MgCl ₂	Magnesium chloride
miRNA	microRNA
MID	Multiplex identifier
MPC	Magnetic particle collector
N	
N	Number
NaCl	Sodium chloride
ncRNA	Non-coding RNA
NOTCH4	Neurogenic locus notch homolog protein 4
P	
PCR	Polymerase chain reaction
PDE4C	cAMP-specific 3',5'-cyclic phosphodiesterase 4C
PGC	Primordial germ cells
PPi	Pyrophosphate
PPiase	Pyrophosphatase
PTP	Picotiter plate
R	
R	Reverse
RAS	Protein family involved in cellular signal transduction
RNA	Ribonucleic acid
RNAi	RNA interference
rpm	Revolutions per min
S	
S	Sequencing
SAM-CH3	S-Adenosyl methionine
SDS	Sodium dodecyl sulfate
.sff	Standard flowgram format
siRNA	Small interfering RNA
SNP	Single nucleotide polymorphism

T	
T	Thymine
TET	Ten-eleven translocation dioxygenase
TDG	Thymine-DNA glycosylase
TAE	Tris acetate-EDTA buffer
TE	Tris-EDTA buffer
TP	Transition protein
TSH	Thyroid-stimulating hormone
TNXB	Tenascin XB gene
U	
U	Uracil
UV	Ultraviolet electromagnetic radiation
W	
WHO	World Health Organization
5-mC	5-Methylcytosine
5-hmC	5-Hydroxymethylcytosine
5-caC	5-Carboxylcytosine
5-Fc	5-Formylcytosine
5-hmU	5-Hydroxymethyluracil

I. INTRODUCTION

In the past few decades a social transformation took place in several Western countries, where the achievement of career goals and economic stability postponed marriage, childbearing and family formation (Peterson et al. 2012). The woman's work status and high educational attainment are reported to be the most important predictors of parenthood timing (De Wit et al. 1992). Young female academics perceive problems related to balancing work and family life and are pessimistic about the effects of parenthood on their status in the labor market (Skoog Svanberg 2006). On this account the influence of delayed parenthood on the offspring's development is discussed in the literature from demographic, medical and ethical points of view (de la Rochebrochard et al. 2002; Schmidt et al. 2012; Cedars et al. 2015; Smith et al. 2015). According to current studies, offspring of elder parents have a higher chance of developing type 1 diabetes (Cardwell et al. 2005), obsessive compulsive behaviors, stuttering and autism (Comings et al. 2006; King et al. 2009), schizophrenia (Sipos et al. 2004), and some forms of cancer (Johnson et al. 2009; Lu et al. 2010). While an increased maternal age increases the risk for pregnancy complications such as spontaneous abortion, ectopic pregnancies, trisomy 21, preterm- and stillbirths (Sartorius et al. 2010; Schmidt et al. 2012), on the other hand paternal age seems to have even a greater negative influence on the offspring's health regarding neurodevelopmental disorders (Cedars et al. 2015). The different implications of male versus female age on the offspring might be explained by the different biology of the sperm compared to the oocyte and the different underlying mechanisms of gamete aging (Cedars et al. 2015). Since spermatogenesis is a lifelong process where spermatogonial cells divide up to 840 times in a 50-year-old male (Goriely et al. 2013), the incidence of paternal *de novo* mutations increases significantly with aging (doubles every 16.5 years) (Kong et al. 2012). This results in a higher risk of cardiac defects, developmental disorders and neurological disease in the offspring (Paul et al. 2013). However, the numerous genetic factors of complex phenotypes discerned in genome wide-association studies (GWAS), clarify just a minority of the heritable traits (Trerotola et al. 2015). Therefore, recent research focusses on strategies for finding the underlying causes and the "missing heritability" of complex diseases (Manolio et al.

2009; Eichler et al. 2010; Koch et al. 2014; Szyf et al. 2015; Trerotola et al. 2015). Non-genomic mechanisms would explain the heritable adaptations to changing environmental conditions and evolutionary processes (Tripaldi et al. 2013; Szyf et al. 2015; Trerotola et al. 2015). These mechanisms are influenced by stochastic events during development, and might also be epigenetically transmitted to the next generation (Kahn et al. 2009). Parental exposure to external and internal environmental disruptive factors, such as diet regimes, stress, drugs and metabolic dysfunction impairs DNA methylation and leads to a transgenerational transmission of altered DNA (Anway et al. 2005; Baccarelli et al. 2009). Apart from environmental factors, predominantly the process of aging influences the human epigenome, since changes in DNA methylation occur during a person's lifetime (Jones et al. 2015). Microarray studies identified a global gain of DNA methylation in early life and a global loss of DNA methylation in later life (Drinkwater et al. 1989; Fuke et al. 2004; Fraga et al. 2007; Martino et al. 2011; Herbstman et al. 2013). Inconsistent with the assumption that every generation starts with a refreshed epigenome due to epigenetic reprogramming after fertilization, genome-wide methylation screens found transgenerational effects of the parental age on the DNA methylation (Adkins et al. 2011; Jenkins et al. 2014; Milekic et al. 2015). Milekic et al. (2015) reported age-associated DNA methylation aberrations in sperm of inbred mice and similar abnormalities in the brain of their offspring. Such methylation alterations lead to a dysregulation in genes associated with autism and schizophrenia. Similar studies in humans confirmed those findings. Jenkins et al. (2014) identified altered methylated regions in sperm samples of fertile donors collected at different points in time. These age-associated epigenetic changes could be transmitted via the germline to the next generation through several transmission mechanisms (Wei et al. 2015) and affect sensitive epigenetic checking points in cell differentiation during the embryonic development (Curley et al. 2011). Disorganization of the epigenetic developmental program might contribute to the development of complex diseases.

To meet the actual need for research in this area, the present study is concerned with the question whether there is an influence of an abnormal paternal sperm-epigenome

on the next generation. This assumption would consequently lead to an arising risk for the offspring of developing impaired phenotypes.

1 Fundamental epigenetic principles

1.1 Epigenetic mechanisms

Epigenetic mechanisms account for the strict regulation of gene-transcription, gene-expression and cell differentiation in the developing organism and is independent from changes in the DNA nucleotide sequence. Apart from several different mechanisms, DNA methylation, posttranslational modification of histones and non-coding RNAs are the best understood and most commonly investigated epigenetic modifications. DNA methylation occurs on the cytosine base by adding a methyl group to the C-5 position of the cytosine ring in cytosine-phosphate-guanine dinucleotides (CpG). CpGs are often accumulated in promotor regions of housekeeping and tumor suppressor genes and form the so-called CpG islands (Bird et al. 2002). Methylated CpG are commonly related to repression of gene-expression by modulating the access to the transcriptional machinery (Lande-Diner et al. 2007). Establishment, maintenance and erasure of methylation patterns are executed by various DNA methyltransferases (DNMT). DNMT3A, DNMT3B and DNMT3L execute de novo methylation, while DNMT1 maintains DNA methylation through copying methylation patterns from hemimethylated DNA-strands during DNA replication (Inbar-Feigenberg et al. 2013; Trerotola et al. 2015). While the enzymatic processes of DNA methylation have been clearly elucidated, there is no consensus about the exact biochemical definition of DNA demethylation. Three strategies have been suggested: (1) The replacement of methylated bases or whole nucleotides with the use of the DNA repair pathway (BER for base excision repair and NER for nucleotide excision repair), (2) active enzymatic DNA demethylation by dedicated demethylase enzyme complexes or (3) DNA demethylation during DNA replication (Wolffe et al. 1999). The replacement of methylated bases (1) is processed by the enzymatic translation of 5-mC to 5-hydroxymethylcytosin (5-hmC) and subsequently to 5-formylcytosine (5-fC) and 5-carboxylcytosine (5-caC) by the TET family enzymes (ten-eleven translocation dioxygenase). 5-fC and 5-caC are erased by the thymine DNA glycosylase (TDG) and the resulting a-basic site is re-established by the

base-excision repair mechanism (Tahiliani et al. 2009; Ficz et al. 2011; Hackett et al. 2013; Trerotola et al. 2015). A direct removal of the methyl-group (2) requires high activation energy, as a C-C binding should be disrupted. Though, Cedar et al. (1999) propose a specific demethylation enzyme complex that hydrolyses 5-methylcytosine to cytosine and methanol. Since the DNMT1 methyltransferase restores DNA methylation on the generated daughter strand during DNA replication (3), a progressive loss of methylation during each cell division event has been discussed (Wolffe et al. 1999). Chromatin structures and protein-complexes would bind sequence-specifically on sites of DNA methylation and thereby prevent the access of the DNMT1 to these sites. In addition, DNMT1 destabilization results in a loss of 5-mC (Trerotola et al. 2015). Due to chemical instability, 5-mC and 5-hmC are often deaminated by enzymes of the AID (activation-induced cytidine deaminase) and APOBEC (Apolipoprotein B mRNA-editing enzyme catalytic polypeptide-like) enzyme families to 5-hydroxymethyluracil (5-hmU) and thymine (T) which leads to partly unadjustable base mismatches and therefore to consistent DNA sequence variations and DNA damage (Fu et al. 2015; Grin et al. 2016).

Epigenetic changes are also associated with alterations in the chromatin structure. The chromatin fibers are constructed of nucleosomes, consisting of a complex interaction between coiled DNA, histone-proteins and non-histone proteins that allow binding between DNA and the DNA binding proteins (Inbar-Feigenberg et al. 2013). Each Histone is built out of a globular octamer-domain formed of each of the two subunits H2A, H2B, H3 and H4 and a highly dynamic N-terminal tail. This tail can be posttranslationally modified by acetylation, methylation, phosphorylation, ubiquitinylation, ADP-ribosylation, etc. (Inbar-Feigenberg et al. 2013) and influences profoundly the chromatin structure (Imhof et al. 2006). The posttranslational modifications of the histone tails are executed by chromatin associated enzymes of the polycomb (Pc-G) and trithorax group (Trx-G) that consequently repress (Pc-G) or activate (Trx-G) gene expression (Imhof et al. 2006; Trerotola et al. 2015). Parts of these groups are both the acetyltransferase with a high turnover rate and the histone methyltransferase with a slow turnover rate. Both modifications are translated into a

defined chromatin structure and might lead to an epigenetic change. The slow turn-over rate might play a key role in epigenetic inheritance as it might be able to maintain a stable chromatin state throughout several rounds of cell divisions without changing the DNA sequence (Imhof et al. 2006). Furthermore, histone codes and DNA methylation are closely interacting factors. For instance, H3 contains a docking site for the DNMT3A at the unmethylated lysine-4 (H3K4) that regulates the methyltransferase's activity (Suetake et al. 2004; Chen et al. 2005).

The third epigenetic mechanism is the activity of non-coding RNAs (ncRNA). While 75% of the genomic DNA are transcribed, just 3% are coding for proteins (Inbar-Feigenberg et al. 2013). NcRNA such as small-interfering RNA (siRNA), micro-RNA (miRNA) and long non-coding RNA (lncRNA) regulate the gene expression through post-transcriptional gene silencing (siRNA), recruiting chromatin-modifying complexes and therefore altering the chromatin conformation (siRNA and miRNA), targeting specific mRNAs for degradation (miRNA) and guiding chromatin-modifying complexes to specific genomic loci (lncRNA) (Inbar-Feigenberg et al. 2013).

1.2 Epigenetic reprogramming

As mentioned before, DNMT are responsible for the preservation of DNA methylation during cell division. Though, between generations in mammals, totipotency of the newly formed zygote is required. Consequently, in both the oocyte and sperm more than 90 percent of the parental epigenetic patterns are removed and again re-established. This phenomenon is termed as “epigenetic reprogramming” (Cantone et al. 2013). The parental epigenetic signature will be firstly reprogrammed by demethylation and remethylation processes during gametogenesis and secondly removed after fertilization during the early embryonal development. A genome-wide methylation wave during the implantation stage of the early embryo will re-establish tissue-specific methylation patterns on somatic cells in order to generate individual and stable cell types. During the first wave of genome-wide demethylation and remethylation processes, around one hundred genes are known to escape the epigenetic reprogramming (Murphy et al. 2003). This phenomenon is called “genomic imprinting”. Regions on the paternal genome that escape from reprogramming due to the imprinting process differ from the

maternal genome. Besides these so-called “imprinted regions”, also other persisting genomic regions might be transmitted to the next cell generation and are still mostly unknown. Embryonic cells that should become germ cells migrate to the germinal ridge of the newly formed embryo and are epigenetically reprogrammed during gametogenesis. The parental DNA methylation patterns are completely erased and are re-established sex-specifically for the newly developed embryo (Cantone et. al 2013)

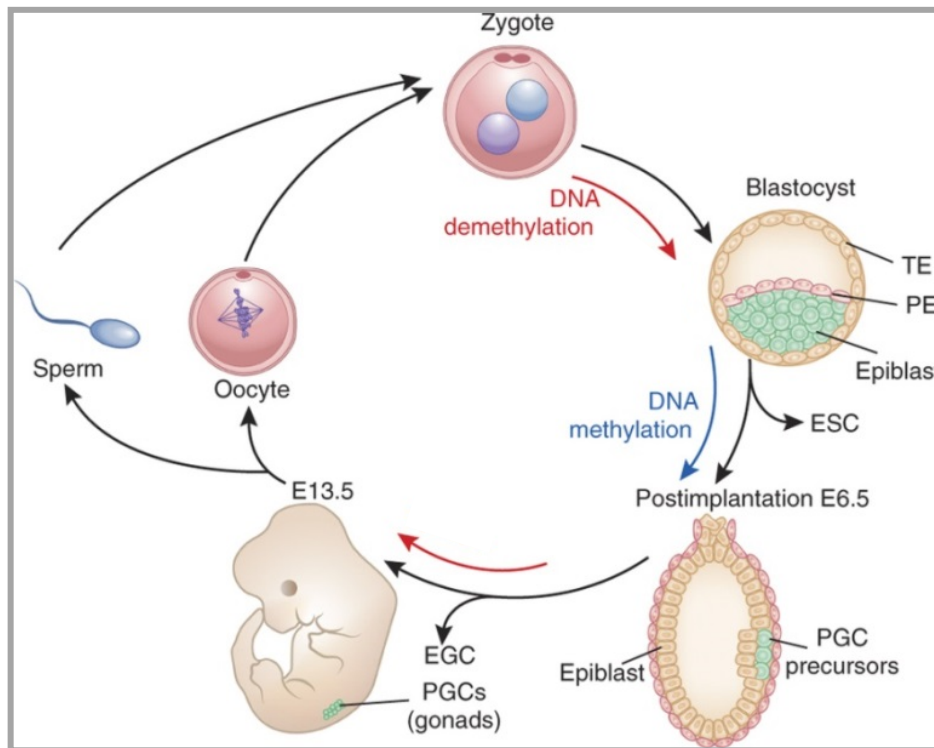


Figure 1: Schematic illustration of epigenetic reprogramming

Oocyte and sperm form the zygote where demethylation and remethylation occur during the implantation stage in order to generate tissue-specific cell types. In gametogenesis on the germinal ridge the biparental DNA methylation patterns of PGC precursors are erased and re-established sex-specifically for the newly developed embryo. (Modified figure cf. Cantone et al. 2013)

1.3 Genomic imprinting

Genomic imprinting is an exceptional inheritance mechanism, whereby a certain allele is only expressed when it is inherited from one parent, while the identical copy of the other parent is inactive by methylation. In a broader sense, the expression of only one of two identical gene copies regardless of the DNA sequence, can be termed as “monoallelic inheritance”. From around one hundred known imprinted genes, *H19* is a

well-studied example for paternal imprinting as the paternal gene copy stays silenced and *IGF2* is a well-studied example for maternal imprinting, as hereby only the paternal gene copy is expressed (Mutter et al. 1993; Jinno et al. 1995; Walsh et al. 1995). After fertilization, primordial germ cells are put aside for germ cell development. Hereby, the parentally transmitted imprints of the previous generation will be erased to create epigenetically equivalent germ cells and during spermatogenesis or oogenesis the promotor regions of imprinted genes are methylated. Therewith, epigenetic marks such as DNA methylation and histone modification can be steadily transmitted to a next cell generation (Griffiths 2008). During DNA replication, existing histone codes and DNA methylation patterns contribute to the regeneration of the chromatin structure as it existed before DNA synthesis (Griffiths 2008). Semiconservative replication creates two hemimethylated daughter strands that are methylated by DNMT1 (Inbar-Feigenberg et al. 2013, Trerotola et al. 2015). Apart from these known imprinted regions that are escaping fetal reprogramming, it is often postulated that also other genomic regions persist in the germline and play an important role in epigenetic inheritance mechanisms.

2 Epigenetic impacts of aging

The underlying genetic background of aging is increasingly being understood. Single gene mutations compromising the life expectancy and the genetic influence on aging processes have been discussed in several reports (Capri et al. 2014; Robert et al. 2015). However, despite known heritable components for aging processes, genes account just 25% for a person's probability of longevity (Kahn et al. 2009). Consequently, the knowledge about longevity-related genes uncover just a minority of this complex trait (Capri et al. 2014) and non-genomic contributing mechanisms are identified on one hand as stochastic events and on the other hand as epigenetic mechanisms. Stochastic occurrences are likely to happen e.g. in altered protein folding with structural and functional consequences or in an altered exposure to cytokines and growth factors leading to differences in the proliferative cell activity (Kahn et al. 2009). Aging, as well as environmental influences alter epigenetic processes over the lifetime. Supporting the assumption that everyone's epigenome is the reflection of lifelong environmental influences, Fraga et al. (2005) detected epigenetically identical patterns in the peripheral

blood of monozygotic twins in their early stages of life, while older monozygotic twins showed an epigenetic discordance. Epigenetic processes are highly dynamic and regulate the cell differentiation, gene expression and the gene-environment interaction. In addition, they are crucial for aging processes and show a high variation during the life span. Thus, special importance must be attached to epigenetic processes in investigating the impact of aging on the cell organization.

2.1 Epigenetic changes in the life span

Specific epigenetic alterations during aging are functionally associated with the aged phenotype (Calvanese et al. 2009). Thereby, aging modifies the DNA methylation by a reduced ability to maintain epigenetic marks and make the resulting alterations heritable throughout cell division (Fraga et al. 2005). From birth to old age, highly coordinated developmental programs determine each cell's DNA methylation patterns and the resulting changes in gene expression, growth and physiology can be seen in physical manifestations, functional loss and enrichment of cellular damage (Jones et al. 2015). The DNA methylation variability during life span was investigated by several research groups. From birth to age 3, Herbstman et al. (2013) detected in a longitudinal birth cohort study of 165 children a significant increase of DNA methylation, with inter-individual differences. These differences suggest that other - potentially environmental - mechanisms influence the dynamics of epigenetic changes. From age 3 to 17, Alisch et al. (2012) identified more rapidly occurring age-associated DNA methylation changes in the blood of younger patients, indicating that in early life there is a much stronger relationship between DNA methylation and age than in later life. In later adulthood, global DNA methylation analyses detected age-dependent decreases (Drinkwater et al. 1989; Fuke et al. 2004; Johansson et al. 2013). Drinkwater et al. (1989) compared the 5mC levels in the peripheral blood of young and old individuals and found a global loss of 10% within 50 years of age. Similar findings in a cohort of individuals aged from 4 to 94 years (N = 76) were reported by Fuke et al. (2004). Furthermore, there was a strong evidence for inter-individual variation of global DNA methylation that indicate that such variation is related to aging (Fuke et al. 2004). Johansson et al. (2013) detected in a study cohort of 421 individuals aged from 14 to 94 years old, age-dependent

methylation variations enriched for hypomethylated sites. In summary, the aforementioned studies indicate an evident global gain of DNA methylation in early life and global loss in later life. Nonetheless it must be noted that CpG islands usually gain DNA methylation and non-islands lose methylation (Jones et al. 2015). Since most CpGs are located outside of islands, in later life there will be a loss of global DNA methylation (Jones et al. 2015). DNA methylation at some CpG sites across the genome is highly associated with age and is consistently related to age across various individuals and tissues. These sites can be used to predict the individuals' chronological age like the "epigenetic clock" (Horvath et al. 2012; Weidner et al. 2014). Apart from this age-related loss of methylation, the variability within individuals increases during life span due to both environmental and stochastic events (Weidner et al. 2014; Jones et al. 2015). **Figure 2** shows how some individuals' epigenomes are more corresponding to their chronological ages than others (Jones et al. 2015). This process is highly diverse across individuals and is identified as "epigenetic drift" (Jones et al. 2015). In contrast to the epigenetic clock and due to the high inter-individual variability, the regions that are susceptible for the epigenetic drift are difficult to distinguish (Jones et al. 2015). The authors concluded that the epigenome in different tissues is a fragile construct and highly vulnerable to aging processes.

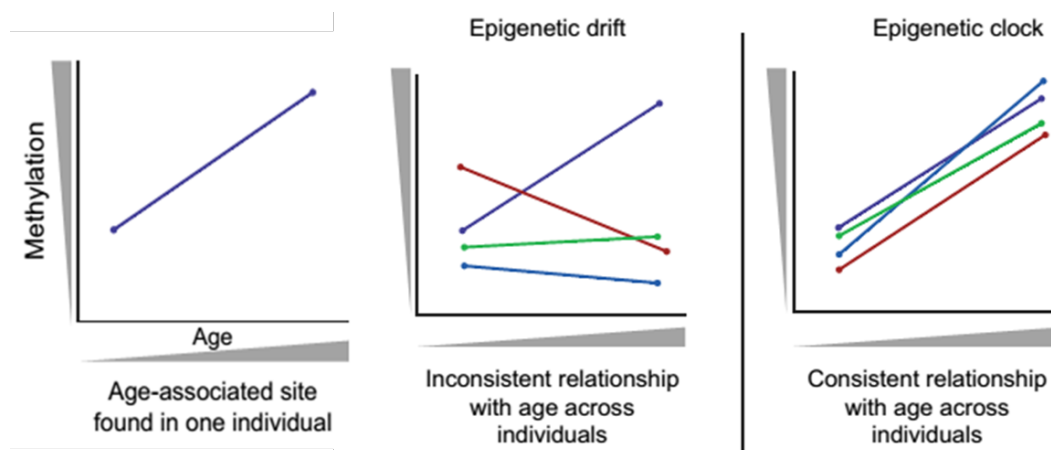


Figure 2: Epigenetic drift vs. epigenetic clock of an age-associated site found in one individual

Figure taken from Jones et al. (2015)

2.2 Male aging

With decreasing testosterone and increasing FSH and LH levels during a male's lifetime, aging has far-reaching impacts on the male reproduction as it compromises the testes in size and volume. Thus, the destruction of the epithelial cells is influenced by hormonal levels. Furthermore, aging-related seminal vesicle inadequacy and prostate atrophy impair the seminal fluids and lead to abnormal semen parameters (Sharma et al. 2015). Normal semen parameters are characterized by the WHO guidelines of 2010 (Cooper et al. 2010) as an ejaculate with a minimal volume of 1.5 ml, a sperm count of at least 15 million/ml, a progressive motility of at least 32 % motile sperm and a morphology of at least 4% normally shaped sperms. Nonetheless it was reported, that until the age of 34 years the parameters do not change and that aging less likely affects the sperm concentration compared to other parameters (Kidd et al. 2001). Besides the influence of male ageing on the testicular function, reproductive hormones and semen parameters, the genetics of male ageing is subject to current research. The genetics of male aging include the aging's influence on sperm DNA integrity, telomere length, chromosomal structure, *de novo* mutation rate and, lastly, the epigenetics of the male germline.

2.2.1 Genetics of male aging

Contrary to popular opinion, semen parameters are said to be less likely predictors of male infertility in comparison to disturbances in the DNA integrity (Sharma et al. 2015). To name just a few, the DNA integrity can be compromised by abnormal protamination (Aoki et al. 2005), oxidative stress because of inflammation, as well as infection, mutations, chromosomal disjunction and apoptosis (Sakkas et al. 1999). Since the sperm-DNA integrity is in turn correlated to male age (Moskovtsev et al. 2006), advanced paternal age negatively influences early embryonic development. It impairs implantation and blastocyst formation and leads ultimately to pregnancy loss (Sharma et al. 2015). Furthermore, various studies are focusing on telomeres while inspecting aging cells. Telomeres are repeating hexameric DNA sequences that are shortened during each cell division to protect coding DNA on the chromosomal ends. In highly proliferative cells like germ cells, the enzyme telomerase sustains telomeres and

indicates a biological resistance against aging (Sharma et al. 2015). Telomere length as a heritable component can be passed to the offspring and seems to be foremost paternally influenced (Njajou et al. 2007). Unryn et al. (2005) previously reported a strong relationship between advanced paternal age and offspring's telomere length.

2.2.2 Arising *de novo* mutations during spermatogenesis

Among all body cells, the sperm cell has an exceptional status, since it is highly specialized to overcome the different environments of both male and female reproduction tracts. In addition, sperm carries the paternal DNA information in a compacted nucleus by a highly motile body. The production of gametes, namely spermatozoa, is in the germinal epithelium of the seminiferous tubules within the testes (Lüllmann-Rauch 2015). The germinal epithelium is overlying the basal membrane and is formed by testicular sertoli cells that are connected by tight junctions and are forming a blood-testis barrier with an adluminal and a basal compartment. In a process lasting 10 weeks, the basally located spermatogonial stem cells undergo three phases: proliferation by mitosis, maturation by meiosis and differentiation to motile spermatozoa (cf. **Figure 3**) (Lüllmann-Rauch 2015). In both the embryonic and pubescent testes, the spermatogonial stem cells produce by mitosis one self-renewing reserve spermatogonium "type A" that stays in the basal compartment not undergoing meiosis and one actively dividing spermatogonium "type B" that goes on further maturation in the sexually mature testes by DNA-duplication (Clermont et al. 1966, Lüllmann-Rauch 2015). Due to the two different trajectories, which the two daughter cells follow, this division process is referred to as asymmetrical division (Clermont et al. 1966; Momand et al. 2013). All diploid sub-clones of the original parental spermatogonium, so-called primary spermatocytes, are connected by cytoplasmatic bridges and undergo the first meiotic division within three weeks, segueing synchronically from the basal to the adluminal compartment (Lüllmann-Rauch 2015). Immediately afterwards, the now evolved secondary spermatocytes pass into the second meiotic division without DNA duplication and four immature haploid spermatids emerge (Lüllmann-Rauch 2015). Those spermatids are differentiated to mature spermatozoa. They are equipped with an acrosome consisting of a modified lysosome filled with hydrolytic enzymes and a tail

consisting of microtubules (Clermont et al. 1966; Clermont et al. 1966). By replacing the histones with strong alkaline protamines, the cell nucleus is compacted to only 10% of its original volume, transforming the spermatozoa into a small and fast courier of DNA (Lüllmann-Rauch 2015).

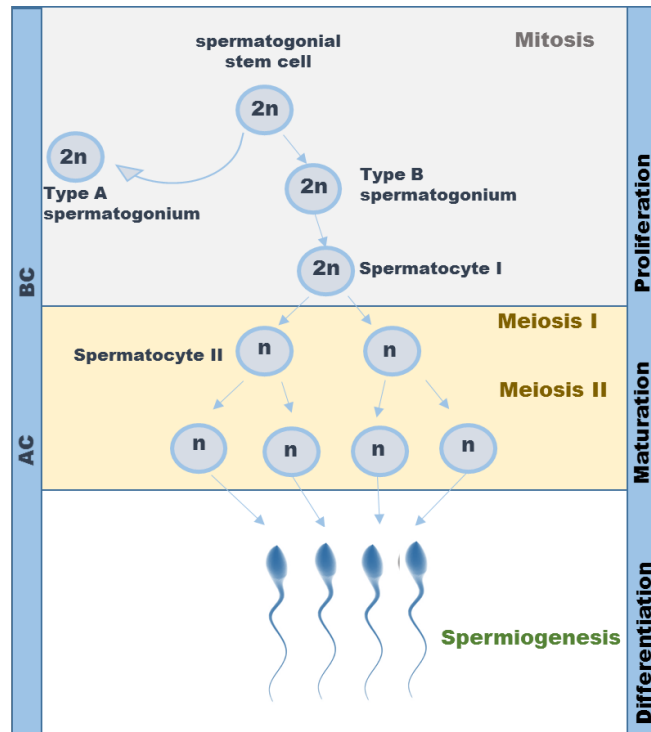


Figure 3: Spermatogenesis

Asymmetric divisions of spermatogonial stem cells replenish the stem cell pool. In case of mutation, the total number of mutant stem cells does not increase. Accordingly, asymmetric division creates a lower risk for transmission of de novo mutation to the offspring. 2n: diploid genome, n: haploid genome, AC: Adluminal compartment, BC: Basal compartment (own illustration)

Due to this disproportion between the oocyte and spermatozoon in size and number of cellular components, this created the assumption that the spermatozoa make only a small contribution to the developing embryo. Paternal determinants - such as paternal age - affect less likely the newborn than maternal influence factors. One could assume that irrelevant to the age of the father at conception, each new born child begins its life with the same biological and chronological age. Nonetheless recent researches indicate a discrepancy between epidemiological and genetic studies and the increasing importance of paternal effects (Goriely et al. 2013). Considering that spermatogenesis

is a lifelong continuing process supports the fact that the sperm of elder men are more prone to *de novo* mutations and the offspring of older fathers are more susceptible to various Mendelian diseases (Momand et al. 2013). Compared to the ovarian stem cell, that undergoes only 22 mitotic divisions in utero before it arrests until ovulation, the spermatogonial stem cell divides by mitosis every 16 days. Overall, this results in 150 mitotic cell divisions in a 20-year old and 840 divisions in a 50-year old male (Goriely et al. 2012). Genome-wide sequencing studies detected an exponential increase of *de novo* mutations per year in the male germline, which means a doubling of paternal mutations every 16.5 years (Kong et al. 2012). Despite being equally distributed through the spermatogonial stem cell stock, the histological dissection of testes tissue revealed that the mutation carrying cells were enriched in clusters that account for no more than 5% of the male testes (Choi et al. 2008). As mentioned above, cell divisions during spermatogenesis occur usually asymmetrically with occasional symmetrical divisions (Clermont et al. 1966; Choi et al. 2008). **Figure 4** shows the impact of a *de novo* germline mutation carrying spermatogonial stem cell that divides symmetrically rather than asymmetrically. Hereby, both mutated daughter cells proliferate and boost the number of mutation carrying cells that will appear in clusters as previously mentioned (Momand et al. 2013).

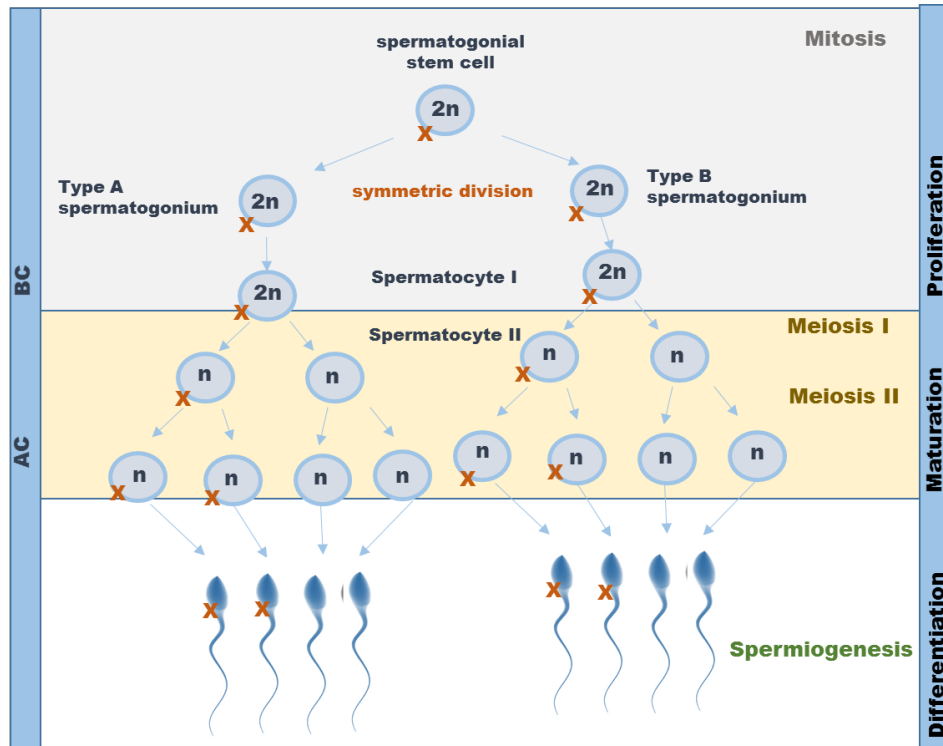


Figure 4: Consequences of symmetric cell division in spermatogenesis

Symmetrical divisions of spermatogonial stem cells increase the total number of mutant stem cells and consequently the total number of mutant sperm.

2n: diploid genome, n: haploid genome, AC: Adluminal compartment, BC: Basal compartment (own illustration)

This expansion of mutation carrying spermatogonial stem cells is described in the literature as the germline selective advantage model (Momand et al. 2013) or the selfish spermatogonial selection model (Goriely et al. 2012; Lim et al. 2012; Goriely et al. 2013). *De novo* germline mutations in genes that are involved in the regulation of growth and differentiation could transfer a selective advantage to the mutated spermatogonial cells that lead to their clonal expansion. A frequently mentioned example are mutations in the growth factor receptor – RAS signaling pathway that determines the spermatogonial cell's choice between self-renewal or being transferred to further maturation (Goriely et al. 2010). In the offspring, a mutation in the RAS-pathway leads to a group of congenital diseases, so-called RASopathies, which are characterized by disorders in neurogenesis, organ homeostasis and tumorigenesis, and in premeiotic cells having a growth advantage compared to wild type cells (Goriely et al. 2012, Momand et al. 2013). These pre-meiotic spermatogonial cells, in which the RAS pathway mutation arose are

positively selected, expand over time and will result into a higher chance for elder men to transmit the disease-causing mutation to their respective offspring.

2.2.3 Epigenetics of male aging

Apart from *de novo* mutations, ageing processes affect the epigenetic profile of the male germline during spermatogenesis. Though epigenetic patterns are stable and heritable modifications on the DNA sequence, environmental and endogenous factors such as increasing age impair the epigenetic marks (Sharma et al. 2015). The process of spermatogenesis and further fertilization, implantation and embryo development are sensitive events whereby the epigenetic program is reprogrammed through several mechanisms (Dada et al. 2012). Since the process of protamination eliminates histone codes that regulate gene activation or silencing via tail modifications, the idea arose that sperm do not contribute to epigenetic regulation in the embryo (Jenkins et al. 2012). However, 5 to 15% of the histones escape protamination and the incompleteness of histone replacement was foremost found in genes that are important for early embryonic development (Hammoud et al. 2009). The importance of the sperm DNA methylation on infertility, pregnancy loss and impaired embryonic development is elucidated in several studies. Molaro et al. (2011) reported the normal sperm methylome as being methylated in up to 96% of overall CpG sites and a deviating methylation pattern is said to be strongly associated with infertility and sperm defects (Jenkins et al. 2012). El Hajj et al. (2011) found aberrant sperm DNA methylation in imprinted regions and repetitive elements being associated with pregnancy loss. Global hypomethylation in the sperm DNA of IVF patients are said to be correlated with poor pregnancy outcomes (Benchaib et al. 2005). The influence of environmental conditions on the sperm DNA methylation was investigated by Yauk et al. (2008), as the sperm of male mice exposed to polluted air showed global DNA hypermethylation compared to mice exposed to filtered air. Aging as an influence factor was studied by Milekic et al. (2015). Sperm of young and old mice were compared in a genome-wide DNA methylation screen that indicated a significant methylation decrease in genes that regulate the transcription of developmental genes involved in neurodevelopmental disorders. This detected sperm hypomethylation resulted in brain DNA methylation

abnormalities and startle behaviors in the offspring of elder mice. In a prospective longitudinal study, Jenkins et al. (2014) compared the sperm of 19 donors at young age and at old age at >485,000 CpGs using Illumina methylation arrays. From each donor, two sperm samples were taken 9-19 years apart. The authors reported a significant decrease in methylation across 139 regions and a significant increase in methylation in 8 regions spanning a total of 117 genes. Several differentially methylated regions are located at loci that play a role in the development of diseases known to be more frequent in the offspring of elder males, e.g. neurodevelopmental disorders. The authors hint to a causative relationship between the epidemiologically confirmed influence of advanced paternal age on the offspring's health and aging-related epigenetic alterations in the male germline. As a further step to examine this intergenerational effect, Adkins et al. (2011) performed a genome-wide DNA-methylation profiling of 168 newborns and found a general trend towards hypomethylation in genes related to cancer, neurological regulation, glucose metabolism and transcriptional regulation. Thus, correct DNA methylation is key for normal sperm parameters and for early embryonic development (Jenkins et al. 2012). The comprehension of the sperm's epigenetics may contribute to our understanding of the paternal effect on embryogenesis.

3 Intergenerational epigenetic inheritance

3.1 The influence of environmental changes on future generations

The aforementioned studies contradict the hypothesis that each generation starts with a refreshed epigenome. The idea of non-genomic inheritance mechanisms or rather an epigenetic heritability would help explain evolutionary processes and the adaptation to changing environments over generations. Natural selection itself would not explain sufficiently the fast variation of phenotypes (Szyf et al. 2015). Radical environmental events experienced by a large section of the population e.g. famines, wars and extreme natural events allow large retrospective epidemiological studies on the association between environmental influences during conception and disease development in later life. Environmental conditions in early development can affect the human's genome and changes can persist over the course of life. Several studies identified the consequences

of parental exposure to famine on the offspring that resulted in various adverse metabolic and mental phenotypes in the descendants (Ravelli et al. 1999; Stein et al. 2007; Heijmans et al. 2008; Lumey et al. 2009; Li et al. 2011). Extensive epidemiologic studies about individuals conceived during the Dutch Hunger Winter in 1944-45 revealed that maternal malnutrition during early pregnancy leads to higher obesity rates in the respective female offspring (Ravelli et al. 1999). Similar findings were revealed by a study of Li et al. (2011) about the Chinese famine in 1959-1961, whereby famine exposure during conception shows an association to hypertension in the offspring's later life. Heijmans et al. (2008) went further and postulated an influence of epigenetic dysregulation, as they found individuals conceived during the Dutch famine having less DNA methylation in certain regions compared to the unaffected control group. Studies with animal models show the consequences of environmental toxins on the epigenome. Baccarelli et al. (2009) proved, that chemicals like metals, peroxisome proliferators, air pollutants and endocrine-disrupting toxicants can alter epigenetic patterns and that these changes increase the risk for diseases. These toxin-induced epigenetic changes can be possibly transmitted to the next generation.

3.2 Impacts of aged gametes on the offspring

If experienced environmental changes affect the offspring via epigenetic inheritance, one might assume that advanced paternal age as an interfering factor could also affect the offspring through changes in the germline. As aforementioned, aging affects DNA methylation in several tissues throughout the human body (Christensen et al. 2009; Horvath et al. 2013), including the paternal germline. Repetitive epidemiological studies confirm the existence of a paternal age effect. Thereby, advanced paternal age shows an association to neuropsychiatric disorders in the respective offspring (Susser et al. 1999; Naserbakht et al. 2011; Lehrer et al. 2015). By a meta-analysis of several case-control and cohort studies Miller et al. (2011) postulate, that advanced paternal age contributes to the development of schizophrenia in the offspring and its influence is equivalent to any known candidate gene. Since advanced paternal age appears as a determinant irrelevant to the family disease history, Lehrer et al. (2015) suggest other than genomic mechanisms, epigenetic mechanisms to be involved in disease

development. The idea that both *de novo* mutations as well as epigenetic changes in the germline contribute to the disease risk in the offspring is not surprising, since the mechanisms of DNA replication and DNA methylation are closely interacting factors on the molecular level and are both susceptible to changes in the environment (Naserbakht et al. 2011).

3.3 The “missing heritability” problem

As mentioned before, literature on the issue describes the “missing heritability” problem (Trerotola et al. 2015), since on their own genomic variations cannot sufficiently explain the underlying causes of these epidemiological observations (Manolio et al. 2009; Eichler et al. 2010; Koch et al. 2014; Szyf et al. 2015; Trerotola et al. 2015). The involvement of epigenetic mechanisms at this point becomes comprehensive, since they define cell type identity and are thus required to be highly stable throughout mitosis (Szyf et al. 2015). Heritability and persistence of DNA methylation over cell division is executed by the DNMT1 enzyme that maintains the methylation sites throughout cell division as it is highly affine to hemimethylated DNA strands obtained during semiconservative DNA replication. The question whether these mechanisms can be extended additionally during meiosis is often dismissed due to the fact, that primordial germ cells undergo an erasure of DNA methylation immediately after fertilization, known as “fetal reprogramming”. Nevertheless, this erasure of DNA methylation is proven to be incomplete at so-called “imprinted” regions that escape the phase of reprogramming.

3.4 The sperm cell as a carrier of epigenetic information

Looking back at spermatogenesis, age-associated methylation alterations in the male germline detected by Jenkins et al. (2014) were significantly enriched in regions escaping histone replacement. Regions with histone retention play an important role in the spermatogenic epigenetic organization, since they regulate gene activation and silencing (Carrell et al. 2012). Lacking protamination leads to a looser chromatin structure and therefore to a better access to the transcriptional machinery. Thus, the age-associated differentially methylated regions are localized in genes that are important to processes in spermatogenesis. Increasing age-related methylation alterations will give a

developmental advantage to the affected sperm cells and in accordance with the selfish spermatogonial theory, the number of differentially methylated sperm cells will expand (Jenkins et al. 2014). Sperm cells function as carriers of epigenetic information to the developing organism and depending on the localization of differentially methylated regions. Sperm cells also function as transmitters of disease predisposition factors. Thus, it is important to understand the male epigenetics to investigate the paternal age effect on embryogenesis and on the developing offspring (Carrell et al. 2012).

4 Aims of this thesis

The aim of this study was firstly to detect the influence of aging on the male germline (see **Table 1**). Therefore, five gene regions (*DMPK*, *GET4*, *FOXK1*, *TNXB*, and *PDE4C*) exhibiting age-associated methylation alterations (previously identified in the study by Jenkins, et al. (2014)) were studied by pyrosequencing in sperm samples of donors who fathered a child through Assisted Reproductive Technology (ART) (cohort 1, N=165). Significant results were confirmed in sperm samples of donors where fertility treatment has not lead to a live birth (control cohort 2, N=176). For an analysis at the single allele level, a group comparison of a young versus an aged sperm sample subset (N=26) was executed by deep bisulfite sequencing. Gene regions that showed a paternal age effect were additionally studied by pyrosequencing in the fetal cord blood (FCB) of the respective offspring (N=190). To focus on the exclusively paternal influence, a subset of fetal cord blood samples was genotyped and a comparison of maternal versus paternal allele was executed by deep bisulfite sequencing and pyrosequencing. Lastly, the father's impact on the offspring's disease susceptibility was investigated through a comparison study of *FOXK1* in patients with Autism Spectrum Disorders (ASD) and control patients without ASD. **Table 1** gives an overview about the key-questions and experiments that were conducted to investigate age-induced methylation alteration in the male germline, the possible transmission of epigenetic marks to the offspring, the exclusively paternal influence and the impact on the offspring's disease susceptibility.

Table 1: Aims of this thesis

Key-question	Analyzed samples	Method	Analyzed regions
Is there an age-induced methylation alteration in the male germline?	sperm cohort 1 (N=165)	Pyrosequencing	<i>DMPK, GET4, FO XK1, TNXB, PDE4C</i>
	sperm control cohort 2 (N=176)	Pyrosequencing	<i>FO XK1</i>
	sperm sample subset (N=26)	DBS	<i>FO XK1</i>
Is the methylation alteration transmitted to the offspring?	FCB (N=190)	Pyrosequencing	<i>FO XK1, DMPK</i>
Is the methylation alteration exclusively paternally inherited?	FCB (N=23)	Genotyping by pyrosequencing	<i>FO XK1</i>
		DBS	
		Allele-specific pyrosequencing	
Is there an impact on the offspring's disease susceptibility?	ASD-patients (N=46)	Pyrosequencing	<i>FO XK1</i>
	control cohort without ASD (N=29)		

The table gives an overview about the four key-questions and about the experiments that were executed to investigate an age-induced methylation alteration in the male germline, the possible transmission of epigenetic marks to the offspring, the exclusively paternal influence and the impact on the offspring's disease susceptibility.

5 Genes of interest

Five gene regions exhibiting age-associated methylation alterations observed by Jenkins et al. (2014) were analyzed in the present study: *DMPK, GET4, TNXB, PDE4C* and *FO XK1*.

DMPK encodes the myotonic dystrophy protein kinase. In the 3' non-coding region of *DMPK*, an instability and expansion of CTG repeats leads to the autosomal dominant inherited disease myotonic dystrophy (Meservy et al. 2003). The dystrophin protein kinase usually forms a protein complex and anchors the myocyte's cytoskeleton on the basal membrane. Lacking dystrophin leads to muscular necrosis and therefore muscular weakness. An epigenetic intermediation of this genetic disease is assumed, as this CTG triplet repeat expansion is said to be linked with impaired chromatin, differential methylation and altered gene expression (Tapscott et al. 1998). Intriguingly,

affected male patients show premature aging which diminishes the life-expectancy by around 20 years (Brisson et al. 2002). The severity of myotonic dystrophy symptoms and age-related hormonal levels correlated positively which emphasizes the complexity of male aging (Brisson et al. 2002).

The gene *GET4* encodes the “Golgi to ER traffic protein 4”, which guides the entry of tail-anchored proteins into the endoplasmatic reticulum membrane (Chang et al. 2010). Thus, the *GET4* protein participates in complex cascades and interactions between protein machineries for a precise delivery of membrane proteins (Rome et al. 2014). These mechanisms are important for the synthesis of lysosomal proteins that are responsible for macromolecular degradation and processes for both cell survival and cell death (Ricarte et al. 2011). In a complex with the other proteins *BAG6* and *UBL4A*, *GET4* is an intermediary for signaling DNA damage and damage-induced cell death (Krenciute et al. 2013).

TNXB encodes the Tenascin-X protein, a large extracellular matrix protein that is involved into the collagen synthesis and deposition in dermal fibroblasts (Mao et al. 2002). Missing expression of tenascin X causes the Tenascin-X (TNX) deficient type Ehlers-Danlos syndrome (EDS) (Demirdas et al. 2016), a syndrome that is characterized with symptoms of the connective tissue organization such as soft skin, joint hypermobility and hernias (Gardella et al. 2004). Causing cervical incompetence in the prenatal period, the *TNXB* gene revealed as candidate gene for prematurity and preterm birth (Anum et al. 2009). Furthermore, Tenascin-X is utilized as a diagnostic marker for ovarian malignant mesothelioma as the gene is differentially expressed (Yuan et al. 2009; Kim et al. 2010). Intriguingly, the *TNXB* locus is closely localized to the *NOTCH4* locus, a susceptibility gene for schizophrenia (Wei et al. 2004). In British, Japanese and Chinese studies a significant association between SNPs in the *TNXB* locus and schizophrenia was confirmed (Wei et al. 2004; Tochigi et al. 2007; Wang et al. 2011). The methylation status of *TNXB* revealed sensitive to environmental changes, since *TNXB* was found to be significantly hypermethylated under periods of starvation (Kesselmeier et al. 2016). Considering the vast consequences of methylation changes on the population’s health during famines, changes in *TNXB* methylation might lead to

implications on the organism regarding the connective tissue organization, development of malignancies, and susceptibility to schizophrenia.

PDE4C encodes the “phosphodiesterase 4C”, an isoenzyme of the phosphodiesterase enzymes that eliminate the second messenger molecules cAMP and cGMP and regulates therefore signal transduction. The *PDE4C* enzyme is expressed in the tissue of lung, testis, kidney, brain, liver and in leucocytes (Obornolte et al. 1997; Perez-Torres et al. 2000). By regulating the cAMP activity in the lungs, the *PDE4C* enzyme is an important mediator in airway inflammation (Tang et al. 2006). More interestingly, in extensive human epidemiological studies, the *PDE4C* gene was identified as a high-confidence age-associated differentially methylated region (Spiers et al. 2016). DNA methylation levels in the *PDE4C* gene were even utilized as a biomarker to predict biological aging in blood. This prediction is more accurate than age measurements on the telomere length (Weidner et al. 2014).

FOXK1 encodes the “forkhead box protein K1”. The forkhead box protein family consists of at least 43 members encoding transcriptional factors that are important for proliferation and differentiation mechanisms and developmental processes during the embryonic period (Kato et al. 2004). Both in animal models and humans, *FOXK1* revealed to be expressed in so-called satellite cells that form a quiescent myogenic stem cell pool in the adult muscle and that are essential for muscular remodeling and regeneration processes (Bassel-Duby et al. 1994; Garry et al. 1997). Knockout or lacking murine *Foxk1* expression showed highly adverse effects on the muscular growth and function evoking a similar phenotype to the human’s Duchenne muscular dystrophy (Garry et al. 2000; Hawke et al. 2003). Furthermore, a human *FOXK1* knockdown resulted in an inhibition of cell proliferation defining *FOXK1* as an important mediator in the cell cycle kinetics (Grant et al. 2012; Shi et al. 2012). This enhanced cell proliferation driven by *FOXK1* expression might play a possible role in cancer development, since it was found to interact with oncoproteins of different types of human papillomaviruses (Komorek et al. 2010). Furthermore, the overexpression of *FOXK1* found in several neoplasias and malignant tissues (Huang et al. 2004) correlates with advanced stages of cancer, revealing *FOXK1* as a significant prognosis marker for colorectal cancer and

breast cancer (Sun et al. 2016; Wu et al. 2016). The repression of autophagy driven by *FOXK1* expression might build a possible underlying mechanism for the observed processes (Bowman et al. 2014). Besides malignant tissues, *FOXK1* overexpression was also found in several embryonic tissues, foremost in the embryonic neural system (Huang et al. 2004; Wijchers et al. 2006), indicating *FOXK1*'s important role in transcriptional activity during neuronal and embryonic development. The embryonic and fetal phase represents a highly dynamic period of epigenetic regulation and significant DNA methylation changes mark key processes in the prenatal period (Spiers et al. 2015). *FOXK1* regulates transcription and chromatin states by binding on cytosine derivatives such as formylcytosine (5fC) that plays a role in demethylation processes and epigenetic signaling (Iurlaro et al. 2013). Microarray data of mouse embryonic stem cells showed a linear increase in murine *Foxk1* expression, revealing *Foxk1* as a marker for neuronal development (Suh et al. 2008). In individuals with an autism spectrum disorder, Nardone et al. (2014) identified altered methylated CpG sites in the *FOXK1* gene body using a 450K methylation array study. The involvement of the FOX protein family in impaired brain development is furthermore highlighted in studies focusing on mutations in the FOX-family member *FOXP1*, that revealed to be highly associated with intellectual disability, language deficits, behavioral and social disorders as found in patients with autism spectrum disorders (Deriziotis et al. 2014; Bacon et al. 2015; Lozano et al. 2015). In summary, the transcriptional activity of the *FOXK1* protein plays an important role in processes affected by cell proliferation (e.g. muscular regeneration by myogenic progenitor cells), cell cycle control (e.g. development of cancer) and cell differentiation (e.g. neuronal differentiation during embryonic development).

II. MATERIAL AND METHODS

1 Material

1.1 Chemicals

Table 2: List of utilized chemicals

Chemicals	Manufacturer
10 x PCR Rxn Buffer with Mg₂Cl	Invitrogen (Darmstadt, Germany)
6 x loading dye	Thermo Fisher Scientific Inc. (Waltham, USA)
Agencourt AMPure XP beads	Beckmann Coulter GmbH (Krefeld, Germany)
Ethanol absolute, p.A.	Carl Roth GmbH & Co KG (Karlsruhe, Germany)
Ethylenediaminetetraacetic acid (EDTA)	Applichem GmbH (Darmstadt, Germany)
Fast Start Taq DNA Polymerase	Roche Diagnostics GmbH (Mannheim, Germany)
Gene ruler DNA Ladder Mix (100 bp ladder)	Thermo Fisher Scientific Inc. (Waltham, USA)
HotStarTaq[®] Master Mix	Qiagen (Hilden, Germany)
Hypochloride acid	Applichem GmbH (Darmstadt, Germany)
Isopropanol	Carl Roth GmbH & Co KG (Karlsruhe, Germany)
PCR grade nucleotide mix (dNTPs)	Roche Diagnostics GmbH (Mannheim, Germany)
peqGOLD universal agarose	Peqlab (Erlangen, Germany)
PureSperm[®] 40	Nidacon (Mölndal, Sweden)
PureSperm[®] 80	Nidacon (Mölndal, Sweden)
PyroMark Annealing Buffer	Qiagen (Hilden, Germany)
PyroMark Binding Buffer	Qiagen (Hilden, Germany)
redSafe	iNtRON Biotechnology (Seongnam-si, Korea)
Sodium chloride (NaCl)	Applichem GmbH (Darmstadt, Germany)
Sodium dodecylsulfate (SDS)	Applichem GmbH (Darmstadt, Germany)
Streptavidin Sepharose high performance	GE Healthcare (Munich, Germany)
Tris	Applichem GmbH (Darmstadt, Germany)
β-mercaptoethanol	Applichem GmbH (Darmstadt, Germany)

1.2 Kits

Table 3: List of utilized Kits

Kit	Manufacturer
Dneasy® Blood and Tissue Kit (250)	Qiagen (Hilden, Germany)
EpiTect® Fast 96 DNA Bisulfite Kit	Qiagen (Hilden, Germany)
EpiTect® Fast DNA Bisulfite Kit (50)	Qiagen (Hilden, Germany)
FlexiGene® DNA Kit (250)	Qiagen (Hilden, Germany)
Genomic DNA Clean and Concentrator™- 10	Zymo Research
GS Junior Titanium emPCR Kit (Lib-A)	Roche Diagnostics GmbH (Mannheim, Germany)
GS Junior Titanium Pico Titer Plate Kit	Roche Diagnostics GmbH (Mannheim, Germany)
GS Junior Titanium Sequencing Kit	Roche Diagnostics GmbH (Mannheim, Germany)
PyroMark Gold Q96 CDT and NDT reagents	Qiagen (Hilden, Germany)

1.3 Buffers

Table 4: Content of prepared buffers

Buffer	Content
1 xTE	1 ml 1M Tris (pH=8), 0.2 ml 0.5 EDTA, 98.8 ml dH ₂ O
50 x TAE	242 g Tris, 100 ml 0.5 M EDTA (pH=8), 57.1 ml acedic acid, 9943 ml dH ₂ O, autoclaved
70 % ethanol	700 ml ethanol, 300 ml dH ₂ O
Buffer 2	1 ml 0.5 M EDTA (pH=8), 5 ml 5M NaCl, 5 ml 1 M Tris (pH=8), 5ml 10% SDS (pH=7.2), 1 ml 100% β-mercaptoethanol, 33 ml dH ₂ O
Denaturation buffer	8 g NaOH, 1 l dH ₂ O
Secret buffer	40% dH ₂ O, 50% 1 xTE, 10% 10xPCR Rxn buffer
Wash buffer	1.21 g Tris, 1 l dH ₂ O, HCl for pH=7.6

1.4 Equipment

Table 5: List of utilized equipment

Equipment	Manufacturer
1.5, 2.0 ml reaction tubes	Eppendorf (Hamburg, Germany), Sarsted (Nümbrecht, Germany)
96-well non skirted plate	Hartenstein (Würzburg, Germany)
Bandelin Sonorex RK52	Hartenstein (Würzburg, Germany)
Bioanalyzer 2100	Agilent (Böblingen, Germany)
Biosphere® Filter Tips	Sarstedt (Nümbrecht, Germany)
Heraeus Fresco 17, Heraeus Multifuge X1R	Thermo Fisher Scientific Inc. (Waltham, USA)
Centrifuge 5424	Eppendorf (Hamburg, Germany)
DNA Engine Tetrad 2 Thermal Cycler	Bio-RAD Laboratories GmbH (Munich, Germany)
Gel Imager	Intas Science Imager Instruments GmbH (Göttingen, Germany)
Glass tubes	Nidacon (Mölndal, Sweden)
Gloves	Carl Roth GmbH & Co KG (Karlsruhe, Germany)
GS Junior 454	Roche Diagnostics GmbH (Mannheim, Germany)
Magnetic particle collector	Invitrogen (Darmstadt, Germany)
NanoDrop 2000c	Peqlab (Erlangen, Germany)
Pipettes	Eppendorf (Hamburg, Germany)
PyroMark Q96 HS Plate	Qiagen (Hilden, Germany)
PyroMark Q96 Working Station	Qiagen (Hilden, Germany)
PyroMark Vakuum Prep Tool 60-0236	Qiagen (Hilden, Germany)
UV bench Model 300	Airclean Systems (Raleigh, USA)
Vortex Genie 2	Scientific Industries, Inc. (New York, USA)
Water bath GFL Type 1002	Gesellschaft für Labortechnik mbH (Burgwedel, Germany)

1.5 Software

Table 6: List of utilized software to generate and analyze data

Software	Developer
Amplifyzer	Sven Rahmann
Pyro Q CpG	Biotagebio
Python	Python Software Foundation
SPSS	IBM
2100 Expert	Agilent

Assay	Direction	Modification 5'	Sequence (5'-3')	Chromosomal location	Primer length	Amplicon length	Annealing temperature PCR	No. of analyzed CpG-sites
GET4	forward		TGAGAGTGGGTTGATTTGTAAA	Chr 7: 875,407- 875,595	23 bp	188 bp	58.8 °C	6
	reverse	biotin	AACTTCCAACCCTATCAAACT		21 bp			
	sequencing 1		GTGGGTTGATTTGTAAAT		19 bp			
	sequencing 2		AGGGTTGGGTTTAG		15bp			
DMPK	forward		GAGTAGGGGATAAATAAGGATTTTAGTT	Chr 19: 45,771,835- 45,772,027	29 bp	192 bp	60.0 °C	5
	reverse	biotin	CACCTCCTCCTCCAAAACCTC		21 bp			
	sequencing		ATATAIAGGTTGAAGTGG		18 bp			
	forward		GTGGGAATAGTTTATAGGGTTTAGAT		25 bp			
	reverse	biotin	ACCCCACTCACCTTATTTAAAAA	Chr 19: 18,220,390- 18,220,617	23 bp	227 bp	60.0 °C	9
PDE4C	sequencing 1		AGGGTTTAGATGAAAGAG		17 bp			
	sequencing 2		GGTAGGTTTTGATTGTTT		19 bp			
	sequencing 3		GGATTGGTGTGGATTA	18 bp				
TNXB	forward		GGGGTTTTGAGAAGTTGT	Chr 6: 32,097,126- 32,097,340	18 bp	214 bp	60.0 °C	5
	reverse	biotin	AAATACTAAAAATCCCTCCCTCTTC		24 bp			
	sequencing 1		GGGTTTGAGAAAGTTTGT		18 bp			
	sequencing 2		AGTTGGGGTTAGTGTA	16 bp				
FOXP1	forward		AGGGTAGTGGAGTTGGAAG	Chr 7: 4,683,841 - 4,684,107	20 bp	266 bp	58.8 °C	6
	reverse	biotin	TACATCCCCCACTAATACTCTTAAATA		28 bp			
	sequencing 1		GTGGAGTTGGAAAAGGA		16 bp			
	sequencing 2		GGTTTTTTTGTTTGGTGA	19 bp				

Table 7: List of primers used for bisulfite pyrosequencing

For each gene a forward and reverse PCR primer was designed. The assay-specific annealing temperature was identified by Gradient-PCR. According to the number of analyzed CpG sites, 1-3 pyrosequencing primers were designed for each assay.

1.6 Primers

FO XK1 Assay	Direction	Modification 5'	Sequence (5'-3')	Chromosomal location	Primer length	Amplicon length	Annealing temperature PCR	No. of analyzed CpG-sites
Geno-typing	forward		AGTGTGGGTTGTGTTGAAG	Chr 7: 4,683,841- 4,684,012	19 bp	171 bp	64.0 °C	2
	reverse	biotin	CCCAACTAAATCTCTACCCTAATA		26 bp			
	sequencing 1		TGAAGGAGTAGAGGT		15 bp			
	sequencing 2		GAGGATAGGAAGTTTGT		17 bp			
DBS 1st round PCR	forward		CTTGCTTCCTGGCAGGAG AGTGTGGGTTGTGTTGAAG	Chr 7: 4,683,841- 4,684,012	40 bp	171 bp	60.0 °C	5
	reverse		CAGGAACACAGCTATGAC CCCAACTAAATCTCTACCCTAATA		44 bp			
Allele-specific Pyro-sequencing	forward	biotin	AGGAGTGTGGGTTGTGTT	Chr 7: 4,683,838- 4,684,012	18 bp	174 bp	61.3 °C	2
	reverse		CCCAACTAAATCTCTACCCTAATA		26 bp			
	sequencing A		ACTAATTAATAAATATAAATAAAT		25 bp			
	sequencing G		ACTAATTAATAAATATAAATAAAC		25 bp			

Table 8: List of primers for FO XK1 genotyping, 1st round PCR of Deep Bisulfite Sequencing and allele-specific pyrosequencing
The genotyping assay was used to study the informative SNP rs9791644. The allele-specific pyrosequencing assay was designed that the 3'end of the sequencing primers binds directly on that SNP. The primers for the 1st round PCR amplification of the deep bisulfite sequencing assays contained the adaptor sequences A (red) and B (blue) (cf. Figure 6)

Table 9: List of 2nd round PCR primers for deep bisulfite sequencing of FO XK1

MID	Direction	Sequence (5'-3')	Primer length [bp]
1	AUT	CGTATCGCCTCCCTCGCGCCATCAGACGAGTGCCTTGCTTCCTGGCACGAG	53
	BUT	CTATGCGCCTTGCCAGCCCGCTCAGACGAGTGCCTCAGGAAACAGCTATGAC	52
2	AUT	CGTATCGCCTCCCTCGCGCCATCAGACGCTCGACACTTGCTTCCTGGCACGAG	53
	BUT	CTATGCGCCTTGCCAGCCCGCTCAGACGCTCGACACAGGAAACAGCTATGAC	52
3	AUT	CGTATCGCCTCCCTCGCGCCATCAGAGACGCACTCCTTGCTTCCTGGCACGAG	53
	BUT	CTATGCGCCTTGCCAGCCCGCTCAGAGACGCACTCCAGGAAACAGCTATGAC	52
4	AUT	CGTATCGCCTCCCTCGCGCCATCAGAGCACTGTAGCTTGCTTCCTGGCACGAG	53
	BUT	CTATGCGCCTTGCCAGCCCGCTCAGAGCACTGTAGCAGGAAACAGCTATGAC	52
5	AUT	CGTATCGCCTCCCTCGCGCCATCAGATCAGACACGCTTGCTTCCTGGCACGAG	53
	BUT	CTATGCGCCTTGCCAGCCCGCTCAGATCAGACACGCAGGAAACAGCTATGAC	52
6	AUT	CGTATCGCCTCCCTCGCGCCATCAGATATCGCGAGCTTGCTTCCTGGCACGAG	53
	BUT	CTATGCGCCTTGCCAGCCCGCTCAGATATCGCGAGCAGGAAACAGCTATGAC	52
7	AUT	CGTATCGCCTCCCTCGCGCCATCAGCGTGTCTCTACTTGCTTCCTGGCACGAG	53
	BUT	CTATGCGCCTTGCCAGCCCGCTCAGCGTGTCTCTACAGGAAACAGCTATGAC	52
8	AUT	CGTATCGCCTCCCTCGCGCCATCAGCTCGCGTGTCTTGCTTCCTGGCACGAG	53
	BUT	CTATGCGCCTTGCCAGCCCGCTCAGCTCGCGTGTCCAGGAAACAGCTATGAC	52
9	AUT	CGTATCGCCTCCCTCGCGCCATCAGTAGTATCAGCCTTGCTTCCTGGCACGAG	53
	BUT	CTATGCGCCTTGCCAGCCCGCTCAGTAGTATCAGCCAGGAAACAGCTATGAC	52
10	AUT	CGTATCGCCTCCCTCGCGCCATCAGTCTCTATGCGCTTGCTTCCTGGCACGAG	53
	BUT	CTATGCGCCTTGCCAGCCCGCTCAGTCTCTATGCGCAGGAAACAGCTATGAC	52
11	AUT	CGTATCGCCTCCCTCGCGCCATCAGTGATACGTCTCTTGCTTCCTGGCACGAG	53
	BUT	CTATGCGCCTTGCCAGCCCGCTCAGTGATACGTCTCAGGAAACAGCTATGAC	52
12	AUT	CGTATCGCCTCCCTCGCGCCATCAGTACTGAGCTACTTGCTTCCTGGCACGAG	53
	BUT	CTATGCGCCTTGCCAGCCCGCTCAGTACTGAGCTACAGGAAACAGCTATGAC	52
13	AUT	CGTATCGCCTCCCTCGCGCCATCAGCATAGTAGTGCTTGCTTCCTGGCACGAG	53
	BUT	CTATGCGCCTTGCCAGCCCGCTCAGCATAGTAGTGCAGGAAACAGCTATGAC	52
14	AUT	CGTATCGCCTCCCTCGCGCCATCAGCGAGAGATACCTTGCTTCCTGGCACGAG	53
	BUT	CTATGCGCCTTGCCAGCCCGCTCAGCGAGAGATACCAGGAAACAGCTATGAC	52
15	AUT	CGTATCGCCTCCCTCGCGCCATCAGATACGACGTACTTGCTTCCTGGCACGAG	53
	BUT	CTATGCGCCTTGCCAGCCCGCTCAGATACGACGTACAGGAAACAGCTATGAC	52
16	AUT	CGTATCGCCTCCCTCGCGCCATCAGTACGTACTACTTGCTTCCTGGCACGAG	53
	BUT	CTATGCGCCTTGCCAGCCCGCTCAGTACGTACTACAGGAAACAGCTATGAC	52
17	AUT	CGTATCGCCTCCCTCGCGCCATCAGCGTCTAGTACCCTTGCTTCCTGGCACGAG	53
	BUT	CTATGCGCCTTGCCAGCCCGCTCAGCGTCTAGTACCAGGAAACAGCTATGAC	52
18	AUT	CGTATCGCCTCCCTCGCGCCATCAGTCTACGTAGCCTTGCTTCCTGGCACGAG	53

	BUT	CTATGCGCCTTGCCAGCCCGCTCAGTCTACGTAGCCAGGAAACAGCTATGAC	52
19	AUT	CGTATCGCCTCCCTCGCGCCATCAGTGTACTACTCCTTGCTTCCTGGCACGAG	53
	BUT	CTATGCGCCTTGCCAGCCCGCTCAGTGTACTACTCCAGGAAACAGCTATGAC	52
20	AUT	CGTATCGCCTCCCTCGCGCCATCAGACGACTACAGCTTGCTTCCTGGCACGAG	53
	BUT	CTATGCGCCTTGCCAGCCCGCTCAGACGACTACAGCAGGAAACAGCTATGAC	52
21	AUT	CGTATCGCCTCCCTCGCGCCATCAGCGTAGACTAGCTTGCTTCCTGGCACGAG	53
	BUT	CTATGCGCCTTGCCAGCCCGCTCAGCGTAGACTAGCAGGAAACAGCTATGAC	52
22	AUT	CGTATCGCCTCCCTCGCGCCATCAGTACGAGTATGCTTGCTTCCTGGCACGAG	53
	BUT	CTATGCGCCTTGCCAGCCCGCTCAGTACGAGTATGCAGGAAACAGCTATGAC	52
24	AUT	CGTATCGCCTCCCTCGCGCCATCAGTAGAGACGAGCTTGCTTCCTGGCACGAG	53
	BUT	CTATGCGCCTTGCCAGCCCGCTCAGTAGAGACGAGCAGGAAACAGCTATGAC	52
25	AUT	CGTATCGCCTCCCTCGCGCCATCAGTCGTGCTCGCTTGCTTCCTGGCACGAG	53
	BUT	CTATGCGCCTTGCCAGCCCGCTCAGTCGTGCTCGCAGGAAACAGCTATGAC	52
26	AUT	CGTATCGCCTCCCTCGCGCCATCAGACATACGCGTCTTGCTTCCTGGCACGAG	53
	BUT	CTATGCGCCTTGCCAGCCCGCTCAGACATACGCGTCAGGAAACAGCTATGAC	52
27	AUT	CGTATCGCCTCCCTCGCGCCATCAGACGCGAGTATCTTGCTTCCTGGCACGAG	53
	BUT	CTATGCGCCTTGCCAGCCCGCTCAGACGCGAGTATCAGGAAACAGCTATGAC	52
28	AUT	CGTATCGCCTCCCTCGCGCCATCAGACTACTATGTCTTGCTTCCTGGCACGAG	53
	BUT	CTATGCGCCTTGCCAGCCCGCTCAGACTACTATGTCAGGAAACAGCTATGAC	52
29	AUT	CGTATCGCCTCCCTCGCGCCATCAGACTGTACAGTCTTGCTTCCTGGCACGAG	53
	BUT	CTATGCGCCTTGCCAGCCCGCTCAGACTGTACAGTCAGGAAACAGCTATGAC	52
30	AUT	CGTATCGCCTCCCTCGCGCCATCAGAGACTATACTCTTGCTTCCTGGCACGAG	53
	BUT	CTATGCGCCTTGCCAGCCCGCTCAGAGACTATACTCAGGAAACAGCTATGAC	52

Each sample for deep bisulfite sequencing was tagged with an individual multiplex identifier (MID, marked in red). Furthermore, a key sequence (marked in blue), the 454 Titanium primer A, 454 Titanium primer B and the Universal Adaptor A and B were added (cf. 2.3.3 Library preparation p.45)

1.7 Samples

1.7.1 Samples for the age-associated methylation analysis by pyrosequencing

All analyzed samples were provided by the Fertility Center in Wiesbaden, Germany. The study of human sperm and FCB samples was approved (no. 111/13) by the Ethics Committee at the Medical Faculty of Würzburg University and informed consent was acquired from all participating couples. For this study, the sperm-DNA of 165 semen samples (left-over swim-up sperm fraction, frozen at -80 °C until further use) with a volume of 0.2 to 0.8 ml each were analyzed. The assisted reproductive treatment (ICSI or IVF) led to a live birth in all analyzed cases. Therefore, the respective offspring's DNA was analyzed in the provided 190 fetal cord blood samples. Since the probability of

multiple births is increased when using assisted reproductive techniques, the fetal cord blood sample set contained 23 twins and 1 triplet. Besides information about the father, such as age (ranging from 26 to 55 years), weight, height and BMI, additional information (**Figure 5**) was known about the semen samples such as spermiogram parameters (per WHO criteria: sperm concentration, morphology, motility), abnormalities and low sperm count (such as oligozoospermia, kriptozoospermia, asthenozoospermia). Furthermore, the father's hormonal status was registered (TSH, testosterone, prolactin and FSH). For the fetal cord blood cohort, information about the gender, birth mode and birth parameters (such as weight, length and head circumference) was available. Furthermore, the assisted reproductive treatment mode (ICSI/IVF) of each case was recorded. In addition, the testing in an independent cohort of 176 semen samples served as a confirmation analysis of the *FO XK1* results. Those semen samples originated from donors whose assisted reproductive treatment did not lead to a live birth. Clinical information similar to the main cohort was also obtained for those samples.

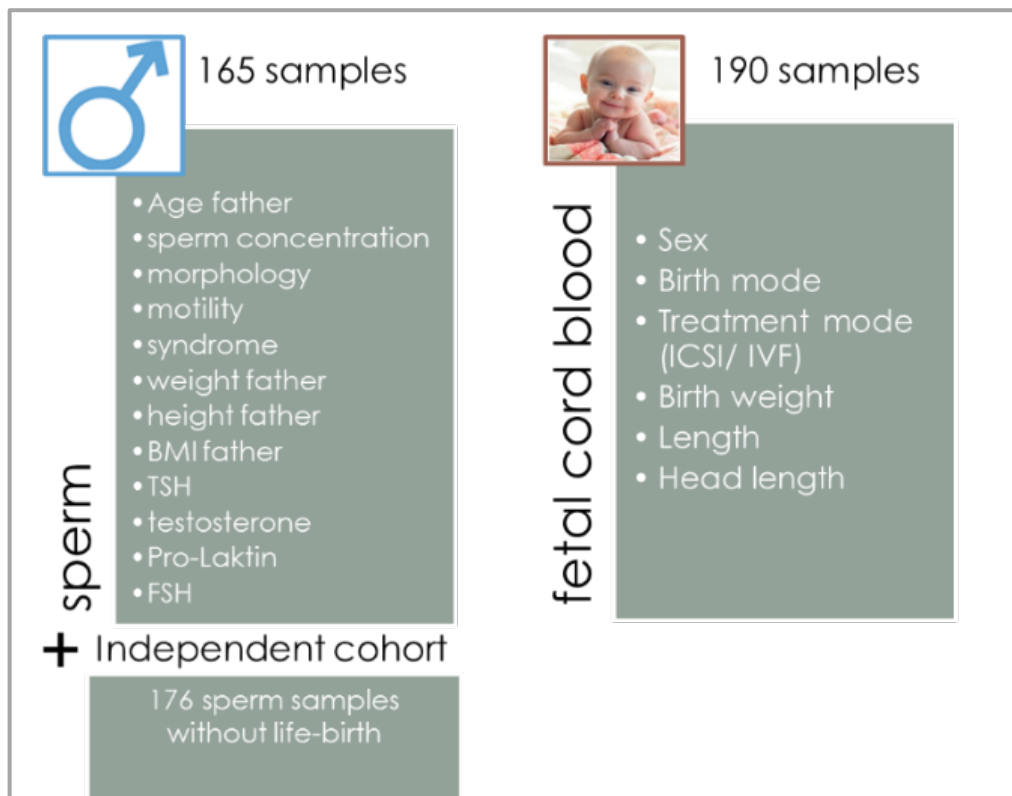


Figure 5: Overview of the analyzed samples (*own illustration*)

1.7.2 Samples for the age-associated methylation analysis by deep bisulfite sequencing

For the deep bisulfite sequencing of the *FOXK1* age-associated region, a subset of 26 sperm and 23 fetal cord blood samples were chosen since 29 MID barcoded samples can only be sequenced per run. For sperm analysis, 13 samples were selected from the oldest and 13 from the youngest donor groups (young group under 35 years old; aged group over 40 years old). For the fetal cord blood analysis, the samples were chosen after genotyping an informative SNP. Therefore, heterozygous cord bloods with a homozygous father were chosen for an allele-specific analysis (cf. 2.2.2 Application fields). In addition to the 26 selected samples, two artificially methylated DNA standards (0% and 100% methylated) were included as sequencing quality controls in both runs (samples listed in **Table 10**).

Table 10: Fetal cord blood and sperm sample sets for DBS

MID	Fetal cord blood samples for DBS			Sperm samples for DBS		
	<i>FCB number</i>	<i>Paternal allele</i>	<i>Maternal allele</i>	<i>Sperm sample number</i>	<i>Group</i>	<i>Age of the father</i>
MID01	FCB 25	G	A	sperm 282	young	35
MID02	FCB 26	G	A	sperm 209	aged	41
MID03	FCB 47	G	A	sperm 1133	young	32
MID04	FCB 61	A	G	sperm 195	young	34
MID05	FCB 70	G	A	sperm 745	young	28
MID06	FCB 85	G	A	sperm 723	young	34
MID07	FCB 86	G	A	sperm 218	young	33
MID08	FCB 91	G	A	sperm 750	aged	49
MID09	FCB 89	G	A	sperm 281	aged	43
MID10	FCB 89 r	G	A	sperm 077	young	26
MID11	FCB 90	G	A	sperm 169	aged	42
MID12	FCB 90 r	G	A	sperm 001	aged	43
MID13	FCB 105	A	G	sperm 389	aged	55
MID14	FCB 114	A	G	sperm 736	young	35
MID15	FCB 120	G	A	sperm 258	young	32
MID15	100% met	-	-	sperm 143	aged	49
MID17	FCB 131	G	A	sperm 061	young	28
MID18	FCB 139	G	A	sperm 224	aged	44
MID19	FCB 155	G	A	sperm 597	young	33
MID20	-	-	-	100% met	-	-
MID21	FCB 178	A	G	sperm 342	young	33
MID22	FCB 184	G	A	sperm 353	aged	43
MID24	FCB 206	G	A	sperm 511	young	35
MID25	FCB 206 r	G	A	sperm 086	aged	41
MID26	FCB 209	G	A	sperm 657	aged	46
MID27	FCB 210	G	A	sperm 1084	aged	44
MID28	FCB 223	A	G	sperm 254	aged	40
MID29	0% met	-	-	0% met	-	-

In both DBS runs, a MID (multiplex identifier) number was assigned to each fetal cord blood or sperm sample. The fetal cord blood sample set consists of 26 heterozygous

fetal cord blood samples with homozygous fathers, 3 replicates (r) and 2 artificially methylated DNA controls (0% met and 100% met). The table also displays paternal and maternal allele, determined after genotyping by pyrosequencing. The sperm sample set consists of 26 sperm samples of 13 young (< 35 years old) and 13 aged (> 40 years old) fathers and 2 artificially methylated DNA controls (0% met and 100% met).

1.7.3 Samples for the FO XK1 study in patients with autism spectrum disorders

For the *FO XK1* autism study, 46 peripheral blood leucocyte (PBL) samples of exclusively male patients with autism spectrum disorders were provided by the “Institut du Cerveau et de la Moelle Epinière” and the “Hôpital Pitié-Salpêtrière” in Paris, France. A control cohort was composed of 29 age- and sex-matched (**Figure 6**) PBL samples of patients with hemophilia. The age range for the autism cohort was 2 to 42 years and for the control cohort 1-43 years.

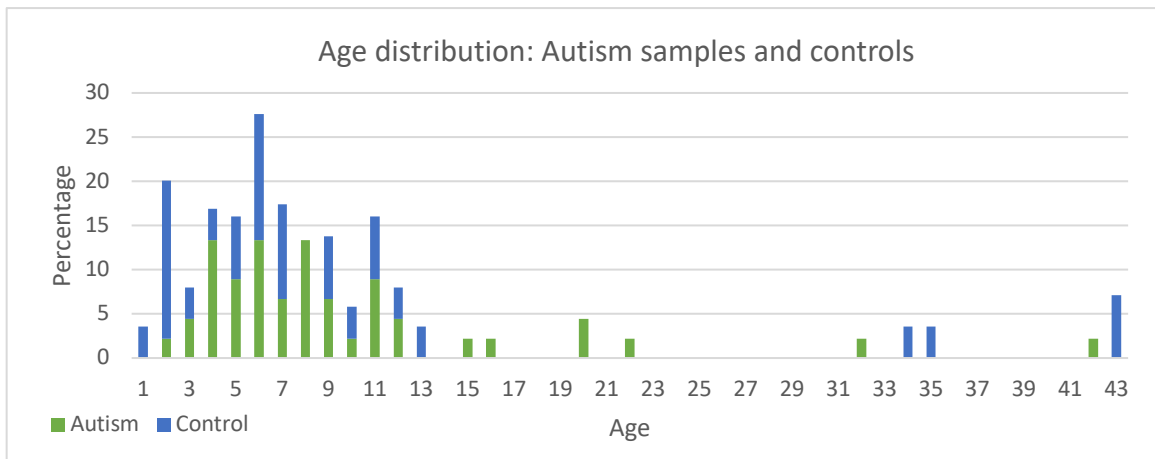


Figure 6: Age distribution for the autism and control cohort.

The figure shows the age distribution across the two cohorts with the autism samples (green) and controls (blue) in percent (own illustration).

2 Methods

2.1 Sample preparation

2.1.1 Purification

For this study the left-over swim-up sperm fraction of the semen donors were analyzed. Though all fluids from the seminal vesicles and prostate gland were already removed and though motile spermatozoa were concentrated by the swim-up method, for a sensitive methylation analysis it was still necessary to purify the samples from bacteria and any somatic contamination, such as Sertoli cells, epithelial cells and lymphocytes.

Hence, the gently thawed semen samples (starting from an initial temperature of -80°C to -20°C and consequently to 4°C for 15 min each and followed by an incubation at 37°C for 30 min) were purified using silane-coated silica density gradients PureSperm® (Nidacon). With each 1 ml of PureSperm®80 and PureSperm®40 the two-phase density gradient was created in 15 ml Nidacon glass tubes, on which a maximum amount of 0.5 ml of the semen sample was carefully pipetted without any interference of the gradient. Using a centrifuge without breaks (Heraeus multifuge) the glass tubes were centrifuged for 20 min at 300 x g at room temperature. After centrifugation, all upper layers were removed by careful aspiration in circular movements, except 4-6 mm PureSperm®80 with the remaining pellet that contained the purified sperm or in case no pellet was apparent the lowest 0.5 ml.

2.1.2 DNA Isolation and quantification

2.1.2.1 Sperm-DNA Isolation

DNA was extracted from the purified semen samples using the Qiagen DNeasy Blood and Tissue Kit. Therefore, the procedure was implemented following the User-developed protocol (2006), whereby each sperm sample was supplemented with 300 µl Buffer 2 (consisting of 2 ml 0.5 EDTA [pH = 8], 5ml 5 M NaCl, 5 ml 1 M Tris [pH = 8], 5 ml 10 % SDS [pH = 7.2], 1 ml 100 % β-mercaptoethanol and 33 ml dH₂O) in a 1.5 ml microcentrifuge tube. For lysing the spermatozoa, the samples were incubated in a slightly shaking thermomixer for two hours at 56°C after adding 100 µl of proteinase K. This incubation step was repeated by adding 20 µl of proteinase K after 2 hours. After incubation, the lysate was mixed thoroughly by vortexing with 400 µl each of Buffer AL and ethanol (96-100%) until yielding a homogenous solution. Step by step the entire amount of the solution was pipetted into the DNeasy Mini spin column placed into the provided 2 ml collection tube that was subsequently centrifuged at 13,300 x g for 1 min, while the flow-through was discarded. Two washing steps were carried out by placing the column into a new collection tube, adding 500 µl of Buffer AW1 and centrifuging at 13,300 x g for 1 min followed by 500 µl of Buffer AW2 and centrifuging at 20,000 x g for 3 min. The flow-through was discarded after each centrifugation step. As it is important to dry the membrane of the DNeasy Mini spin column, since residual ethanol would

interfere with subsequent reactions, another centrifugation step for 1 min at 20,000 x g was performed. After placing the DNeasy Mini spin column in a clean 1.5 ml tube, 100 µl Buffer AE was pipetted directly onto the DNeasy membrane. Followed by incubation at room temperature for 1 min, the solution was eluted by centrifuging at 13,300 x g for 1 min. By repeating the elution while using a new collection tube, two eluates with different DNA concentrations were obtained.

2.1.2.2 Fetal cord blood and peripheral blood leucocyte DNA Isolation

After quickly thawing the fetal cord blood and peripheral blood leucocyte samples in a shaking water bath of 37°C, the DNA was extracted using the FlexiGene Kit (Qiagen). The procedure was implemented according to manufacturer's instructions "Purification of DNA from clotted blood using the FlexiGene® DNA Kit" (2010). Briefly, 500 µl of fetal cord blood was mixed with 1250 µl of buffer FG1 in a 2ml tube by inverting the tube 5 times. Two centrifugation steps were carried out for 1 min at 10,000 x g, whereby the supernatant was discarded each time. Subsequently the tube was left inverted on a clean piece of absorbent paper for two minutes. During this time, a mix of 500 µl FG2 and 2.5 µl Qiagen Protease was prepared and 250 µl of the mixture was added to the dried pellet. Immediately the tube was vortexed until yielding a homogeneous solution, which was heated for 5 min at 65 °C. By mixing the solution with 250 µl isopropanol (100 %), the DNA precipitate became visible as a clump. After centrifuging for 3 min and discarding the supernatant, the pellet was vortexed for 5 s with 250 µl of ethanol (70 %). After removing the supernatant by centrifugation, the tube was inverted again on a clean piece of absorbent paper for 5 min. At this point the DNA should be visible as a small white pellet. For evaporating all the residual liquid, the pellet was air-dried for 5 to 10 min and subsequently dissolved in 200 µl buffer FG3. After incubation at 65°C for 1 h, the samples were left overnight at 37°C in a shaking incubator at low rpm levels.

2.1.2.3 DNA quantification

The DNA concentration was measured on the NanoDrop 2000c spectrophotometer.

2.1.3 Bisulfite conversion

Since the methylation patterns of genomic DNA are not transmitted during amplification by polymerase chain reaction (PCR), it is necessary to convert the DNA into a condition that preserves information about the methylation status. Bisulfite

treatment of the DNA is suitable for this purpose as it changes the DNA sequence in a manner, in which

unmethylated and methylated cytosine can be distinguished from each other. While 5-methylcytosine is not interacting with bisulfite, cytosine reacts with bisulfite and is converted to uracil by deamination (described in **Figure 7**). After a PCR-amplification, 5-methylcytosine appears in the sequence as cytosine whereas the unmethylated cytosine is amplified as thymine.

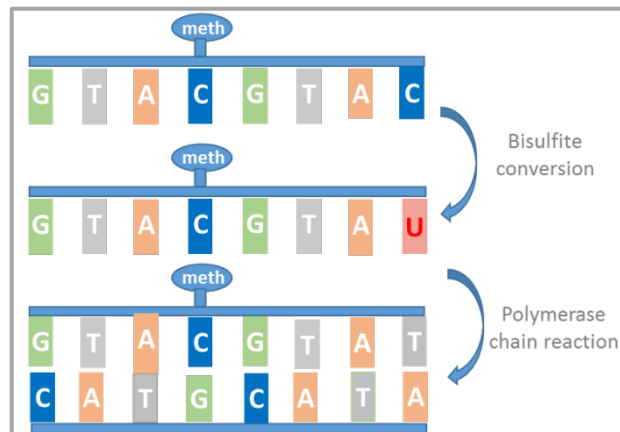


Figure 7: Bisulfite conversion

C = cytosine, T = thymine, A = adenosine, G = guanine, U = uracil, meth = methyl group -CH₃

For performing a bisulfite conversion, the EpiTect® Fast 96 DNA Bisulfite Kit was utilized that consists of a bisulfite reaction step and a clean-up step. Approximately 500 ng of sperm DNA and 1000 ng of leucocyte DNA from fetal cord blood were supplemented with 85 µl bisulfite solution and 15-35 µl DNA protect buffer depending on the concentration level of each DNA sample. The reaction mix (**Table 11**) was filled up to a total volume of 140 µl with RNase-free water. In a thermal cycler denaturation for 5 min at 95°C and incubation for 20 min at 60°C was performed twice each and converted DNA was stored at 20°C. Upon completion of the bisulfite treatment, the converted DNA was cleaned up using the provided EpiTect 96 plate. Each well was filled up with 300 µl buffer BL, the total volume of bisulfite reaction product and 250 µl ethanol (96-100%) and the reagent solution was mixed by pipetting up and down. Next, the EpiTect 96 Plate was centrifuged for 1 min at 5800 x g at room temperature after sealing with an AirPore Tape Sheet. One wash step with 500 µl buffer BW was followed by an incubation at room temperature with 250 µl buffer BD for 15 min. Two wash steps with each 500 µl buffer

BW and one wash step with 250 μ l ethanol (96-100%) were performed. Ultimately the EpiTect 96 plate was centrifuged for 15 min at 5800 x g to remove all residual ethanol. Using the provided EpiTect Elution Plate, each sample was eluted with 70 μ l buffer EB by centrifugation at 5800 x g for 1 min. All bisulfite converted and purified DNA samples were stored at -20°C.

Table 11: Pipetting scheme for bisulfite conversion

Component	Volume for 1 ng - 2 μ g DNA	Volume for 1 - 500 ng DNA
DNA	max. 20 μ l	max. 40 μ l
RNase-free water	filling up to a total volume of 140 μ l	filling up to a total volume of 140 μ l
Bisulfite Mix (dissolved)	85	85
DNA Protect Buffer	35	15
Total volume	140	140

According to each sample's DNA concentration, the pipetting scheme for the bisulfite conversion was modified. For samples with a low amount of DNA (1 ng – 2 μ g) 35 μ l of DNA Protect Buffer was added, while samples with a high amount of DNA (1 – 500 ng) just 15 μ l were added. Depending on the volume of each sample, the reaction mix was filled up with RNase-free water to a total volume of 140 μ l.

2.2 Pyrosequencing

2.2.1 Basic principles

Pyrosequencing is a fast and efficient technique to quantify DNA methylation, with a throughput of 96 samples per run. Using a previously defined sequence as template, the PyroMark 96 MD pyrosequencer can progressively detect incorporation of one of the four nucleotides in the form of deoxyribonucleotide triphosphate (dNTP) present in each sequencing-step (schematic overview in **Figure 8**). DNA polymerase catalyzes the complementary binding of each dNTP, which is followed by a release of pyrophosphate (PPi). As a secondary reaction, PPi is converted to ATP by a sulfurylase, using adenosine 5' phosphosulfate (APS) as substrate and consecutively this ATP converts luciferin to oxyluciferin via a luciferase. That last reaction leads to light emission that is detected by a charge coupled device (CCD) camera and a peak in the pyrogram is generated. Proportional to the intensity of the light signal and therefore to the number of incorporated nucleotides, the peak appears higher or lower in the pyrogram.

Unincorporated dNTPs are degraded by an apyrase as a last step. For characterizing DNA methylation, bisulfite conversion of the amplicon sequence is necessary as it offers a differentiation between methylated and unmethylated cytosines. After that treatment, methylated cytosines remain cytosines, unmethylated cytosines are converted to uracil that is amplified in a following polymerase chain reaction as thymine. Thus, pyrosequencing can distinguish methylated from unmethylated CpG sites and it generates an average methylation value for each analyzed CpG site.

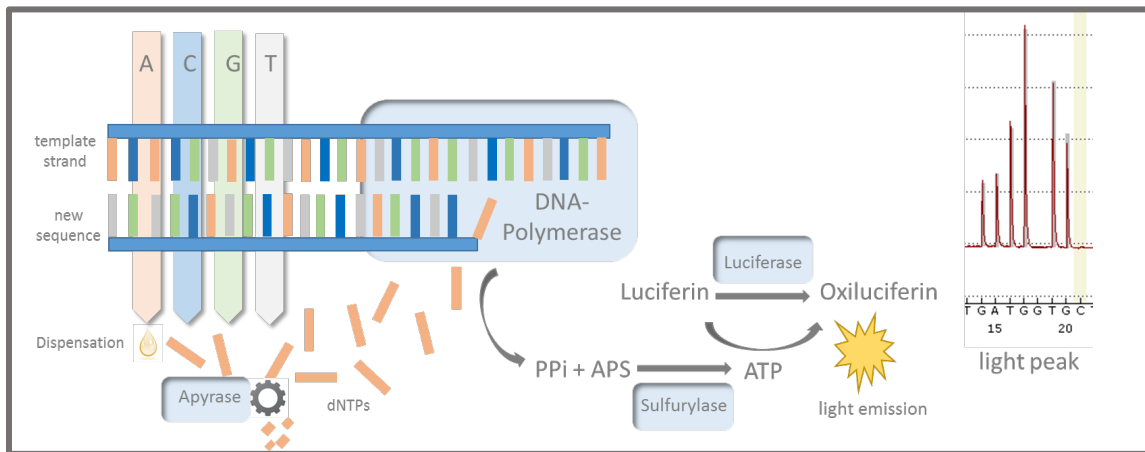


Figure 8: Pyrosequencing scheme

A = adenosine, C = cytosine, G = guanosin, T = thymine, dNTPs = deoxyribonucleotide triphosphate, PPI = pyrophosphate, APS = adenosine 5'phosphosulfate (own illustration).

2.2.2 Application fields

As pyrosequencing generates an average methylation value for the CpG islands in the analyzed region, it was utilized to have a general overview of the methylation status of a high number of samples. In this study, bisulfite pyrosequencing was performed to develop a correlation analysis of methylation status and paternal age both for sperm and fetal cord blood DNA. Since by pyrosequencing of fetal cord blood DNA both paternally and maternally inherited alleles are simultaneously analyzed and a mean methylation value is calculated, further sequencing techniques were necessary to specifically analyze the paternally inherited allele. For this reason, a pyrosequencing assay was designed where the sequencing primer contained a SNP at its 3' end. Two different sequencing primers were applied to ensure allele-specific sequencing.

Furthermore, another pyrosequencing assay was designed to genotype the analyzed samples. In combination with the SNP-specific pyrosequencing assay, it was possible to analyze maternally and paternally inherited allele separately, as heterozygous fetal cord blood samples with homozygous fathers were selected.

To check the change of the FOXP1 methylation status during ageing in patients with ASD and in an age- and sex-matching control cohort, the same pyrosequencing assay used for the sperm and fetal cord blood samples was applied.

Artificially methylated and unmethylated DNA standards (100%, 75%, 50%, 25% and 0% methylated standards) were considered for measuring the quantitative accuracy of all assays. The average methylation difference between technical replicates was approximately 1-2 %.

2.2.3 Sample amplification

For all analyzed samples – sperm, FCB and PBL – the region of interest was amplified by polymerase chain reaction (PCR). Therefore, a gradient-PCR was performed to determine the specific PCR conditions for each analyzed gene. Subsequently all reagents shown in **Table 12** were pipetted to the reaction mixture and PCR carried out according to the reaction steps (denaturation, annealing and elongation) shown in **Table 13**. For verifying a successful and specific amplification, gel electrophoresis was performed, whereby 4 µl of PCR product with 6 µl 1 x loading dye were applied on a 1.5 % agarose gel.

Table 12: Pipetting scheme for PCR sample amplification

Reagent	Volume for one reaction [µl]
10xPCR buffer with MgCl₂	2.5
dNTPs	0.5
10 µM forward primer	1.25
10 µM reverse primer	1.25
Fast start taq DNA polymerase	0.2
Template DNA	1.0
dH₂O	18.8
Total volume	25.0

The volume for one reaction is given.

Table 13: PCR program

Step	Temperature	Duration	
Heating	95°C	5 min	
Denaturation	95°C	30 sec	Repeating steps for 40 cycles
Annealing	see Table 14	30 sec	
Elongation	72°C	45 sec	
Final elongation	72°C	10 min	
Hold	8°C	∞	

The protocol for the PCR thermocycler consisted of the following steps heating – denaturation – annealing – elongation – final elongation – hold. For each gene region, a specific annealing temperature was identified by performing gradient-PCRs.

2.2.4 Pyrosequencing-assays

Table 14: Pyrosequencing assays

Gene	Number of assays	Number of analyzed CpGs	Amplicon length [bp]	Location	PCR annealing temperature [°C]
PDE4C	2	9	227	Chr 19: 18,220,390-18,220,617	60.0
GET4	2	6	188	Chr 7: 875,407-875,595	58.8
FOXK1	3	8	266	Chr 7: 4,683,841 - 4,684,107	58.8
DMPK	1	5	192	Chr 19: 45,771,835-45,772,027	60.0
TNXB	1	5	214	Chr 6: 32,097,126-32,097,340	60.0

For each gene a DNA amplicon was generated by PCR using a specific annealing temperature. Pyrosequencing assays were designed where 5-9 CpGs could be analyzed for each gene.

2.2.5 Sequencing

The pyrosequencing procedure consists of four general steps: Binding the biotinylated PCR-product on sepharose beads, washing and denaturation of unbiotinylated strands, annealing of the sequencing primer and ultimately sequencing via the PyroMark 96 MD pyrosequencer. For each sample, 70 µl of Master Mix 2 (pipetting scheme as shown in **Table 15**) was pipetted with 10 µl PCR-product into a non-skirted PCR-plate. The reagents were vortexed for 5 min to ensure binding of the biotin molecule at the 5' end of the PCR-primers with the sepharose beads. In the PyroMark Q96 vacuum workstation

bead-bound amplicons were captured via aspiration while residual fluids were absorbed. The amplicons were washed for 10 to 15 s in 70 % ethanol, followed by a denaturation step of 10 s, whereby unbiotinylated strands were removed. Next, the beads were cleaned for another 10 to 15 s in washing buffer. By releasing the vacuum, the washed beads were deposited into a PyroMark Q96 well plate, that contained the Master Mix 1 (pipetting scheme as shown in **Table 15**). For annealing the sequencing primers, the PyroMark Q96 well plate was kept for 2 min at 80°C followed by 2 min at room temperature. After these steps, sequencing was performed by the PyroMark 96 MD pyrosequencer, utilizing a previously calculated amount of nucleotide, enzyme and substrate mixes.

Table 15: Pipetting scheme for Pyrosequencing Master Mix 1 & 2

Master Mix 1	Volume for one reaction [μl]	Master Mix 2	Volume for one reaction [μl]
Annealing buffer	11.5	Binding buffer	40.0
Sequencing primer	0.5	dH ₂ O	28.0
		Sepharose beads	2.0
Total volume for each reaction	12.0	Total volume for each reaction	70.0

Volume shown is for one pyrosequencing reaction.

2.2.6 Data processing and analysis

The data was processed by the sequencing software Pyro Q CpG that generated a sequencing table, a pyrogram and a text file of each run. In the sequencing table (representative sequencing table in **Figure 9**) a rough quality estimation of each sample was illustrated through a color code. Thereby, a blue marked well displays a very good, a yellow marked well displays a good and a red marked well an insufficient sequencing quality. Red marked samples were excluded from further analysis. The mean methylation value of all analyzed CpG islands was listed as a percentage value for each sample. In the pyrogram (representative pyrogram in **Figure 10**) the dispensation order of the nucleotides, the peak height of each light emission of the luciferin reaction and the mean methylation value of each single CpG is displayed.

	1	2	3	4	5	6	7	8	9	10	11	12
A	hFOCK1 Pyr FCB 26 14%	hFOCK1 Pyr FCB 34 17%	hFOCK1 Pyr FCB 42 25%	hFOCK1 Pyr FCB 50 13%	hFOCK1 Pyr FCB 58 6%	hFOCK1 Pyr FCB 67 8%	hFOCK1 Pyr FCB 78 13%	hFOCK1 Pyr FCB 88 14%	hFOCK1 Pyr FCB 96 10%	hFOCK1 Pyr FCB 106 13%	hFOCK1 Pyr FCB 117 14%	hFOCK1 Pyr NN
B	hFOCK1 Pyr FCB 25 20%	hFOCK1 Pyr FCB 33 15%	hFOCK1 Pyr FCB 41 19%	hFOCK1 Pyr FCB 49 9%	hFOCK1 Pyr FCB 57 10%	hFOCK1 Pyr FCB 65 9%	hFOCK1 Pyr FCB 77 14%	hFOCK1 Pyr FCB 86 12%	hFOCK1 Pyr FCB 95 11%	hFOCK1 Pyr FCB 105 7%	hFOCK1 Pyr FCB 116 10%	hFOCK1 Pyr FCB 125 6%
C	hFOCK1 Pyr FCB 24 16%	hFOCK1 Pyr FCB 32 9%	hFOCK1 Pyr FCB 40 9%	hFOCK1 Pyr FCB 48 15%	hFOCK1 Pyr FCB 56 10%	hFOCK1 Pyr FCB 64 10%	hFOCK1 Pyr FCB 75 13%	hFOCK1 Pyr FCB 85 15%	hFOCK1 Pyr FCB 94 17%	hFOCK1 Pyr FCB 104 12%	hFOCK1 Pyr FCB 114 6%	hFOCK1 Pyr FCB 124 15%
D	hFOCK1 Pyr FCB 22 15%	hFOCK1 Pyr FCB 31 22%	hFOCK1 Pyr FCB 39 11%	hFOCK1 Pyr FCB 47 11%	hFOCK1 Pyr FCB 55 14%	hFOCK1 Pyr FCB 63 12%	hFOCK1 Pyr FCB 73 8%	hFOCK1 Pyr FCB 84 15%	hFOCK1 Pyr FCB 93 13%	hFOCK1 Pyr FCB 103 9%	hFOCK1 Pyr FCB 113 10%	hFOCK1 Pyr FCB 123 8%
E	hFOCK1 Pyr FCB 21 12%	hFOCK1 Pyr FCB 30 17%	hFOCK1 Pyr FCB 38 12%	hFOCK1 Pyr FCB 46 15%	hFOCK1 Pyr FCB 54 9%	hFOCK1 Pyr FCB 62 9%	hFOCK1 Pyr FCB 72 10%	hFOCK1 Pyr FCB 82 10%	hFOCK1 Pyr FCB 92 8%	hFOCK1 Pyr FCB 102 9%	hFOCK1 Pyr FCB 110 7%	hFOCK1 Pyr FCB 122 22%
F	hFOCK1 Pyr FCB 20 14%	hFOCK1 Pyr FCB 29 10%	hFOCK1 Pyr FCB 37 17%	hFOCK1 Pyr FCB 45 14%	hFOCK1 Pyr FCB 53 13%	hFOCK1 Pyr FCB 61 5%	hFOCK1 Pyr FCB 71 8%	hFOCK1 Pyr FCB 81 11%	hFOCK1 Pyr FCB 91 10%	hFOCK1 Pyr FCB 101 15%	hFOCK1 Pyr FCB 109 10%	hFOCK1 Pyr FCB 121 14%
G	hFOCK1 Pyr FCB 19 8%	hFOCK1 Pyr FCB 28 8%	hFOCK1 Pyr FCB 36 14%	hFOCK1 Pyr FCB 44 14%	hFOCK1 Pyr FCB 51/52? 10%	hFOCK1 Pyr FCB 59/60? 12%	hFOCK1 Pyr FCB 70 10%	hFOCK1 Pyr FCB 80 10%	hFOCK1 Pyr FCB 90 8%	hFOCK1 Pyr FCB 100 16%	hFOCK1 Pyr FCB 108 12%	hFOCK1 Pyr FCB 120 7%
H	hFOCK1 Pyr FCB 18 16%	hFOCK1 Pyr FCB 27 10%	hFOCK1 Pyr FCB 35 18%	hFOCK1 Pyr FCB 43 24%	hFOCK1 Pyr FCB 51/52 9%	hFOCK1 Pyr FCB 59/60 15%	hFOCK1 Pyr FCB 68 8%	hFOCK1 Pyr FCB 79 14%	hFOCK1 Pyr FCB 89 10%	hFOCK1 Pyr FCB 99 9%	hFOCK1 Pyr FCB 107 10%	hFOCK1 Pyr FCB 118 6%

Figure 9: sequencing table generated from the Pyro Q Cpg software

Each well contains information about the analyzed assay (hFOCK1), the analyzed sample (fetal cord blood sample FCB 18 – 125, NN = negative control) and the mean methylation value (percentage value). A color code indicates the sequencing quality (blue = very good, yellow = good, red = insufficient). Red marked samples (e.g. here FCB 54, FCB 101 and FCB 79) were excluded from further analysis

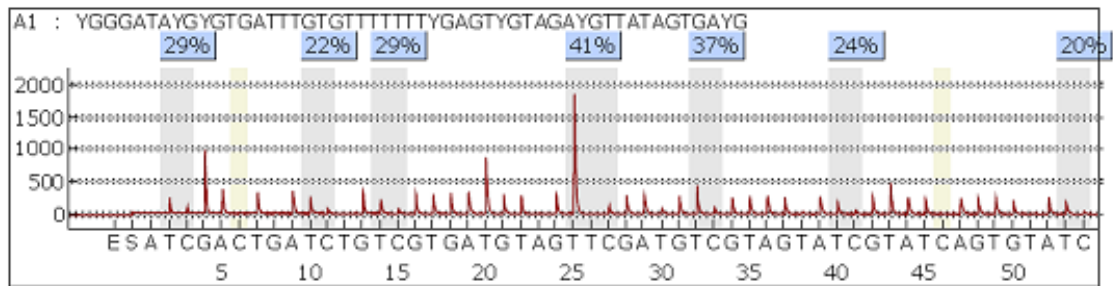


Figure 10: Representative pyrogram

The figure shows a pyrogram created by the sequencing software. The x-axis displays the dispensation order of the nucleotides and the y-axis the peak height of each light emission of the luciferin reaction.

The generated text file was utilized for further data processing in Microsoft Excel and SPSS, where the information about the analyzed CpGs was supplied to the clinical information known about each sample (additional information shown in **Figure 5**). A test of normality was carried out to check whether the data have a standard or a random variable distribution. Since all data sets were not normally distributed, a Spearman correlation analysis in terms of a two-tailed test for significance was performed, where all listed parameters were correlated to each other. For evaluating the analysis, the correlation coefficient and the p-value were considered.

2.3 Deep Bisulfite Sequencing

2.3.1 Basic principles

Deep bisulfite sequencing on the GS Junior System (Roche) is a next generation sequencing based technique suitable for accurate quantification of methylation levels of 29 samples per run. Compared to Pyrosequencing, it offers measurement at the single molecule level where each read represents one allele. Since 500 to 1,000 individual molecules can be analyzed per sample, DBS allows a high-resolution analysis of methylation-abnormalities affecting single alleles. By including a nearby informative SNP and analyzing heterozygous samples, an allele-specific methylation profile can be generated. The sequencing method consists of several steps. As a first step libraries of bisulfite treated DNA are prepared, where PCR is performed using gene-specific primers that include a specific barcode sequence to help sort samples after sequencing. In an

emulsion based PCR the previously generated amplicons are clonally amplified and sequenced via a sequence-by-synthesis technique.

2.3.2 Application fields

After pyrosequencing, regions showing a significant age correlation were chosen for further sequencing with the deep bisulfite method. The first DBS run was performed with sperm samples for a group comparison analysis between 13 samples of the youngest and 13 of the oldest fathers of the cohort. Besides, DBS allowed a data exploration at the single molecule level. Furthermore, for supporting the hypothesis that those detected regions were dominantly influenced by paternal age, DBS was also employed for studying fetal cord blood DNA methylation at the single allele level. Thus, an *in-silico* search of single nucleotide polymorphisms (SNPs) with a high heterozygosity-rate was performed. Next, heterozygous fetal cord blood samples with homozygous fathers were sequenced in the second DBS run. This allowed the separation of the parental alleles and the specific methylation analysis of the paternally inherited allele in cord blood DNA.

2.3.3 Library preparation

For adding all necessary adaptor- and barcode-sequences (illustration in **Figure 11**) to the region of interest, two successive PCRs were carried out. First, bisulfite treated DNA was amplified utilizing specific primers for the region of interest. Those primers were tagged with sequences A and B, that served as adaptors for the further procedure. In the second PCR, primers were utilized that contained the complementary adaptor-sequence, multiplex identifiers (MID) serving as sample-specific barcodes as well as A- and B-primers. All generated PCR-products were purified from secondary products, leftover nucleotides and primers via the Agencourt AMPure XP system (2013) according to the *Amplicon Library Preparation Method Manual* (May 2010 (Rev. April 2011)). Prior to pooling and diluting all samples, quality and quantity were checked using the Agilent Bioanalyzer and the NanoDrop 2000c spectrophotometer.

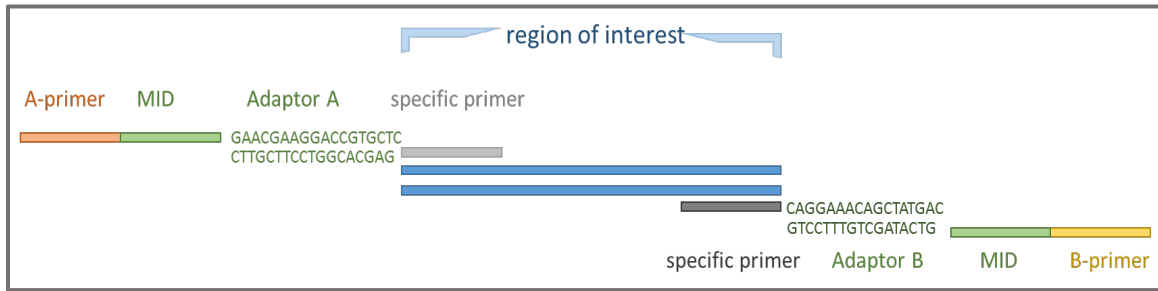


Figure 11: Amplicon library preparation

In a first-round PCR, the region of interest was amplified using specific primers tagged with the adaptor sequences A and B. In the second-round PCR, multiplex identifiers (MID), as well as A- and B-primers were bound to the adaptors serving as sample-specific barcodes (own illustration).

2.3.3.1 Sample Amplification

For both DBS runs, the first-round PCR was performed using a standard-protocol with 2.5 µl 10xPCR buffer, 0.5 µl dNTPs, 1 µl each of forward and reverse 10 µM primers, 0.2 µl Faststart Taq polymerase, 18.8 µl sterile water and 1 µl bisulfite-treated sample-DNA (pipetting scheme as shown in **Table 16**). Three methylation controls (100%, 50% and 0% artificially methylated standards) were included. The PCR cycling conditions consisted of a 5min initiation step at 95°C, 40 cycles of denaturation for 20 s at 95°C, annealing for 30 s at 60°C, as well as an elongation for 45 s at 72°C and a final elongation step for 5 min at 72°C. For verifying a successful and specific amplification (expected amplicon lengths shown in **Table 18**), gel electrophoresis was performed by running 4 µl of PCR product with 6 µl 1 x loading dye on a 1.5 % agarose gel.

Table 16: Pipetting scheme for the 1st round PCR

Reagent	Volume for one reaction [µl]
10xPCR buffer with MgCl₂	2.5
dNTPs	0.5
10 µM forward primer	1.0
10 µM reverse primer	1.0
Fast start taq DNA polymerase	0.2
Template DNA	1.0
dH₂O	18.8
Total volume	25.0

Volume is given for one sample each.

The second-round PCR was performed with 25 µl Hotstartaq polymerase Mastermix, 20 µl sterile water, 1 µl each of forward and reverse primers, as well as 3 µl DNA (pipetting scheme as shown in **Table 17**). Here, the PCR-product of the first round served as template. Primers carried the sample-specific multiplex identifiers (MID 1-30), Titanium 454 A and B primers and a key serving for light calibration during sequencing (primer sequences shown in **Table 9**). The PCR program consisted of a 15 min initiation step at 95°C in addition to 40 cycles of a denaturation step for 20 s at 95°C as well as a combined annealing and elongation step for 30 s at 72°C. A final elongation step for 7 min at 72°C was also included. For verifying a successful and specific amplification (expected amplicon lengths shown in **Table 18**), gel electrophoresis was performed, where 4 µl of PCR product with 6 µl 1 x loading dye were analysed on a 1.5 % agarose gel. The samples were stored before further processing at -20°C.

Table 17: Pipetting scheme for the 2nd round PCR

Reagent	Volume for one reaction [µl]
Hotstartaq Mastermix Kit	25.0
Forward primer	1.0
Reverse primer	1.0
Template DNA	3.0
dH2O	20.0
Total volume	50.0

Volume is given for one sample each

Table 18: Expected amplicon lengths for FOXK1

FOXK1	Sequence length [bp]	Forward primer [bp]	Reverse primer [bp]	Total expected amplicon length [bp]
1st round PCR	310	17	18	345
2nd round PCR	345	35	35	415

The expected amplicon lengths were calculated by considering all added sequences such as forward and reverse primer. In the second round PCR the primer sequences A and B included Adaptor sequences and multiplex identifiers

2.3.3.2 Library purification

For purifying the samples from remaining PCR reagents, such as leftover nucleotides and primers, the Agencourt AMPure XP system (2013) was utilized.

Therefore, 35 μl of AMPure XP bead suspension was mixed in 1.5 ml tubes by pipetting up and down with 40 μl of second-round PCR product. The mixture was incubated for 10 min at room temperature to allow amplicons longer than 150 bp to bind on the magnetic beads. By incubating the tubes for further 5 min in a magnetic particle collector (MPC), unbound free amplicons were separated from bound ones which were later removed with the supernatant. A washing step was performed twice by pipetting and removing 180 μl of freshly prepared ethanol (75%) was performed. Removing all residuals, the tubes were left opened for 10 min. Next, the air-dried pellets were eluted in a last elution step using 20 μl of buffer per sample. Thus, the tubes were incubated again for 2 min in the MPC and the pure and DNA-containing supernatant was carefully pipetted into fresh 1.5 ml tubes. The eluate was stored at -20°C until further processing.

2.3.3.3 Amplicon quantification and quality control

The verification of a successful and specific amplification on the Agilent BioAnalyzer 2100 is a more accurate method than gel electrophoresis. Therefore, a subset of samples and controls were loaded on a DNA 7500 LabChip following the *Agilent DNA 1000 Kit Guide (2013)*. 25 μl of DNA dye concentrate and DNA gel matrix were mixed by vortexing and centrifuged on a provided spin filter for 10 min at 1500 x g. Utilizing the provided chip priming station, a specially marked G-well of the DNA chip was loaded with 9 μl of the prepared gel dye mix. Afterwards pressure was applied by closing the priming station and waiting for 30 s. All other G-wells were loaded with 9 μl of the gel-dye mix, sample-wells (1-12) were filled up with 5 μl marker such as 1 μl of sample-DNA and 1 μl ladder was loaded on the ladder-well. After vortexing the chip horizontally for 1 min at 2400 rpm, the bioanalyzer run was started within 5 min and the measured data was analyzed with the Expert 2100 software. For FOXX1 the expected amplicon length after both amplifications was 415 bp (**Table 18**).

The DNA concentration of each sample was measured on the NanoDrop 2000c, where 400 ng per sample was needed for the sequencing and subsequently a second purification was performed.

2.3.3.4 Pooling and dilution

As the sequencing capacity of the GS Junior sequencer allows 29 samples per DBS run, the 58 samples were sequenced in two separate DBS runs. For each run, samples were combined and diluted twice to achieve the desired concentration of molecules/ μl (Figure 12).

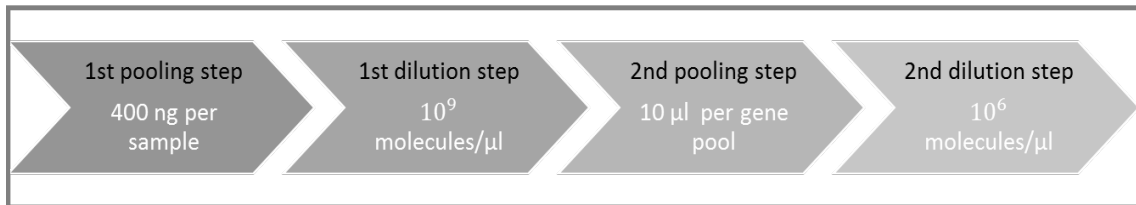


Figure 12: Pooling and dilution of the DBS samples

By two pooling and two dilution steps the DBS samples were prepared for the sequencing (own illustration).

In the first step, all 29 amplified and purified samples from one DBS-assay were pooled equimolar amounts (400 ng each). The required volume was calculated using the concentration values generated by the NanoDrop 2000c spectrophotometer. Subsequently, the two generated pools were again purified using the Agencourt AMPure XP system and quantified twice using the NanoDrop 2000c spectrophotometer. For *FOXK1*, the median was calculated as 175.7 ng/ μl for the sperm pool and 110.9 ng/ μl for the fetal cord blood pool. The measured concentration was utilized to calculate each pool's concentration in the unit [molecules/ μl] (1). In a first dilution step, the pools were diluted to a concentration of 10^9 molecules/ μl by adding a calculated amount of 1x TE buffer (2). Subsequently the second pooling step was performed by combining the same amount of each gene pool and then the single gene pool was diluted with sterile H_2O to 10^6 molecules/ μl . For the sequencing procedure, a ratio of 2-3 molecules per capture bead was desired. The needed volume of the diluted DNA library was calculated as shown in (3).

$$(1) \quad \text{molecules}/\mu\text{l} = \frac{\text{measured concentration} \left[\frac{\text{ng}}{\mu\text{l}} \right] \times 6,022 \times 10^{23}}{656,6 \times 10^9 \times \text{amplicon length [bp]}}$$

$$(2) \quad \frac{\text{molecules}/\mu\text{l}}{10^9} - 1 [\mu\text{l}]$$

$$(3) \quad \mu\text{l of DNA library} = \frac{\text{desired molecules per bead} \times 5 \times 10^6 \text{ beads}}{\text{library concentration} \left[\frac{\text{molecules}}{\mu\text{l}} \right]} \times 1.5$$

2.3.4 Deep bisulfite sequencing assay

The deep bisulfite sequencing assay for *FOXK1* included 5 CpGs and one SNP A/G (rs9791644). By genotyping the fetal cord blood samples, this SNP was useful to distinguish the paternal allele from the maternal allele. The heterozygosity rate for this SNP is 26.4 % in Europeans, while 71.2 % of the samples are homozygous for G and 2.4 % of the samples are homozygous for A (cf. **Figure 13**)

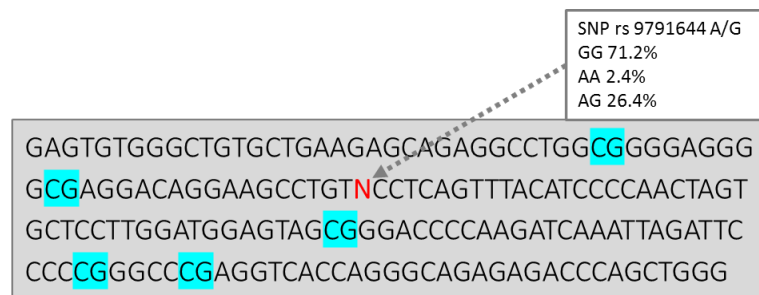


Figure 13: Deep bisulfite sequencing assay for FOXK1
CpG sites marked in blue, SNP (N) marked in red (own illustration).

2.3.5 Emulsion based PCR amplification

To clonally amplify DNA molecules, a single molecule was attached to DNA capture beads in a one-to-one ratio and each capture bead was amplified in one oil droplet of a water-in-oil emulsion. The binding of each amplicon to the DNA capture beads was enabled by the Titanium 454 primers A and B, that were previously added in the second-round PCR. This emulsion based clonal amplification was performed as described in the provided protocol *emPCR Amplification Method Manual (May 2010 (Rev. April 2011))* and consists of seven general steps. First, the reagents such as the emulsion oil and the amplification mixes were prepared (step 1). Subsequently the DNA library was attached to capture beads where the necessary amount of DNA library for an optimal amplicon-to-bead ratio was calculated as shown in 2.3.3.4. (step 2). In the provided Ultra Turrax Tube Drive (UTTD), an emulsion was generated as the reagents were mixed in a stirring tube (step 3). Using a Combitip, the emulsion was dispensed into a 96 well plate and the amplification reaction was carried out by a thermocycler (4 min at 94°C, followed by 50

cycles of 30 s at 94°C, 4.5 min at 58°C and 30 s at 68°C and hold at 10°C) (step 4). Subsequently the emulsion was collected by a vacuum-assisted set-up and the water-in-oil emulsion was retracted by several wash steps in isopropanol and ethanol to recover the beads (step 5). To separate the DNA-carrying beads of a successful amplification from unbound beads of an unsuccessful emPCR, enrichment primers were annealed to the amplicons that allow them to bind to complementary sequences of magnetic enrichment beads. A magnetic particle collector enabled the collection of enriched beads and hence the removal of all beads without any amplification product (step 6). The last step served for the annealing of the sequencing primers A and B (step 7). One run with the GS Junior necessitates an intake of 500,000 enrichment beads. This amount was estimated via the provided GS Junior Bead Counter, by measuring the bead pellet's size. The prepared beads could be stored at + 4°C for approximately two weeks before further processing.

2.3.6 Sequencing

As described in the provided *Sequencing method manual (May 2010 (Rev. June 2010))* the GS Junior Titanium Sequencing Kit and the GS Junior Titanium Pico Titer Plate (PTP) Kit were utilized for sequencing on the GS Junior. This procedure consists of four general steps: washing the instrument's fluidics with pre-wash buffer, preparation of the PTP by loading the bead and enzyme layers, priming the instrument with buffers and reagents and finally sequencing of the generated library. While the instrument performed two pre-wash steps with the kit's pre-wash buffer, the DNA beads were combined with packing beads and several wash steps were carried out. Thus, the PTP was set onto a bead deposition device (BDD) whose lid exerted pressure onto the PTP to generate a liquid-tight seal. Accessible through a loading hole, four different layers were created by centrifugation: an enzyme beads pre-layer, a layer containing the DNA and packing beads, an enzyme beads post-layer and a PPIase bead layer. Each kind of microparticles had to be prepared. The loaded PTP was set into the GS Junior instrument and the sequencing run was performed with 200 cycles sufficient for sequencing approximately 500 bases.

2.3.7 Data processing and analysis

The GS Junior software generated standard flowgram format files (.sff) and the data was analyzed by the Amplifyzer software. Bisulfite filter settings were applied after the run with the sperm samples. This setting has a less stringent filter for discarding reads thus it helped us increase the number of reads for further analysis. The Amplifyzer program allowed a low-quality rate of 20 % CpGs (1 out of 5 CpGs for *FOXP1*). For the run with the fetal cord blood samples there were no filter settings applied, as the determination of the informative SNP required an accurate sequence and high amplicon quality between each analyzed CpG. Here, 20 % of CpGs with a low sequencing quality were allowed for further analysis. For identifying the respective sample in the analysis, the MID sequences, universal tag sequences and genomic sequences of the amplicons were taken into consideration. A generated excel file for each sample served as basis for the further statistical analysis in SPSS. Furthermore, for each sample a diagram indicated methylated CpGs with a red line and unmethylated CpGs with a blue line. Those CpGs with a low sequencing quality were marked with a grey line (representative diagram in **Figure 14**). **Table 19** records the number of generated reads and the average read-count per MID for the GS Junior deep bisulfite sequencing runs with sperm and fetal cord blood samples. As mentioned above, the application of bisulfite filter settings results in a higher number of generated reads in the run with the sperm samples (34,351 reads) compared to the run with the fetal cord blood samples (13,441 reads), where no bisulfite filter was applied.

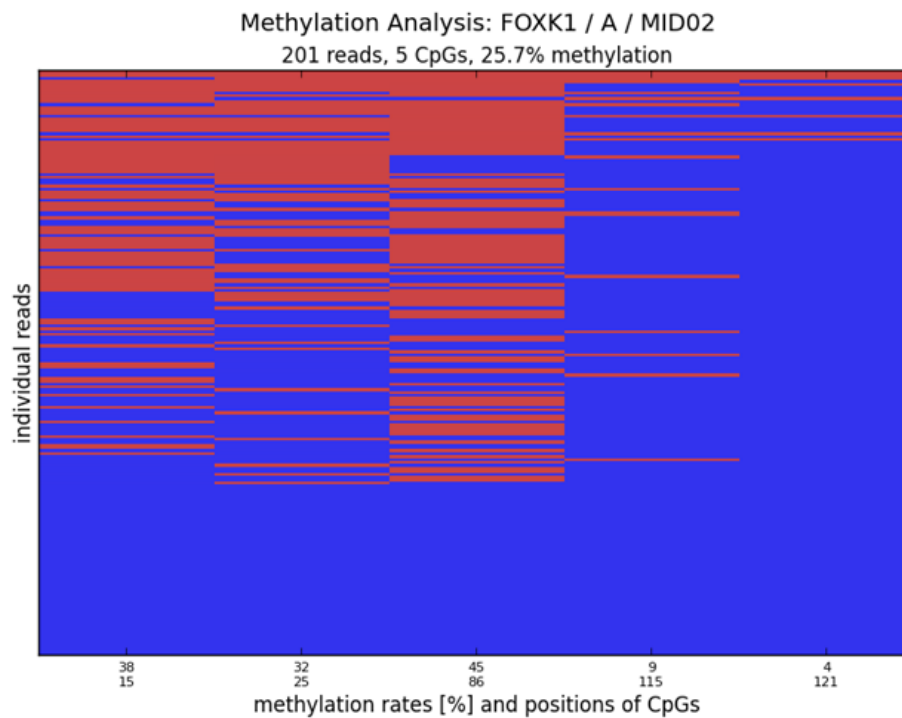


Figure 14: Representative diagram generated by the Amplifyzer software
This diagram displays the methylation status for the A allele of the fetal cord blood sample with MID02. CpG methylation (horizontal axis) is delineated for every single read (vertical axis) in different colors. Red = methylated, blue = unmethylated, grey = low sequencing quality

Table 19: Number of generated reads and average read count per MID for both runs

Run	Number of generated reads	Average read count per MID
Sperm	34,351	1,272.3
Fetal cord blood	13,441	268.8

For both runs the number of generated reads and the average read count per MID was recorded.

III. RESULTS

1 Age-associated methylation analysis in fathers and their resulting offspring

For investigating the link between advanced paternal age and changes in the epigenome, five genes (*DMPK*, *GET4*, *FOXK1*, *TNXB* and *PDE4C*) were studied by pyrosequencing in the main sperm cohort of 165 donors (undergoing ICSI/IVF). Two genes (*FOXK1* and *DMPK*) exhibited age-associated methylation changes in sperm and were therefore studied in the resulting offspring's fetal cord blood. As *FOXK1* displayed age-associated methylation changes in cord blood, it was further confirmed in an independent sperm cohort and additionally analyzed in a subset of 26 sperm samples by deep bisulfite sequencing.

1.1 Age-associated methylation analysis in sperm-DNA

By pyrosequencing, five genes (*DMPK*, *FOXK1*, *GET4*, *TNXB*, and *PDE4C*) were studied in the main sperm cohort of 165 samples. The measured methylation values were correlated to the father's clinical information (e.g. weight, height, hormonal status; cf. **Figure 5**) to exclude any confounding factors (**Table 21**). Paternal age showed a significant correlation to maternal age and to the levels of the hormones TSH, testosterone and prolactin. Furthermore, a correlation analysis of paternal age versus measured methylation in the sperm samples is shown in **Table 20**. *FOXK1* was additionally confirmed in an independent sperm cohort by pyrosequencing and in a subset of 26 sperm samples by deep bisulfite sequencing (**Table 22**).

1.1.1 Pyrosequencing results for DMPK, FOXK1, GET4, PDE4C and TNXB in the sperm cohort 1

The correlation analysis (**Table 20**) showed age-associated methylation changes in the analyzed regions of *FOXK1* and *DMPK*. Both regions displayed a significant decrease of methylation with advanced paternal age with a correlation coefficient of -0.219 ($p = 0.009$) for *DMPK* and of -0.377 ($p = 0.000$) for *FOXK1*. *GET4* and *TNXB* showed only a few significant CpGs whereas in *PDE4C* there was no significant correlation detected. The number of analyzed samples varies for each gene, since samples with an insufficient pyrosequencing quality were excluded from further analysis.

Gene	Number of analyzed CpGs	Number of analyzed samples	Correlation coeff.		CpG1	CpG2	CpG3	CpG4	CpG5	CpG6	CpG7	CpG8	CpG9	Mean methylation
DMPK	5	142	Correlation coeff.	p-value	-0.231 **	-0.166 *	-0.165 *	-0.239 **	-0.206 *	-	-	-	-	-0.219 **
					0.006	0.049	0.050	0.004	0.014	-	-	-	0.009	
FO XK1	8	122	Correlation coeff.	p-value	-0.398 **	-0.379 **	-0.288 **	-0.266 **	-0.314 **	-0.283 **	-0.301 **	-0.252 **	-	-0.377 **
					0.000	0.000	0.001	0.003	0.000	0.002	0.000	0.003	-	0.000
GET4	6	127	Correlation coeff.	p-value	-0.077	-0.139	-0.132	-0.126	-0.178 *	-0.775	-	-	-	-0.119
					0.395	0.122	0.143	0.157	0.045	0.225	-	-	-	0.181
TNXB	5	117	Correlation coeff.	p-value	-0.185 *	-0.196 *	-0.070	-0.112	-0.125	-	-	-	-	-0.128
					0.046	0.034	0.456	0.230	0.181	-	-	-	-	0.171
PDE4C	9	131	Correlation coeff.	p-value	-0.069	0.034	-0.068	0.065	0.011	-0.125	-0.117	-0.086	-0.037	-0.068
					0.410	0.658	0.419	0.443	0.895	0.140	0.166	0.327	0.674	0.442

Table 20: Correlation analysis paternal age vs. sperm methylation for DMPK, GET4, FOXK1, PDE4C and TNXB in the main sperm cohort

*In the main sperm cohort all genes were studied. A Spearman correlation analysis in terms of a two-tailed test for significance was performed. This table shows the correlation coefficients and the p-values for the analysis paternal age vs. methylation for all analyzed CpGs and for the mean methylation. Values labeled with * and yellow are significant on a level of $p < 0.05$ and values labeled with ** and green are significant on a level of $p < 0.01$. The number of analyzed samples varies for each gene, since samples with an insufficient pyrosequencing quality were excluded from further analysis.*

Table 21: Correlation between paternal age and possible confounding factors

Paternal age	Correlation coeff.		p-value	birth weight	length	head length	age mother	sperm concentration	morphology	total motility	weight father	height father	BMI father	TSH	testosterone	prolactin	FSH
	0.023	0.035	0.001	0.563**	-0.099	0.078	0.044	0.084	-0.026	0.040	-0.224**	-0.184*	-0.170*	0.011			
	0.762	0.644	0.993	0.000	0.236	0.326	0.583	0.482	0.830	0.736	0.002	0.013	0.022	0.879			

1.1.2 Pyrosequencing results for FO XK1 in the sperm cohort 2

Due to the strong effect that FO XK1 showed in the main sperm cohort, the results were replicated in the independent cohort (**Table 22**). On this behalf, the previously detected hypomethylation with advanced paternal age was significantly confirmed with a correlation coefficient of -0.261 ($p=0.000$)

Table 22: Correlation analysis paternal age vs. sperm methylation for FO XK1 in the independent cohort

Gene	No. of analyzed CpGs	No. of analyzed samples		CpG1	CpG2	CpG3	CpG4	CpG5	CpG6	Mean methylation
FO XK1	6	176	coeff.	-0.277**	-0.299**	-0.307**	-0.164*	-0.181*	-0.256**	-0.261**
			p-value	0.000	0.000	0.000	0.032	0.018	0.001	0.000

*Values that are significant on a level of $p < 0.05$ are labeled with * and yellow and values that are significant on a level of $p < 0.01$ labeled with ** and green.*

1.1.3 Deep bisulfite sequencing results for FO XK1 in sperm-DNA

In a subset of 26 sperm samples, 13 young and 13 old fathers were chosen for a group comparison analysis (samples listed in **Table 10**). Here, the measured methylation values were correlated to paternal age (cf. 1.1.3.1), a group comparison (cf. 1.1.3.2) and a methylation analysis on the single read level were executed (cf. 1.1.3.3).

1.1.3.1 Correlation analysis methylation versus paternal age

The correlation analysis (**Table 23**) showed age-associated methylation changes in the analyzed regions of FO XK1. The region displayed a significant hypomethylation with advanced paternal age in all analyzed CpGs. The mean methylation versus paternal age was significant with a correlation coefficient of -0.630 ($p = 0.001$).

Table 23: GS Junior results: Correlation analysis methylation vs. paternal age for the sperm samples

Gene	No. of analyzed CpGs	No. of analyzed samples		CpG1	CpG2	CpG3	CpG4	CpG5	Mean methylation
FOXX1	5	26	coeff.	-0.648**	-0.673**	-0.655**	-0.650**	-0.623**	-0.630**
			p-value	0.000	0.000	0.000	0.000	0.001	0.001

*In all 5 analyzed CpGs the region was significantly hypomethylated with advanced paternal age. Values that are significant on a level of $p < 0.05$ are labeled with * and yellow and values that are significant on a level of $p < 0.01$ labeled with ** and green.*

1.1.3.2 Group comparison young versus aged group

In the group comparison, the analyzed region showed a mean methylation value of 60.48 % in the sperm samples of the young group, while the aged group was significantly hypomethylated with a mean methylation value of 23.62 % (**Table 24**). This results in a group difference of 36.85 % when comparing sperm of young and old males. Within each group, sperm DNA methylation showed small variation (**Figure 15**).

Table 24: GS Junior results: Group comparison young vs. aged group for methylation

Group	Mean methylation value [%]	Group difference in methylation [%]
Young	60.48	36.85
Old	23.62	

The table shows the mean methylation value of sperm from 13 young and 13 aged fathers. The group methylation difference is listed in %.

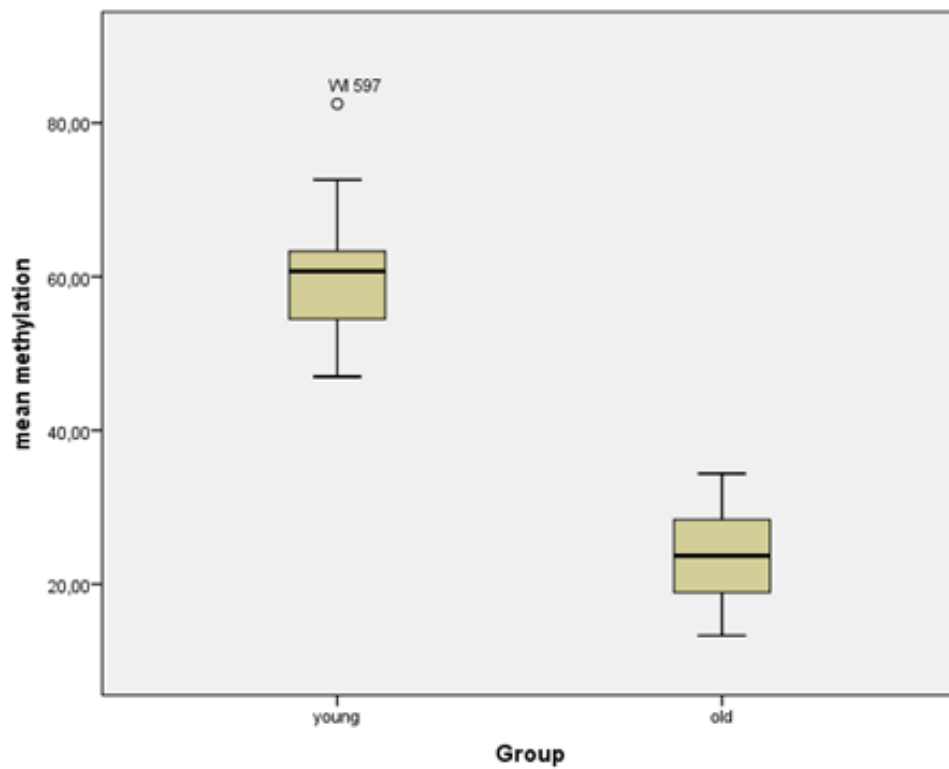


Figure 15: GS Junior results: Boxplot for group comparison young vs. aged group for sperm methylation

The boxplot displays a small range for the methylation values within each group. Young samples' displayed sperm methylation values around 60.48 %, while aged samples' had methylation values around 23.62 % (own illustration).

1.1.3.3 Methylation analysis at the single read level

For both groups, the number of fully unmethylated, 20 % methylated (1 out of 5 CpGs is methylated), 40 % methylated (2 out of 5 CpGs are methylated), 60 % methylated (3 out of 5 CpGs are methylated), 80 % methylated (4 out of 5 CpGs are methylated) and fully methylated reads were counted and the data of both groups was compared to each other. Here, the number of fully unmethylated sperm alleles increases significantly with advanced age. For the aged group 36.26 % of all generated reads were fully unmethylated, while for the young group just 4.64 % of all generated reads were fully unmethylated.

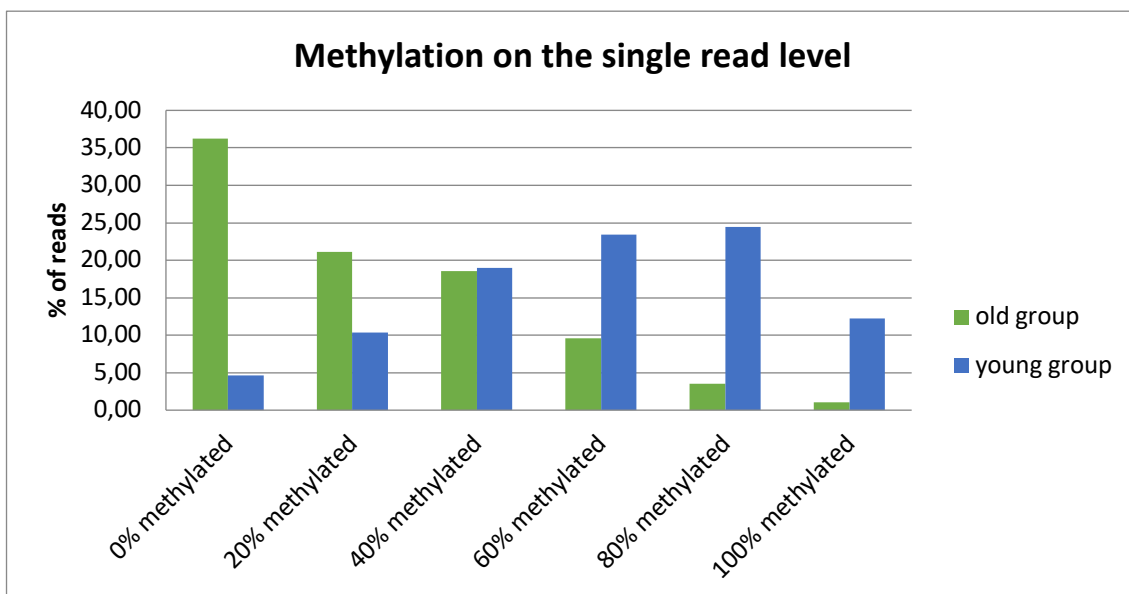


Figure 16: Sperm methylation on the single read level

For both groups, the number of fully unmethylated, 20 % methylated (1 out of 5 CpGs is methylated), 40 % methylated (2 out of 5 CpGs are methylated), 60 % methylated (3 out of 5 CpGs are methylated), 80 % methylated (4 out of 5 CpGs are methylated) and fully methylated reads were counted and the data of both groups was compared to each other. Green indicates the old group whereas blue indicates the young group.

1.2 Paternal age effect on methylation in the offspring

Since the analyzed regions in the *FOXK1* and *DMPK* genes showed a significant methylation change with advanced paternal age, the same pyrosequencing assay was performed in the fetal cord blood cohort to check whether those methylation alterations are transmitted to the offspring. The sperm and cord blood samples originated from

fathers and their respective children. The sperm used for the ICSI/IVF procedure leading to a live birth were analyzed in this thesis. On this account, the measured methylation values of all analyzed CpGs in the offspring's blood were correlated to each father's age (**Table 25**). Additionally, all relevant clinical information about fathers and offspring (e.g. birth weight, length, head circumference; cf. **Figure 5**) was correlated to the measured methylation values to exclude any confounding factors. In the *FOXK1* gene, there was a significant correlation coefficient of -0.199** ($p=0.009$) with paternal age, while there was no significance detected for *DMPK*.

Table 25: Correlation analysis fetal cord blood methylation vs. paternal age

Gene	No. of analyzed CpGs	No. of analyzed		CpG1	CpG2	CpG3	CpG4	CpG5	CpG6	CpG7	CpG8	Mean methylation
FOXK1	8	170	coeff.	-0.170*	-0.166*	-0.207*	-0.208**	-0.271**	-0.164*	-0.170*	-0.228**	-0.199**
			p-value	0.027	0.031	0.022	0.007	0.000	0.033	0.030	0.003	0.009
DMPK	5	173	coeff.	-0.133	-0.076	-0.091	-0.040	-0.052	-	-	-	-0.073
			p-value	0.082	0.323	0.235	0.603	0.494	-	-	-	0.341

Values that are significant on a level of $p < 0.05$ are labeled with * and yellow and values that are significant on a level of $p < 0.01$ labeled with ** and green.

2 Allele specific methylation analysis in the offspring

Since somatic cells carry two genome copies i.e. one paternal and one maternal allele, it was important to focus exclusively on the paternally inherited allele. As pyrosequencing generates a mean methylation value of both alleles, the objective was to measure allele-specific methylation analysis. For that reason, it was necessary to genotype fetal cord blood samples in order to separate maternally and paternally inherited alleles. Subsequently both alleles were separately analyzed via deep bisulfite sequencing and by an allele-specific pyrosequencing assay in a subset of 23 heterozygous cord blood samples.

2.1 Genotyping fetal cord blood samples by pyrosequencing

2.1.1 Analyzed region

An *in-silico* search of SNPs with a high heterozygosity-rate was performed and a methylation assay was designed to genotype the SNP and measure the methylation of additional CpGs. By means of the peak-height in the pyrogram, it was possible to determine whether adenosine or guanine was incorporated for each sample (representative pyrograms for each genotype in **Figure 17**).

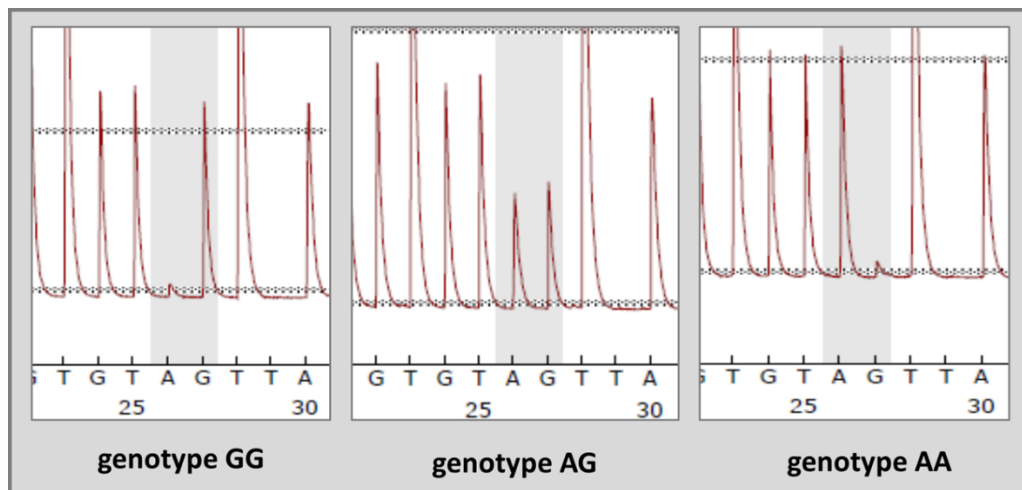


Figure 17: Representative pyrograms for the genotypes GG, AG and AA
(own illustration)

2.1.2 Genotypes for sperm and fetal cord blood samples

Thus, the genotypes of all sperm and fetal cord blood samples were determined. 133 fetal cord blood and 101 sperm samples were homozygous for G, 48 fetal cord blood and 40 sperm samples were heterozygous and 1 fetal cord blood and 6 sperm samples were homozygous for A (**Table 26**). Samples with an insufficient sequencing quality were excluded. The results correspond largely to the available allele frequency information in the European population (www.ensembl.org AA 2.4%, AG 26.4%, GG 71.2%). For the allele-specific analysis, heterozygous fetal cord blood samples with homozygous fathers were chosen. 26 of the fetal cord blood samples complied with those conditions (**Table 27**).

Table 26: Genotyping Results

Genotype	AA	AG	GG
No. of FCB samples	1 (0.55 %)	48 (26.37 %)	133 (73.08 %)
No. of sperm samples	6 (4.08 %)	40 (27.21 %)	101 (68.70 %)

The results correspond largely to the information about the allele frequency in the genome database www.ensembl.org (AA 2.4 %, AG 26.4 %, GG 71.2 %)

Table 27: List of heterozygous fetal cord blood samples with homozygous fathers

Fetal cord blood sample number	genotype	Sperm sample number of the father	genotype	Age of the father
FCB 25	heterozygous AG	sperm 048	homozygous GG	32
FCB 26	heterozygous AG	sperm 048	homozygous GG	32
FCB 47	heterozygous AG	sperm 153	homozygous GG	33
FCB 61	heterozygous AG	sperm 159	homozygous AA	36
FCB 70	heterozygous AG	sperm 256	homozygous GG	31
FCB 85	heterozygous AG	sperm 373	homozygous GG	36
FCB 86	heterozygous AG	sperm 373	homozygous GG	36
FCB 89	heterozygous AG	sperm 342	homozygous GG	33
FCB 90	heterozygous AG	sperm 353	homozygous GG	43
FCB 91	heterozygous AG	sperm 353	homozygous GG	43
FCB 105	heterozygous AG	sperm 092	homozygous AA	39
FCB 114	heterozygous AG	sperm 371	homozygot AA	38
FCB 120	heterozygous AG	sperm 086	homozygous GG	41
FCB 131	heterozygous AG	sperm 511	homozygous GG	35
FCB 139	heterozygous AG	sperm 293	homozygous GG	37
FCB 155	heterozygous AG	sperm 363	homozygous GG	30
FCB 167	heterozygous AG	sperm 671	homozygous GG	48
FCB 178	heterozygous AG	sperm 736	homozygous AA	35
FCB 184	heterozygous AG	sperm 233	homozygous GG	38
FCB 206	heterozygous AG	sperm 926	homozygous GG	47
FCB 209	heterozygous AG	sperm 449	homozygous GG	35
FCB 210	heterozygous AG	sperm 962	homozygous GG	40
FCB 223	heterozygous AG	sperm 893	homozygous AA	40

For the allele-specific analysis, heterozygous fetal cord blood samples with homozygous fathers were chosen. 26 of the fetal cord blood samples complied with those conditions.

2.2 Allele-specific deep bisulfite sequencing results in fetal cord blood

For the 26 determined heterozygous cord blood samples, the region downstream the SNP rs9791644 (*FOXK1*) was sequenced and reads containing the paternally inherited allele were separately analyzed from those reads containing the maternal allele. Across the 26 samples, the methylation of the paternal allele displayed a strong correlation with paternal age with a correlation coefficient of -0.529 ($p=0.005$), while the methylation of the maternal allele only showed significant correlation with the maternal age in 2 single CpGs (**Table 28**). On the single read level, most of the reads showed no methylation or 20 % methylation and just few reads had higher methylation values.

Table 28: GS Junior Results: Allele comparison in fetal cord blood

Correlation analysis	No. of analyzed samples		CpG1	CpG2	CpG3	CpG4	CpG5	Mean methylation
Paternal allele vs. father's age	26	coeff.	-0.345	-0.438*	-0.446*	-0.619**	-0.408*	-0.529**
		p-value	0.085	0.025	0.022	0.001	0.038	0.005
Maternal allele vs. mother's age	26	coeff.	-0.410*	-0.200	-0.189	-0.268	-0.506**	-0.383
		p-value	0.042	0.339	0.336	0.195	0.010	0.059

*For allele comparison in fetal cord blood, paternally and maternally inherited alleles were separately analyzed. Two correlation analyses (paternal allele versus father's age and maternal allele versus mother's age) were executed. Values that are significant on a level of $p < 0.05$ are labeled with * and yellow and values that are significant on a level of $p < 0.01$ labeled with ** and green.*

2.3 Allele-specific pyrosequencing results in fetal cord blood

Next, the observed association of methylation at the paternally inherited allele with advanced paternal age was confirmed via allele-specific pyrosequencing. Therefore, two different sequencing primers specific for either A or G of the informative SNP were designed. This assay measured methylation of the two CpG sites (CpG4 and CpG5). Here, methylation at the studied CpGs of the paternally inherited allele showed a significant association to father's age with a correlation coefficient of -0.442 ($p = 0.039$). The maternally inherited allele showed no age-associated methylation alteration (**Table 29**).

Table 29: Allele specific pyrosequencing results

Correlation analysis	No. of analyzed samples		CpG4	CpG5	Mean methylation
Paternal allele vs. father's age	26	coeff.	-0.549**	-0.301*	-0.442**
		p-value	0.008	0.174	0.039
Maternal allele vs. mother's age	26	coeff.	-0.228	-0.175	-0.198
		p-value	0.307	0.436	0.378

*In an allele-specific pyrosequencing assay, the age-associated methylation alteration was confirmed for CpG4 and the mean methylation value for the paternal allele. Values that are significant on a level of $p < 0.05$ are labeled with * and yellow and values that are significant on a level of $p < 0.01$ labeled with ** and green*

3 FO XK1 and Autism Spectrum Disorders

In a previously published study, copy number variations (CNV) were found in the region of FO XK1 in 2 of 23 patients with autism spectrum disorders (ASD) (Stobbe et al. 2014). For that reason, FO XK1 methylation was measured in an ASD cohort. The ASD cohort consisted of peripheral blood leukocyte (PBL) samples of 45 children and young adults with ASD (2 – 43 years old) and 27 age and sex-matched controls (2–42 years old). Though the two groups did not differ in FO XK1 average methylation ($p = 0.137$), nevertheless a significant age-associated methylation was measured for FO XK1 ($p = 6.98e-05$). For that reason, an analysis using an age-status model was applied. This test displayed an accelerated methylation decrease for the patients with ASD during ageing ($p = 0.0152$) (**Figure 18**).

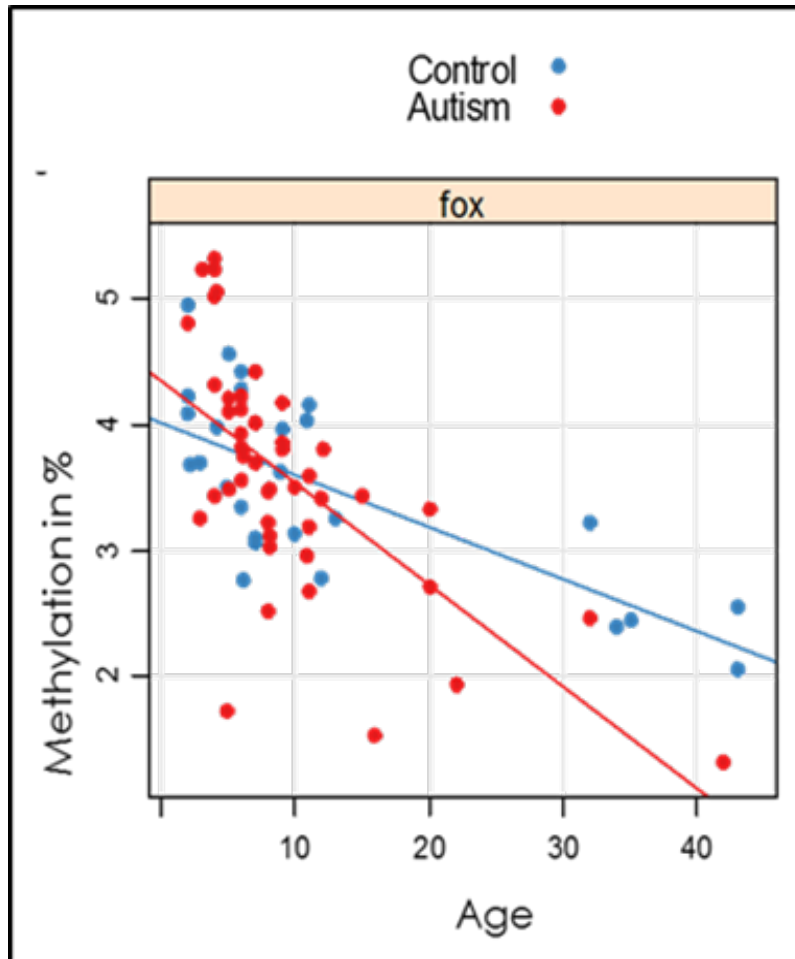


Figure 18: FOXP1 and autism - correlation analysis of age vs. methylation for ASD patients and controls

In the correlation analysis of age versus methylation both groups – ASD patients (red) and controls (blue) – show a significant methylation decrease with age. In the ASD cohort methylation change is faster than in the control group.

(Figure cf. Atsem et al. (2016))

IV. DISCUSSION

1 Age-associated methylation alterations in sperm of elder men

1.1 *FOXK1*-hypomethylation in the sperm of elder men

Several reports have shown clinical evidence for an association between advanced male age and male subfertility. Since male subfertility is known to be associated with altered sperm DNA methylation (Kuhnert et al. 2004), it is plausible that advanced male age affects sperm methylation as well. Several studies showed a relationship between sperm DNA methylation alteration in the aging male in both humans and animal models (De Jonge et al. 2013; Jenkins et al. 2014; Niederberger et al. 2014; Milekic et al. 2015). In this study, two of five analyzed regions (*DMPK* and *FOXK1*) displayed a significant decrease in sperm DNA methylation with advanced age. This result was additionally replicated in an independent sperm cohort. Therefore, *FOXK1* revealed as the most promising gene region for altered age-related methylation, since it showed a strikingly significant correlation with advanced paternal age in two independent sperm cohorts. This observed age-related methylation alteration is common among individuals at different ages. Because the analyzed sperm samples were provided of an Infertility center, they exhibit a wide spectrum of aberrant semen parameters. Thus, infertility cannot surely be excluded as a possible confounding factor. Nevertheless, the analyzed regions also exhibited age-associated methylation alterations in fertile, healthy donors (Jenkins et al. 2014). Furthermore, semen parameters as predictors for infertility become less important in arising studies at the expense of other factors such as DNA damage (Sharma et al. 2015).

1.2 The inter-allelic sperm *FOXK1* methylation variability

A single allele analysis by deep bisulfite sequencing confirmed the observed hypomethylation in the *FOXK1* region with advanced age and allowed a more detailed analysis of how the methylated CpGs are distributed among the individual sperm alleles of one donor. While in sperm of young donors the DNA methylation of each sperm allele showed a high inter-allelic variability of methylation values between 0% (fully unmethylated) and 100% (fully methylated), in the sperm of older donors there was a decrease of methylation variation observed where most of the measured sperm alleles

showed a fully unmethylated status. Considering that young paternal age at fertilization leads to higher pregnancy and live-birth rates, one can assume that there is no optimal *FO XK1* methylation status leading to a developmental advantage for the embryo, since the sperm alleles of young donors were highly variably methylated. The reduced methylation variation in sperm of old donors might be explained via the “selfish spermatogonial selection” model where the certain differentially methylated regions would lead to a proliferation advantage of spermatogonial stem cells.

1.3 Possible consequences of *FO XK1* hypomethylation in sperm of elder men

A dual-luciferase reporter assay developed by our laboratory for the *FO XK1* gene promoter showed that an unmethylated *FO XK1* differentially methylated region (DMR) caused increased gene expression (Atsem et al. 2016). Demethylation of the *FO XK1* region and therefore higher *FO XK1* expression might lead to a growth advantage and therefore to an expansion of demethylated sperm alleles over the course of a man’s life. The transcriptional factor *FO XK1* is reported to be an important regulator in the cell cycle control and high *FO XK1* expression enhances cell proliferation (Grant et al. 2012; Shi et al. 2012). A possible explanation how the observed hypomethylation in sperm of older donors might occur is described by Jenkins et al. (2014) as either due to active or passive demethylation events. Passively, since the hypomethylated regions detected in his study were mainly located in sites escaping protamination and therefore associated with a loose chromatin structure which makes the region susceptible to DNA damage over time. DNA repair mechanisms could passively delete methylation patterns and sperm cells with lost methylation marks would accumulate throughout male reproductive life (Jenkins et al. 2014). The loose chromatin structure indicates regions of developmental importance, since the transcriptional machinery should have access to regions relevant for spermatogenesis and developing processes. If hypomethylation of these sites favors spermatogenesis, then an active enzymatic demethylation is possible as an additional mechanism (Jenkins et al. 2014). Nevertheless, the biological and clinical role of this *FO XK1* hypomethylation and therefore higher *FO XK1* expression remains to be elucidated. As aforementioned, transmitted epigenetic alterations through the male germline are quite likely to be potential triggers for diseases related to paternal age and

therefore a possible explanation to the missing heritability problem observed in several studies (Manolio et al. 2009; Eichler et al. 2010; Goriely et al. 2010; Sadee et al. 2014; Trerotola et al. 2015).

2 Intergenerational inheritance of age-associated methylation alterations

2.1 Transmission of paternal *FOXK1*-hypomethylation to the next generation

The question of whether the methylation alterations observed in sperm are transmitted to the offspring was clarified. An epigenetic signature for *FOXK1* similar to the donors' sperm was detected in somatic cells (fetal cord blood) of the donors' respective offspring by bisulfite pyrosequencing. The blood of children conceived at advanced paternal age showed lower methylation values in the same analyzed *FOXK1* gene region when compared to the blood of children conceived at a young paternal age. This result was replicated by an independent method - deep bisulfite sequencing - which allowed an allele-specific methylation analysis. Interestingly, the region is evidently differentially methylated only on the paternally inherited allele, while the maternally inherited allele remains unaffected. An allele-specific pyrosequencing assay supported and replicated these findings. It could be expected that in accordance to Mendelian mechanisms inherited epigenetically altered alleles will show either fully unmethylated or half methylated or fully methylated (0, 50 or 100%) CpG patterns. However, the detected sperm methylation values showed anything in between 0 and 100%, which suggests that changes to the methylome occur during subsequent development. Nevertheless, the methylation profile can resemble to a certain extent the original methylation pattern transmitted by the sperm. Since the spermatocytes of older males show a decrease in methylation, this hypomethylated pattern will be reflected in the fertilized zygote. In conclusion, offspring of elder males have a higher probability of being created from a low methylated paternal *FOXK1* allele.

2.2 The influence of sperm methylation on early embryonal development processes

Even though both maternal and paternal gametes contribute a genetically equal part to the differentiating individual, the importance of the sperm genome to early developmental processes has been underestimated. However, the obtained data show

that the sperm cell contributes more than just the paternal DNA sequence to the embryo and that paternal epigenetic signatures play an important role in early embryonic development (Hammoud et al. 2009). A precise epigenetic program regulates germ cell function and embryonic development after fertilization (Oakes et al. 2007). Thus, reprogramming events in both the male germline and the zygote are highly vulnerable developmental phases. Incomplete replacement of epigenetic signatures by somatic patterns in other than imprinted regions during postzygotic reprogramming might lead to a persistence of epigenetic patterns and therefore to a transgenerational epigenetic inheritance (Reik et al. 2001; Curley et al. 2011; Ly et al. 2015). The processes of imprinting and reprogramming are yet not fully understood, since establishment, maintenance and erasure of epigenetic marks seem to follow precise timing within the differentiation process (Boyano et al. 2008). Adverse environmental conditions at fertilization might lead to inappropriate methylation and therefore altered epigenetic programs, that might have an impact on the future health of the developing individual (Oakes et al. 2007). Possibly, non-imprinted regions in the paternal genome can be transmitted through the sperm to the offspring and persist in the differentiating somatic cells over the course of development.

3 The impact of inherited methylation alterations on the offspring's disease susceptibility

3.1 Epigenetic processes and the development of autism spectrum disorders

Autism defines a wide spectrum of neuropsychiatric deficits associated with a triad of symptoms that consists of impaired social interaction, problems in social communication and comporment and repetitive behavioral patterns or island talents. Though candidate genes responsible for the development of autism were detected in single individuals, there are still a large proportion of autism types whose etiology remains unknown. Numerous studies assume a multimodal interaction of environmental and genetic predisposition factors that lead to this complex neuropsychiatric disease. Especially the prenatal period is said to be a vulnerable developmental phase and susceptible to influencing factors resulting in implications on future mental and physical health (Susser et al. 1999). Influencing factors such as the

paternal age are subject to recent research. There is epidemiological evidence for an association between advanced paternal age and neuropsychiatric disorders in the respective offspring, which might be caused by changes in the epigenetic program during embryonic development (Malaspina et al. 2015).

The importance of epigenetic regulation during fetal brain development, was highlighted by Schneider et al. (2016), who detected more than 2000 sites that are developmentally regulated and significantly hypo- or hypermethylated during development. An impaired methylation program during fetal brain development might increase the susceptibility to intellectual and neurodevelopmental disorders (Schneider et al. 2016). Spiers et al. (2015) confirmed changes in DNA methylation over brain development by a dynamic expression of de novo DNMTs in fetal brains where loci related to neurodevelopmental processes were especially affected by demethylation. By comparing the post mortal brain tissues of autistic subjects to the brain of healthy controls, there was an evidence for genome wide differentially methylated regions across autistic individuals (Ladd-Acosta et al. 2014). Nardone et al. (2014) detected via a 450K methylation array analysis, a high amount of demethylated CpG sites in different brain regions of autistic patients which strengthens the role of epigenetic processes in disease development. Furthermore, a negative correlation between DNA methylation and gene expression was observed which is consistent with the overexpression of *FOXK1* by hypomethylation in this study.

3.2 *FOXK1*-methylation as a possible contributing factor to the development of complex neuropsychiatric diseases

The transcription factor *FOXK1* revealed as an important regulator in neural differentiation and marker for embryonic brain development (Suh et al. 2008). Furthermore, copy number variations in the *FOXK1* region were found in the DNA of autistic patients (Stobbe et al. 2014). The observed decrease in DNA methylation in the somatic cells (FCB) of children of older fathers might display a possible explanation for the epidemiological findings linking higher paternal age to higher risk for neurodevelopmental disorders in the respective offspring.

In this thesis, *FO XK1* methylation was also measured in the blood of autistic subjects. Though the average methylation values did not deviate between the autistic and control group, a linear regression model displayed a trend for a faster regression of *FO XK1* demethylation in autistic individuals. Since DNA methylation and gestational age show a strong relation, precise timing of DNA methylation is of high importance during development (Schneider et al. 2016). The faster regression observed would lead to a higher *FO XK1* expression and therefore to alternate differentiation processes in the brain of autistic patients. Furthermore, this analysis shows a consistent methylation decrease with increasing age as previously observed in sperm and fetal cord blood samples, which further strengthens the relationship between *FO XK1* methylation changes and aging. All these findings support the assumption that certain differentially methylated regions are transmitted through the aged male germline to the offspring, which leads to an altered epigenetic program during brain development and thus contribute to the etiology of complex neuropsychiatric diseases such as autism spectrum disorders.

V. CONCLUSION

The present study gives striking evidence about the role of epigenetic changes in the sperm of aging men and a possible transmission to the developing offspring resulting in future health implications. Advanced paternal age influences the sperm DNA methylation in the gene region of the transcriptional factor *FOXK1* and leaves an epigenetic signature in the resultant embryo. Highly dynamic epigenetic programs during fetal brain development and the importance of *FOXK1* expression for neural differentiation strengthen the assumption that precise timing of *FOXK1* methylation in the prenatal period is essential to normal embryonic development. The accelerated *FOXK1* methylation dynamics observed in the blood of autistic patients gives a hint for understanding the role of epigenetic processes in the etiology of autism spectrum disorders. Future research in this area is needed to elucidate the effects of paternal influencing factors on the developing offspring and their future health. The present results of this thesis highlight that age-associated epigenetic signatures in the male germline and possible transmission mechanisms to the resulting offspring play an underestimated role in complex neuropsychiatric diseases.

VI. ABSTRACT

The effect of late parenthood on the offspring's physical and mental health status has recently become an increasingly important topic of discussion. Studies on neurodevelopmental disorders in children of older parents (Naserbakht et al., 2011) outline the negative consequences of aging fathers as unpredictable compared to the better-understood unfavorable maternal influences (Cedars et al. 2015). This may be due to the fact that lifelong production of male gametes becomes more susceptible to error, not only for somatic mutations. Non-genomic mechanisms such as epigenetic methylation also alter DNA dynamically throughout life (Jones et al., 2015) and influence the aging human sperm DNA (Jenkins et al., 2014). These methylation changes may be transmitted to the next generation via epigenetic inheritance mechanisms (Milekic et al., 2015), which may negatively impact the sensitive epigenetic regulation of cell differentiation in the embryonic period (Curley et al., 2011; Spiers et al., 2015). Accordingly, Nardone et al. (2014) reported several hypomethylated regions in autistic patients, illustrating potential epigenetic influences on the multifactorial pathogenesis of neuropsychiatric disorders. In the present study, the methylation status of five gene regions in the sperm DNA of males of different ages was analyzed by two techniques - pyrosequencing and deep bisulfite sequencing. Two gene regions, *FOXK1* and *DMPK*, showed a highly significant age-related methylation loss and *FOXK1* a reduced methylation variation at the level of single alleles. In addition, the examined gene region of *FOXK1* showed significant methylation changes in the fetal cord blood DNA of the respective offspring of the sperm donor. This fact suggests a transfer of age-related methylation loss to the next generation. Interestingly, a methylation analysis at the level of single alleles showed that the methylation loss was inherited exclusively by the father. *FOXK1* is a transcription factor that plays an important role in the epigenetic regulation of the cell cycle during embryonic neuronal development (Huang et al., 2004; Wijchers et al., 2006). For this reason, the methylation status of *FOXK1* in the blood of autistic patients and an age- and sex-matched control group was investigated. While both groups showed age-associated *FOXK1* methylation loss, a faster dynamics of methylation change was observed in the autistic group. Although further studies are

needed to uncover inheritance mechanisms of epigenetic information, the present results show an evident influence of age-related methylation changes on offspring. When advising future fathers, it is important to consider how the paternal epigenome is altered by aging and can have a negative impact on the developing embryo.

VII. ZUSAMMENFASSUNG

Die Auswirkungen einer späten Elternschaft auf die körperliche und geistige Gesundheit der Nachkommen wurde in letzter Zeit zunehmend diskutiert. Studien zu neurologischen Entwicklungsstörungen bei Kindern älterer Eltern (Naserbakht et al. 2011) skizzieren insbesondere die negativen Folgen alternder Väter (Cedars et al. 2015). Dies ist möglicherweise darauf zurückzuführen, dass die lebenslange Produktion männlicher Gameten im Laufe des Lebens nicht nur für somatische Mutationen fehleranfälliger wird. Auch nicht-genomische Mechanismen wie die epigenetische Methylierung verändert die DNA im Laufe des Lebens dynamisch (Jones et al. 2015) und beeinflussen die alternde menschliche Spermien-DNA (Jenkins et al. 2014). Möglicherweise werden diese Methylierungsveränderungen über epigenetische Vererbungsmechanismen an die nächste Generation übertragen (Milekic et al. 2015), was sich negativ auf die empfindliche epigenetische Regulation der Zelldifferenzierung in der Embryonalperiode auswirken kann (Curley et al. 2011; Spiers et al. 2015). Mögliche epigenetische Einflüsse auf die multifaktorielle Pathogenese neuropsychiatrischer Erkrankungen veranschaulichend, zeigten Nardone et al. (2014) mehrere hypomethylierte Regionen bei autistischen Patienten auf. In der vorliegenden Arbeit wurde der Methylierungsstatus von fünf Genregionen in der Spermien-DNA von Männern unterschiedlichen Alters durch zwei Techniken analysiert – das Pyrosequencing und das Deep Bisulfite Sequencing. Zwei Genregionen, *FO XK1* und *DMPK*, zeigten einen hochgradig signifikanten altersbedingten Methylierungsverlust und *FO XK1* auf der Ebene einzelner Allele eine verringerte Methylierungsvariation. Darüber hinaus zeigte die untersuchte Genregion von *FO XK1* signifikante Methylierungsveränderungen in der Nabelschnurblut-DNA der jeweiligen Nachkommen der Samenspende. Diese Tatsache spricht für eine Übertragung des altersbedingten Methylierungsverlustes auf die nächste Generation.

Anhand einer Methylierungsanalyse auf der Ebene einzelner Allele konnte interessanterweise gezeigt werden, dass der Methylierungsverlust ausschließlich durch den Vater vererbt wurde. *FO XK1* ist ein Transkriptionsfaktor, der eine wichtige Rolle bei der epigenetischen Regulation des Zellzyklus während der embryonalen neuronalen

Entwicklung spielt (Huang et al. 2004; Wijchers et al. 2006). Aus diesem Grund wurde der Methylierungsstatus von *FOXP1* im Blut autistischer Patienten und einer alters- und geschlechtsentsprechenden Kontrollgruppe untersucht. Während beide Gruppen einen altersassoziierten *FOXP1*-Methylierungsverlust zeigten, wurde in der autistischen Gruppe eine schnellere Dynamik der Methylierungsänderung beobachtet. Obwohl weitere Studien erforderlich sind, um Vererbungsmechanismen epigenetischer Information aufzudecken, zeigen die vorliegenden Ergebnisse einen offensichtlichen Einfluss altersbedingter Methylierungsveränderungen auf die Nachkommen. Bei der Beratung zukünftiger Väter ist es wichtig zu berücksichtigen, wie das väterliche Epigenom durch das Altern verändert wird und negative Auswirkungen auf den sich entwickelnden Embryo haben kann.

VIII. INDEX OF FIGURES

Figure 1: Schematic illustration of epigenetic reprogramming	6
Figure 2: Epigenetic drift vs. epigenetic clock of an age-associated site found in one individual.....	9
Figure 3: Spermatogenesis.....	12
Figure 4: Consequences of symmetric cell division in spermatogenesis	14
Figure 5: Overview of the analyzed samples	31
Figure 6: Age distribution for the autism and control cohort.	34
Figure 7: Bisulfite conversion.....	37
Figure 8: Pyrosequencing scheme.....	39
Figure 9: sequencing table generated from the Pyro Q CpG software.....	43
Figure 10: Representative pyrogram.....	44
Figure 11: Amplicon library preparation	46
Figure 12: Pooling and dilution of the DBS samples	49
Figure 13: Deep bisulfite sequencing assay for FOXX1	50
Figure 14: Representative diagram generated by the Amplifyzer software.....	53
Figure 15: GS Junior results: Boxplot for group comparison young vs. aged group for sperm methylation	59
Figure 16: Sperm methylation on the single read level	60
Figure 17: Representative pyrograms for the genotypes GG, AG and AA	62
Figure 18: FOXX1 and autism - correlation analysis of age vs. methylation for ASD patients and controls.....	66

IX. INDEX OF TABLES

Table 1: Aims of this thesis	20
Table 2: List of utilized chemicals.....	24
Table 3: List of utilized Kits	25
Table 4: Content of prepared buffers.....	25
Table 5: List of utilized equipment.....	26
Table 6: List of utilized software to generate and analyze data.....	26
Table 7: List of primers used for bisulfite pyrosequencing	27
Table 8: List of primers for FOXX1 genotyping, 1st round PCR of Deep Bisulfite Sequencing and allele-specific pyrosequencing	28
Table 9: List of 2nd round PCR primers for deep bisulfite sequencing of FOXX1.....	29
Table 10: Fetal cord blood and sperm sample sets for DBS	33
Table 11: Pipetting scheme for bisulfite conversion.....	38
Table 12: Pipetting scheme for PCR sample amplification.....	40
Table 13: PCR program	41
Table 14: Pyrosequencing assays.....	41
Table 15: Pipetting scheme for Pyrosequencing Master Mix 1 & 2.....	42

Table 16: Pipetting scheme for the 1st round PCR	46
Table 17: Pipetting scheme for the 2nd round PCR	47
Table 18: Expected amplicon lengths for FO XK1	47
Table 19: Number of generated reads and average read count per MID for both runs	53
Table 20: Correlation analysis paternal age vs. sperm methylation for DMPK, GET4, FO XK1, PDE4C and TNXB in the main sperm cohort	55
Table 21: Correlation between paternal age and possible confounding factors	56
Table 22: Correlation analysis paternal age vs. sperm methylation for FO XK1 in the independent cohort.....	57
Table 23: GS Junior results: Correlation analysis methylation vs. paternal age for the sperm samples	58
Table 24: GS Junior results: Group comparison young vs. aged group for methylation	58
Table 25: Correlation analysis fetal cord blood methylation vs. paternal age.....	61
Table 26: Genotyping Results	63
Table 27: List of heterozygous fetal cord blood samples with homozygous fathers.....	63
Table 28: GS Junior Results: Allele comparison in fetal cord blood.....	64
Table 29: Allele specific pyrosequencing results	65
Table 30: sperm parameters.....	80
Table 31: FCB parameters.....	88

X. APPENDIX

Table 30: sperm parameters

Sperm sample ID	Paternal age	sperm concentration [$\times 10^6/ml$]	Morphology [% normal formed]	total motility [%]	disease father	TSH [$\mu U/ml$]	Testosterone [$\mu g/l$]	Prolactin [$\mu g/l$]	FSH [IU/ml]
S 001	43	2.80	8	45		2.40	112	568	3.50
S 005	33	41	10	38		3.40	364	101	2.40
S 006	37	9.30	5	23		1.90	456	172	4.70
S 007	44					2.30	176	242	1.60
S 008	33	14	5	45	OAT-syndrome	3	245	112	4.10
S 013	36	1	8	19	cryptozoospermia	1.60	253	289	7.50
S 022	31	73	15	45		0	493	223	3.10
S 026	37	3.20	0	17		0.46	421	89	6.80
S 027	30	1	6	27		1.20	287	237	5.10
S 030	31	0.70	1	44	anomalies in sperm head	0.87	326	80	2
S 031	39	11.80	2	38	OAT-syndrome	1.40	315	154	3.80
S 034	30	29	5	13		1.20	311	134	0.80
S 035	36	6	2	26	OAT-syndrome	1.70	222	13	2.20
S 037	38	20	9	36	asthenozoospermia, anomalies in sperm head	0	411	133	0.70
S 041	34	67	3	54	asthenozoospermia, anomalies in sperm head	0.95	365	24	1.20
S 043	31	33	5	26	asthenozoospermia, anomalies in sperm head	1.10	2	151	11.80
S 044	37	24	3	49		1.20	322	242	2.90
S 047	35	2	1	23	OAT-syndrome		286	223	4
S 048	32	2	4	10	cryptozoospermia	1.60	325	352	12.30
S 049	48	9	3	11	OAT-syndrome	0.95	179	97	4.90
S 050	34	9	3	29	OAT-syndrome	2	336	173	0.90
S 056	32	14	6	6					

S 059	34	80	15	50		1.40	398	99	1.50
S 061	28	9	6	23		1.70	229	180	14.10
S 063	37	23	1	21	asthenozoospermia, anomalies in sperm head	1.50	232	105	5.50
S 070	40	77	10	53		0	0	0	0
S 076	45				cryptozoospermia	1	289	191	37.80
S 077	26	11	16	36	OAT-syndrom	1.20	207	123	7.30
S 086	41	4.30	6	16		0.65	398	111	5.60
S 091	32	26	4	12		1.50	250	179	1.90
S 092	39		0			2	111	56	13.20
S 094	37	30	12	25	asthenozoospermia; anomalies in sperm head	1.50	345	233	5.30
S 097	36	9	4	36	OAT-syndrom	0.96	339	203	2.70
S 100	46	41	12	32	anomalies in sperm head, motility problems	1.20	77	193	3.50
S 1012	31	50	7	40	asthenozoospermia, anomalies in sperm head	1	229	14	2.10
S 106	36	16	1	43	asthenozoospermia, OAT-syndrom, anomalies in sperm head	2.20	125	337	7.40
S 108	34	23	1	27		1.60	473	23	1.30
S 1084	44		7	35	cryptozoospermia		35	299	14.90
S 1097	44					2.80	382	212	19.70
S 1131	30	52	10	45	asthenozoospermia	1.40	229	104	3.70
S 1133	32	110	10	40	asthenozoospermia, anomalies in sperm head				
S 1156	36	61	1	43	asthenozoospermia	1.90	481	60	4.70
S 1161	34						336	125	4.30
S 1169	48	130	12	70					
S 136	31	90	18	45	asthenozoospermia				
S 143	49	31	6	34		0	0	0	0

S 152	36	55	3	38	asthenozoospermia, anomalies in sperm head	1.20	327	84	5.10
S 153	33	95	8	38	asthenozoospermia, anomalies in sperm head				
S 159	36	60	10	32	asthenozoospermia, anomalies in sperm head	4.50	333	384	2.10
S 161	40	0.80	3	50		0.36	135	141	7.90
S 165	49	1.90	9	42		1	132	212	4
S 169	42	6	7	14		0	328	177	1.90
S 172	39		0		cryptozoospermia	0.58	459	177	8.10
S 176	37	110	8	26		2.20	85	78	5
S 189	40	20	5	10	asthenozoospermia, anomalies in sperm head	1.30	244	154	14.80
S 195	34	85	7	13	asthenozoospermia, anomalies in sperm head	2.20	213	227	2.90
S 209	41	82	12	55		0.52	339	145	2.70
S 218	33	91	2	22	asthenozoospermia, anomalies in sperm head	1.20	327	242	1.40
S 224	44	35	7	41	asthenozoospermia, anomalies in sperm head	0	163	166	2.10
S 228	34	16.40	4	26		0.97	446	223	7.10
S 233	38	4.60	5	12			313	142	16.80
S 237	32	31	10	23	asthenozoospermia, anomalies in sperm head	1.90	414	284	4
S 242	43	130	12	40		1.20	330	231	3
S 250	39	38	12	45	asthenozoospermia, anomalies in sperm head	0.48	278	176	13.80
S 254	40	7.20	1	42	OAT-syndrome	1	135	122	2.20
S 256	31	27	9	35		1.60	210	129	1.10

S 258	32	100	12	50		1.20	277	181	4.60
S 263	38	7	3	56	Oligozoospermie, anomalies in sperm head, problems in motility	1.40	326	147	8.60
S 265	35	52	5	48	asthenozoospermia, anomalies in sperm head	1.70	146	168	3.70
S 277	31	3.40	2	39.90	Oligozoospermie, anomalies in sperm head, problems in motility	1.70	32	194	5.20
S 281	43	22	15	55	asthenozoospermia, anomalies in sperm head	0.70	305	161	2.80
S 282	35	32	9	73		0.59	235	65	4.10
S 293	37	3.40	2	40			28	25	14.10
S 297	36	112	10	44		2.10	266	152	1
S 317	36	162	15	25		1.10	228	171	4.10
S 318	44	11	5	30	OAT-syndrome	1.10	291	97	4.30
S 319	40	66	9	52	asthenozoospermia, anomalies in sperm head	0	0	0	0
S 320	37	2.10		4	cryptozoospermia	0.65	222	116	15.30
S 324	36				cryptozoospermia	2.80	234	141	19
S 335	42	58	10	38	asthenozoospermia, anomalies in sperm head	0.63	273	199	3.20
S 339	40	70	10	40	asthenozoospermia, anomalies in sperm head	0.96	143	278	4.20
S 342	33	37	2	20	asthenozoospermia, anomalies in sperm head	1.10	367	12	5.30
S 353	43	4	1	15	OAT-syndrome	1.70	245	151	4.40
S 360	32	5	4	54	OAT-syndrome	0.62	297	187	2.90
S 363	30				immotile sperms				

S 371	38	52	10	32	asthenozoospermia, anomalies in sperm head	3.60	102	227	7
S 373	36	12	7	29	OAT-syndrome	1.30	167	0	5.50
S 389	55	25	4	28		0	0	0	0
S 391	45	6	5	35		1.90	159	271	7.60
S 397	41				cryptozoospermia	1.80	162	218	8.40
S 398	41	20	2	45	OAT-syndrome	1.50	240	100	3.30
S 401	36	46	11	36	asthenozoospermia, anomalies in sperm head	0	0	0	0
S 411	3	243	7	25	asthenozoospermia, anomalies in sperm head		256	211	5.10
S 419	44	92	18	55		1	247	75	5.40
S 435	37	3	10	30	OAT-syndrome	0.88	484	124	7.10
S 439	36	9	8	30	OAT-syndrome	1.20	249	25	3
S 444	32	57	10	42	asthenozoospermia, anomalies in sperm head		291	44	6
S 447	36				cryptozoospermia	2.20	197	211	6
S 448	39	1	5	27	cryptozoospermia	0	274	329	13.30
S 449	35	5	4	31	OAT-syndrome				
S 462	31	24	4	46	asthenozoospermia, anomalies in sperm head	1.70	279	81	2
S 464	40	15	5	43	OAT-syndrome	0	427	132	5.60
S 472	44	16	5	40		1.30	493	75	4.50
S 474	39	17	2	20		0	0	0	0
S 484	29	16	4	12	OAT-syndrome		216	113	2.50
S 485	35	65	10	32	asthenozoospermia, anomalies in sperm head	1.30	649	189	7.40
S 488	43	32	3	28	asthenozoospermia, anomalies in sperm head	0.77	201	137	5.90
S 493	41	14	7	41	OAT-syndrome	0.80	126	95	6

S 499	33	3	5	30	OAT-syndrome	2.60	293	630	3.80
S 501	32	1/4BF			cryptozoospermia	1.40	39	216	13.80
S 504	34	41	7	34	asthenozoospermia, anomalies in sperm head	0.88	219	237	3
S 511	35	3	3	24		2.50	354	134	4.40
S 521	32	84	10	58	asthenozoospermia	1	142	519	1.80
S 533	31	12	5	25	OAT-syndrome	4.10	379	169	1.30
S 537	38	30	6	50	asthenozoospermia, anomalies in sperm head	0	0	0	0
S 547	42	14	7	30	Oligozoospermie, anomalies in sperm head, problems in motility	2.10	333	147	4.50
S 580	46	101	7	48		0.63	275	310	2.30
S 587	36	70	15	55		0.65	378	118	4.20
S 588	37	25	8	65		1.50	187	175	3.50
S 597	33	37	8	50	asthenozoospermia, anomalies in sperm head	1.70	33	13	3.30
S 599	40	31	13	39	asthenozoospermia, anomalies in sperm head	0.72	135	174	2.70
S 601	39	32	10	31	asthenozoospermia, anomalies in sperm head	0.69	404	135	8.70
S 627	41	120	17	65		1.50	124	149	4.60
S 637	40	80	15	55		1.20	387	250	3.20
S 644	34	63	7	41		3	299	187	6.50
S 648	39	38	11	58		2.80	346	178	3.50
S 651	42	56	10	39	asthenozoospermia, anomalies in sperm head	1	240	235	2.80
S 657	46	16	1	32	OAT-syndrome	1.40	358	462	1.50
S 670	37	75	9	32	asthenozoospermia, anomalies in sperm head		234	99.20	3.60

S 671	48	21	3	7		0	0	0	0
S 676	35	4	8	21	OAT-syndrome	1.50	21	146	5.80
S 683	30	81	10	37	asthenozoospermia, anomalies in sperm head	1.30	365	211	2.30
S 684	46	2	1	14	Oligozoospermia, anomalies in sperm head, problems in motility	1.20	288	278	11.40
S 691	32	20	10	40	Oligozoospermia, anomalies in sperm head, problems in motility	1.50	178	145	1.50
S 699	36	22	5	22	anomalies in sperm head, problems in motility				
S 723	34	49	7	59		1.70	308	98	4.80
S 736	35	31	3	10	asthenozoospermia, anomalies in sperm head	1.50	135	16	3.50
S 745	28	40	11	54		1.60	365	123	2.20
S 747	43	17	5	52		1.20	248	161	1.20
S 750	49	52	9	50		1.70	237	107	2.80
S 756	38	23	2	16	asthenozoospermia, anomalies in sperm head	2.30	292	16	3.40
S 767	35	3	8	38	OAT-syndrome	1.80	223	182	6.30
S 777	43	22	7	12	asthenozoospermia, anomalies in sperm head	1.10	431	205	5.60
S 783	33				cryptozoospermia	1.40	237	82	8.10
S 790	51					0.78	421	14	2.90
S 799	32	1	3	30	cryptozoospermia		510	125	14.50
S 805	37					2.70	411	312	3.10
S 820	32	85	5	26	asthenozoospermia, anomalies in sperm head	1.10	271	29	2.30

S 842	34	60	10	50	anomalies in sperm head	1.80	246	363	4
S 851	33	50	5	41		1.30	179	155	3.70
S 857	43				cryptozoospermia	2.80	324	161	5.50
S 881	33	71	11	41		0	0	0	0
S 887	38	41	13	60		1.20	421	129	2.40
S 893	40	9	5	26			279	133	2.40
S 900	40	105	8	59					
S 903	34	3	8	8	OAT-syndrome	1.50	275	167	18.90
S 905	41				Azoospermia	0.89	385	146	24.50
S 910	52				immotile sperm				
S 926	47				cryptozoospermia	0.67	136	174	3.30
S 962	40	6	1	4	OAT-syndrome	0.75	111	108	5.10
S 967	32				cryptozoospermia	1.30	173	229	11.30
S 974	36	33	11	59		0.85	263	223	2.90
S 975	42				cryptozoospermia, anomalies in sperm head	1.10	34	67	18.90
S 977	36	33	2	16	asthenozoospermia, anomalies in sperm head	1.70	175	181	3

Table 31: FCB parameters

FCB sample ID	gender	birth weight [g]	length [cm]	head length [cm]	sample ID father	paternal age	maternal age	treatment
FCB 100	male	2360	45	32	S 005	33	33	
FCB 101	female	1770	42	31	S 005	33	33	
FCB 102	male	4420	56	37	S 318	44	35	ICSI
FCB 103	female	4020	53	34	S 297	36	34	IVF
FCB 104					S 375	35	35	IVF
FCB 105	male	2600	48	35	S 092	39	39	M/T
FCB 106	female	3925	51	34	S 360	32	36	ICSI
FCB 107	male	4140	54	36	S 320	37	35	ICSI
FCB 108	male	3040	49	35	S 401	36	33	IVF
FCB 109	male	3260	52	35	S 411	36	32	ICSI
FCB 110	male	2640	46	33	S 411	36	32	ICSI
FCB 113	male	3280	48	32	S 435	37	35	ICSI
FCB 114	male	3860	56	34	S 371	38	33	IVF
FCB 116	male	2130	45	33	S 165	49	37	ICSI
FCB 117	male	2950	49	35	S 461	36	38	
FCB 118	male	3450	53	35	S 397	41	36	ICSI
FCB 120	male	3840	53	35	S 086	41	31	
FCB 121	female	2990	50	34	S 474	39	34	
FCB 122	male	2940	50	34	S 474	39	34	ICSI
FCB 123	female	3480	49	36	S 448	39	38	ICSI
FCB 124	male	3420	51	36	S 439	36	31	ICSI
FCB 125	female	2640	47	34	S 472	44	37	
FCB 126	male	2910	49	36	S 472	44	37	ICSI
FCB 128	female	3310	54	35	S 109	47	39	IVF
FCB 129	male	2920	52	34	S 493	41	38	ICSI
FCB 130		3840	52	34	S 485	35	30	IVF
FCB 131	female	3160	51	35	S 511	35	36	ICSI
FCB 132	male	3650	50	34	S 281	43	37	IVF
FCB 134	male	3400	51	36	S 537	38	30	ICSI
FCB 135	female	4300	54	37	S 501	32	27	ICSI
FCB 138	female	3470	53	35	S 547	42	33	ICSI
FCB 139	male	3760	52	35	S 293	37	34	ICSI
FCB 140	female	2450	43	32	S 580	46	42	IVF
FCB 141	female	2835	51	31	S 579	39	40	ICSI
FCB 142	female	2580	48	35	S 597	33	30	IVF
FCB 143	male	3280	52	33	S 588	37	39	IVF

FCB 144	female	3040	52	35	S 484	29	31	ICSI
FCB 145	female	3610	53	36	S 622	34	33	ICSI
FCB 146	female	4118	54	35	S 587	36	34	IVF
FCB 147	female	3780	52	37	S 599	40	37	IVF
FCB 150	female	2690	53	35	S 447	36	33	ICSI
FCB 153	female	3150	50	34	S 628	47	37	ICSI
FCB 155	male	3750	52	35	S 363	30	29	M/T Kryo
FCB 156	male	3200	50	36	S 657	46	41	ICSI
FCB 157	male	3200	51	35	S 313	39	36	ICSI
FCB 158	female	3130	51	35	S 648	39	38	IVF
FCB 159	male	3325	51	35	S 637	40	35	
FCB 160	male	3500	52	37	S 291	45	40	M/T
FCB 161					S 291	45	40	M/T
FCB 162	female	3495	51	36	S 683	30	25	IVF
FCB 163	male	3260	51	36	S 659	42	39	ICSI
FCB 164	male	2480	46	34	S 699	36	32	ICSI
FCB 165	female	3225	55	35	S 687	35	34	ICSI
FCB 166	female	2850	50	34	S 533	31	25	ICSI
FCB 167	female	3750	51	34	S 671	48	37	
FCB 168	female	3650	54	36	S 676	35	31	ICSI
FCB 169	male	2480	49	34				IVF
FCB 170		2580	49	32				IVF
FCB 171	female	3030	50	35	S 684	46	32	ICSI
FCB 172	female	2840	47	34	S 745	28	22	IVF
FCB 173	female	3320	50	35	S 723	34	37	IVF
FCB 174	male	3540	54	35	S 750	49	39	IVF
FCB 176	female	4220	52	36	S 464	40	39	
FCB 177	male	3920	52	36	S 767	35	35	ICSI
FCB 178	male	3460	54	36	S 736	35	36	ICSI
FCB 179	female	3150	48	36	S 758	40	32	ICSI
FCB 18	male	2410	52	33	S 050	34	33	
FCB 180	female	2140	49	33	S 820	32	34	ICSI
FCB 181	male	3150	55	36	S 820	32	34	ICSI
FCB 182	female	2650	48	32	S 842	34	33	IVF
FCB 183	female	3150	50	37	S 815	33	32	IVF
FCB 184	female	3215	52	36	S 233	38	33	ICSI
FCB 185	male	4100	55	36	S 756	38	34	ICSI
FCB 186	female	3390	49	35	S 034	30	25	
FCB 187	female	2490	47	32	S 799	32	31	ICSI
FCB 188	male	3480	55	35	S 783	33	28	ICSI
FCB 189	female	2340	46	34	S 398	41	32	ICSI

FCB 19	female	4230	56		S 047	35	30	ICSI
FCB 190	female	2240	45	32	S 398	41	32	ICSI
FCB 191	male	3650	52	36	S 790	51	32	M/T, Kryo
FCB 192	male	2970	50	34	S 499	33	27	
FCB 193	female	4950	57	36	S 851	33	31	ICSI
FCB 194	male	2660	48	33	S 903	34	31	ICSI
FCB 195	female	2010	44	30	S 903	34	31	ICSI
FCB 196	female	2930	49	33	S 888	34	34	IVF
FCB 197	male	3040	50	35	S 887	38	36	IVF
FCB 198	male	2770	49	36	S 881	33	36	ICSI
FCB 20	female	2180	46	33	S 077	26	36	IVF
FCB 200	male	3790	54	37	S 031	39	33	ICSI
FCB 201	male	2690	47	33	S 897	48	38	ICSI
FCB 202	male	3710	53	36	S 910	52	36	M/T
FCB 203	male	3470	52	37	S 900	40	37	IVF
FCB 204	male	3840	53	36	S 905	41	36	ICSI, M/T
FCB 205	male	2815	48	34	S 777	43	37	ICSI
FCB 206	male	2990	52	35	S 926	47	37	
FCB 207	male	3440	54	35	S 670	37	36	ICSI
FCB 208	male	2900	50	34	S 805	37	38	ICSI
FCB 209	male	3630	54	36	S 449	35	31	ICSI
FCB 21	female	2570	50	34	S 059	34	28	IVF
FCB 210	male	3050	51	35	S 962	40	34	ICSI
FCB 212	female	3720	52	35	S 963	47	34	
FCB 213	female	3200	52	33	S 076	45	34	ICSI
FCB 214					S 977	36	30	ICSI
FCB 215					S 977	36	30	ICSI
FCB 217	female	2720	49	33	S 747	43	42	ICSI
FCB 218	female	3410	50	35	S 1012	31	32	ICSI
FCB 22	male	1730			S 091	32	35	ICSI
FCB 220	male	2760	49	35	S 488	43	32	ICSI
FCB 222	female	2700	51	33	S 494	46	36	
FCB 223	male				S 893	40	31	ICSI
FCB 224	male	3100	52	34	S 1084	44	39	ICSI
FCB 225	female	3280	50	33	S 504	34	29	ICSI
FCB 226	male	3820	55	35	S 967	32	28	M/T, Kryo HG
FCB 227	female	3620	52	35	S 476	39	27	ICSI
FCB 228	male	4530	52	38	S 975	42	38	ICSI
FCB 230	female	3450	52	36	S 1133	32	30	ICSI
FCB 231	male	3330	54	35	S 1161	34	34	M/T

FCB 232	female	3135	50	34	S 1156	36	30	ICSI
FCB 233	male	4540	52	38	S 1131	29	33	IVF
FCB 234	female	3540	56	35	S 601	39	41	ICSI
FCB 235	female	3060	50	34	S 1169	48	37	IVF
FCB 236	male	2850	51	34	S 1223	34	32	ICSI
FCB 24	male	2115			S 091	32	35	ICSI
FCB 25	male	2510	49	33	S 048	32	29	ICSI
FCB 26	female	2120	47	31	S 048	32	29	ICSI
FCB 27	male	3920	55	36	S 063	37	35	ICSI
FCB 28	male	3810	51	36	S 070	40	37	IVF
FCB 29	female	3000	51	35	S 082	43	35	
FCB 30	female	1900	47	32	S 001	43		KRYO
FCB 31	male	1980	47	31	S 001	43		KRYO
FCB 32	male	2630	52	52	S 094	37	30	ICSI
FCB 33	male	1910	44	32	S 143	49	38	ICSI
FCB 34	male	2130	43	30	S 143	49	38	ICSI
FCB 35	male	1830	44	30	S 143	49	38	ICSI
FCB 36	female	2540	46	35	S 136	31	32	ICSI
FCB 37	female	2810	48	34	S 136	31	32	ICSI
FCB 38	male	3120	51	35	S 108	34	26	ICSI
FCB 39	female	3190	51	33	S 100	46	39	ICSI
FCB 40	male	3510	53	34	S 097	36	34	ICSI
FCB 41	female	2640	49		S 161	40	32	KRYO
FCB 42	male	1760	43	28	S 265	35	33	ICSI
FCB 43	male	2100	44	29	S 265	35	33	ICSI
FCB 44	male	2250	47	33	S 195	34	32	ICSI
FCB 45	female	2560	50	33	S 195	34	32	ICSI
FCB 46	male	2510	48	36	S 153	33	33	ICSI
FCB 47	male	2770	48	35	S 153	33	33	ICSI
FCB 48					S 145	39	37	IVF
FCB 49					S 145	39	37	IVF
FCB 50					S 196	47	30	M/T
FCB 51	male	2810	51	35	S 179	35	27	ICSI
FCB 52	female	2780	49	36				ICSI
FCB 53	female	3370	54	35	S 176	37	36	
FCB 54	female	3270	52	35	S 172	39	40	
FCB 55	female	3800	56	35	S 189	40	32	ICSI
FCB 56	female	2450	47	33	S 209	41	37	IVF
FCB 57	female	2900	47	32	S 209	41	37	IVF
FCB 58	female	3705	54	36	S 169	42	43	ICSI
FCB 59	male	2090	49	32	S 272	47	34	ICSI

FCB 60	female	2200	49	32	S 272	47	34	ICSI
FCB 61	male	4320	56	37	S 159	36	33	ICSI
FCB 62	male	4450	56	38	S 217	44	33	ICSI
FCB 63	female	2960	49	34	S 258	32	35	
FCB 64	male	2270	46	34	S 258	32	35	IVF
FCB 65	male	2740	51	34	S 254	40	30	ICSI
FCB 67	female	3030	51	35	S 237	32	31	ICSI
FCB 68					S 228	34	35	
FCB 70	female	2130	45	32	S 256	31	30	IVF
FCB 71	male	2560	49	32	S 294	39	34	ICSI
FCB 72	male	3090	52	36	S 224	44	39	ICSI
FCB 73	female	3250	52	35	S 218	33	39	ICSI
FCB 75	female	2060	45	30	S 319	40	36	ICSI
FCB 77	male	2650	48	34	S 277	31	30	ICSI
FCB 78	female	3000	50	34	S 277	31	30	ICSI
FCB 79	male	2550	51	35	S 317	36	30	
FCB 80	male	3410	53	33	S 282	35	35	IVF
FCB 81	male	3940	57	36	S 041	34	34	ICSI
FCB 82	male	2825	50	34	S 061	28	29	ICSI
FCB 84	male	3845	52	36	S 263	37	37	ICSI
FCB 85	female	2490	47	33	S 373	36	30	ICSI
FCB 86	female	2385	47	31	S 373	36	30	ICSI
FCB 88	male	2430	45	33	S 342	33	31	ICSI
FCB 89	male	2300	46	33	S 342	33	31	
FCB 90	male	1900			S 353	43	32	ICSI
FCB 91	female	2360			S 353	43	32	ICSI
FCB 92	female	2630	51	33	S 335	42	38	IVF

XI. REFERENCES

- (2006) "User-Developed Protocol: Purification of total DNA from animal sperm using the DNeasy®."
- (2010) "QIAGEN Supplementary Protocol: Purification of DNA from clotted blood using the FlexiGene® DNA."
- (2013) "Agilent DNA 1000 Kit Guide."
- (2013). Beckman Coulter. Agencourt AMPure XP Information For Use Guide PCR Purification.
- (May 2010 (Rev. April 2011)). emPCR Amplification Method Manual - Lib-A, GS Junior Titanium Series.
- (May 2010 (Rev. June 2010)) "Sequencing Method Manual, GS Junior Titanium Series ".
- Adkins, R. M., F. Thomas, F. A. Tylavsky and J. Krushkal (2011). "Parental ages and levels of DNA methylation in the newborn are correlated." BMC Med Genet **12**: 47.
- Alisch, R. S., B. G. Barwick, P. Chopra, L. K. Myrick, G. A. Satten, K. N. Conneely and S. T. Warren (2012). "Age-associated DNA methylation in pediatric populations." Genome Res **22**(4): 623-632.
- Anthony Griffiths, S. W., Richard Lewontin, Sean Carroll (2008). Regulation of Gene Expression in Eukaryotes. Introduction to genetic analysis. New York, W. H. Freeman and Company: 838.
- Anum, E. A., L. D. Hill, A. Pandya and J. F. Strauss, 3rd (2009). "Connective tissue and related disorders and preterm birth: clues to genes contributing to prematurity." Placenta **30**(3): 207-215.
- Anway, M. D., A. S. Cupp, M. Uzumcu and M. K. Skinner (2005). "Epigenetic transgenerational actions of endocrine disruptors and male fertility." Science **308**(5727): 1466-1469.
- Aoki, V. W., L. Liu and D. T. Carrell (2005). "Identification and evaluation of a novel sperm protamine abnormality in a population of infertile males." Hum Reprod **20**(5): 1298-1306.
- Atsem, S., J. Reichenbach, R. Potabattula, M. Dittrich, C. Nava, C. Depienne, L. Bohm, S. Rost, T. Hahn, M. Schorsch, T. Haaf and N. El Hajj (2016). "Paternal age effects on sperm FOXP1 and KCNA7 methylation and transmission into the next generation." Hum Mol Genet.
- Baccarelli, A. and V. Bollati (2009). "Epigenetics and environmental chemicals." Curr Opin Pediatr **21**(2): 243-251.
- Bacon, C., M. Schneider, C. Le Magueresse, H. Froehlich, C. Sticht, C. Gluch, H. Monyer and G. A. Rappold (2015). "Brain-specific Foxp1 deletion impairs neuronal development and causes autistic-like behaviour." Mol Psychiatry **20**(5): 632-639.
- Bassel-Duby, R., M. D. Hernandez, Q. Yang, J. M. Rochelle, M. F. Seldin and R. S. Williams (1994). "Myocyte nuclear factor, a novel winged-helix transcription factor under both developmental and neural regulation in striated myocytes." Mol Cell Biol **14**(7): 4596-4605.
- Benchaib, M., V. Braun, D. Ressenkoff, J. Lornage, P. Durand, A. Niveleau and J. F. Guerin (2005). "Influence of global sperm DNA methylation on IVF results." Hum Reprod **20**(3): 768-773.
- Bird, A. (2002). "DNA methylation patterns and epigenetic memory." Genes Dev **16**(1):6-

21.

- Bowman, C. J., D. E. Ayer and B. D. Dynlacht (2014). "Foxk proteins repress the initiation of starvation-induced atrophy and autophagy programs." Nat Cell Biol **16**(12): 1202-1214.
- Boyano, M. D., N. Andollo, M. M. Zalduendo and J. Arechaga (2008). "Imprinting of mammalian male gametes is gene specific and does not occur at a single stage of differentiation." Int J Dev Biol **52**(8): 1105-1111.
- Brisson, D., G. Houde, J. St-Pierre, M. C. Vohl, J. Mathieu and D. Gaudet (2002). "The pleiotropic expression of the myotonic dystrophy protein kinase gene illustrates the complex relationships between genetic, biological and clinical covariates of male aging." Aging Male **5**(4): 223-232.
- Calvanese, V., E. Lara, A. Kahn and M. F. Fraga (2009). "The role of epigenetics in aging and age-related diseases." Ageing Res Rev **8**(4): 268-276.
- Cantone, I., Fisher, A.G., 2013. Epigenetic programming and reprogramming during development. *Nat Struct Mol Biol* **20**, pp. 282-289.
- Capri, M., A. Santoro, P. Garagnani, M. G. Bacalini, C. Pirazzini, F. Olivieri, A. Procopio, S. Salvioli and C. Franceschi (2014). "Genes of human longevity: an endless quest?" Curr Vasc Pharmacol **12**(5): 707-717.
- Cardwell, C. R., D. J. Carson and C. C. Patterson (2005). "Parental age at delivery, birth order, birth weight and gestational age are associated with the risk of childhood Type 1 diabetes: a UK regional retrospective cohort study." Diabet Med **22**(2): 200-206.
- Carrell, D. T. (2012). "Epigenetics of the male gamete." Fertil Steril **97**(2): 267-274.
- Cedar, H. and G. L. Verdine (1999). "Gene expression. The amazing demethylase." Nature **397**(6720): 568-569.
- Cedars, M. I. (2015). "Introduction: Childhood implications of parental aging." Fertil Steril **103**(6): 1379-1380.
- Chang, Y. W., Y. C. Chuang, Y. C. Ho, M. Y. Cheng, Y. J. Sun, C. D. Hsiao and C. Wang (2010). "Crystal structure of Get4-Get5 complex and its interactions with Sgt2, Get3, and Ydj1." J Biol Chem **285**(13): 9962-9970.
- Chen, Z. X., J. R. Mann, C. L. Hsieh, A. D. Riggs and F. Chedin (2005). "Physical and functional interactions between the human DNMT3L protein and members of the de novo methyltransferase family." J Cell Biochem **95**(5): 902-917.
- Choi, S. K., S. R. Yoon, P. Calabrese and N. Arnheim (2008). "A germ-line-selective advantage rather than an increased mutation rate can explain some unexpectedly common human disease mutations." Proc Natl Acad Sci U S A **105**(29): 10143-10148.
- Christensen, B. C., E. A. Houseman, C. J. Marsit, S. Zheng, M. R. Wrensch, J. L. Wiemels, H. H. Nelson, M. R. Karagas, J. F. Padbury, R. Bueno, D. J. Sugarbaker, R. F. Yeh, J. K. Wiencke and K. T. Kelsey (2009). "Aging and environmental exposures alter tissue-specific DNA methylation dependent upon CpG island context." PLoS Genet **5**(8): e1000602.
- Clermont, Y. (1966). "Renewal of spermatogonia in man." Am J Anat **118**(2): 509-524.
- Clermont, Y. (1966). "Spermatogenesis in man. A study of the spermatogonial population." Fertil Steril **17**(6): 705-721.

- Comings, D. E. and J. P. MacMurray (2006). "Maternal age at the birth of the first child as an epistatic factor in polygenic disorders." Am J Med Genet B Neuropsychiatr Genet **141B**(1): 1-6.
- Cooper, D. T. G. (2010). WHO laboratory manual for the Examination and processing of human semen. Switzerland, World Health Organization.
- Curley, J. P., R. Mashoodh and F. A. Champagne (2011). "Epigenetics and the origins of paternal effects." Horm Behav **59**(3): 306-314.
- Dada, R., M. Kumar, R. Jesudasan, J. L. Fernandez, J. Gosalvez and A. Agarwal (2012). "Epigenetics and its role in male infertility." J Assist Reprod Genet **29**(3): 213-223.
- De Jonge, C. J. (2013). "Paternal age and sperm methylation status." Fertil Steril **100**(4): 940-941.
- de la Rochebrochard, E. and P. Thonneau (2002). "Paternal age and maternal age are risk factors for miscarriage; results of a multicentre European study." Hum Reprod **17**(6): 1649-1656.
- De Wit, M. L. and F. Rajulton (1992). "Education and timing of parenthood among Canadian women: a cohort analysis." Soc Biol **39**(1-2): 109-122.
- Demirdas, S., E. Dulfer, L. Robert, M. Kempers, D. van Beek, D. Micha, B. G. van Engelen, B. Hamel, J. Schalkwijk, B. Loeys, A. Maugeri and N. C. Voermans (2016). "Recognizing the tenascin-X deficient type of Ehlers-Danlos syndrome: a cross-sectional study in 17 patients." Clin Genet.
- Deriziotis, P., B. J. O'Roak, S. A. Graham, S. B. Estruch, D. Dimitropoulou, R. A. Bernier, J. Gerds, J. Shendure, E. E. Eichler and S. E. Fisher (2014). "De novo TBR1 mutations in sporadic autism disrupt protein functions." Nat Commun **5**: 4954.
- Drinkwater, R. D., T. J. Blake, A. A. Morley and D. R. Turner (1989). "Human lymphocytes aged in vivo have reduced levels of methylation in transcriptionally active and inactive DNA." Mutat Res **219**(1): 29-37.
- Eichler, E. E., J. Flint, G. Gibson, A. Kong, S. M. Leal, J. H. Moore and J. H. Nadeau (2010). "Missing heritability and strategies for finding the underlying causes of complex disease." Nat Rev Genet **11**(6): 446-450.
- El Hajj, N., U. Zechner, E. Schneider, A. Tresch, J. Gromoll, T. Hahn, M. Schorsch and T. Haaf (2011). "Methylation status of imprinted genes and repetitive elements in sperm DNA from infertile males." Sex Dev **5**(2): 60-69.
- Ficz, G., M. R. Branco, S. Seisenberger, F. Santos, F. Krueger, T. A. Hore, C. J. Marques, S. Andrews and W. Reik (2011). "Dynamic regulation of 5-hydroxymethylcytosine in mouse ES cells and during differentiation." Nature **473**(7347): 398-402.
- Fraga, M. F., E. Ballestar, M. F. Paz, S. Ropero, F. Setien, M. L. Ballestar, D. Heine-Suner, J. C. Cigudosa, M. Urioste, J. Benitez, M. Boix-Chornet, A. Sanchez-Aguilera, C. Ling, E. Carlsson, P. Poulsen, A. Vaag, Z. Stephan, T. D. Spector, Y. Z. Wu, C. Plass and M. Esteller (2005). "Epigenetic differences arise during the lifetime of monozygotic twins." Proc Natl Acad Sci U S A **102**(30): 10604-10609.
- Fraga, M. F. and M. Esteller (2007). "Epigenetics and aging: the targets and the marks." Trends Genet **23**(8): 413-418.
- Fu, Y., F. Ito, G. Zhang, B. Fernandez, H. Yang and X. S. Chen (2015). "DNA cytosine and methylcytosine deamination by APOBEC3B: enhancing methylcytosine deamination by engineering APOBEC3B." Biochem J **471**(1): 25-35.

- Fuke, C., M. Shimabukuro, A. Petronis, J. Sugimoto, T. Oda, K. Miura, T. Miyazaki, C. Ogura, Y. Okazaki and Y. Jinno (2004). "Age related changes in 5-methylcytosine content in human peripheral leukocytes and placentas: an HPLC-based study." Ann Hum Genet **68**(Pt 3): 196-204.
- Gardella, R., N. Zoppi, D. Assanelli, M. L. Muiesan, S. Barlati and M. Colombi (2004). "Exclusion of candidate genes in a family with arterial tortuosity syndrome." Am J Med Genet A **126A**(3): 221-228.
- Garry, D. J., A. Meeson, J. Elterman, Y. Zhao, P. Yang, R. Bassel-Duby and R. S. Williams (2000). "Myogenic stem cell function is impaired in mice lacking the forkhead/winged helix protein MNF." Proc Natl Acad Sci U S A **97**(10): 5416-5421.
- Garry, D. J., Q. Yang, R. Bassel-Duby and R. S. Williams (1997). "Persistent expression of MNF identifies myogenic stem cells in postnatal muscles." Dev Biol **188**(2): 280-294.
- Goriely, A., J. J. McGrath, C. M. Hultman, A. O. Wilkie and D. Malaspina (2013). "'Selfish spermatogonial selection": a novel mechanism for the association between advanced paternal age and neurodevelopmental disorders." Am J Psychiatry **170**(6): 599-608.
- Goriely, A. and A. O. Wilkie (2010). "Missing heritability: paternal age effect mutations and selfish spermatogonia." Nat Rev Genet **11**(8): 589.
- Goriely, A. and A. O. Wilkie (2012). "Paternal age effect mutations and selfish spermatogonial selection: causes and consequences for human disease." Am J Hum Genet **90**(2): 175-200.
- Grant, G. D., J. Gamsby, V. Martyanov, L. Brooks, 3rd, L. K. George, J. M. Mahoney, J. J. Loros, J. C. Dunlap and M. L. Whitfield (2012). "Live-cell monitoring of periodic gene expression in synchronous human cells identifies Forkhead genes involved in cell cycle control." Mol Biol Cell **23**(16): 3079-3093.
- Grin, I. and A. A. Ishchenko (2016). "An interplay of the base excision repair and mismatch repair pathways in active DNA demethylation." Nucleic Acids Res **44**(8): 3713-3727.
- Hackett, J. A., R. Sengupta, J. J. Zyllich, K. Murakami, C. Lee, T. A. Down and M. A. Surani (2013). "Germline DNA demethylation dynamics and imprint erasure through 5-hydroxymethylcytosine." Science **339**(6118): 448-452.
- Hammoud, S. S., D. A. Nix, H. Zhang, J. Purwar, D. T. Carrell and B. R. Cairns (2009). "Distinctive chromatin in human sperm packages genes for embryo development." Nature **460**(7254): 473-478.
- Hawke, T. J., N. Jiang and D. J. Garry (2003). "Absence of p21CIP rescues myogenic progenitor cell proliferative and regenerative capacity in Foxk1 null mice." J Biol Chem **278**(6): 4015-4020.
- Heijmans, B. T., E. W. Tobi, A. D. Stein, H. Putter, G. J. Blauw, E. S. Susser, P. E. Slagboom and L. H. Lumey (2008). "Persistent epigenetic differences associated with prenatal exposure to famine in humans." Proc Natl Acad Sci U S A **105**(44): 17046-17049.
- Herbstman, J. B., S. Wang, F. P. Perera, S. A. Lederman, J. Vishnevetsky, A. G. Rundle, L. A. Hoepner, L. Qu and D. Tang (2013). "Predictors and consequences of global DNA methylation in cord blood and at three years." PLoS One **8**(9): e72824.

- Horvath, S. (2013). "DNA methylation age of human tissues and cell types." Genome Biol **14**(10): R115.
- Horvath, S., Y. Zhang, P. Langfelder, R. S. Kahn, M. P. Boks, K. van Eijk, L. H. van den Berg and R. A. Ophoff (2012). "Aging effects on DNA methylation modules in human brain and blood tissue." Genome Biol **13**(10): R97.
- Huang, J. T. and V. Lee (2004). "Identification and characterization of a novel human FOXK1 gene in silico." Int J Oncol **25**(3): 751-757.
- Imhof, A. (2006). "Epigenetic regulators and histone modification." Brief Funct Genomic Proteomic **5**(3): 222-227.
- Inbar-Feigenberg, M., S. Choufani, D. T. Butcher, M. Roifman and R. Weksberg (2013). "Basic concepts of epigenetics." Fertil Steril **99**(3): 607-615.
- Iurlaro, M., G. Ficz, D. Oxley, E. A. Raiber, M. Bachman, M. J. Booth, S. Andrews, S. Balasubramanian and W. Reik (2013). "A screen for hydroxymethylcytosine and formylcytosine binding proteins suggests functions in transcription and chromatin regulation." Genome Biol **14**(10): R119.
- Jenkins, T. G., K. I. Aston, B. R. Cairns and D. T. Carrell (2013). "Paternal aging and associated intraindividual alterations of global sperm 5-methylcytosine and 5-hydroxymethylcytosine levels." Fertil Steril **100**(4): 945-951.
- Jenkins, T. G., K. I. Aston, C. Pflueger, B. R. Cairns and D. T. Carrell (2014). "Age associated sperm DNA methylation alterations: possible implications in offspring disease susceptibility." PLoS Genet **10**(7): e1004458.
- Jenkins, T. G. and D. T. Carrell (2012). "The sperm epigenome and potential implications for the developing embryo." Reproduction **143**(6): 727-734.
- Jinno, Y., Y. Ikeda, K. Yun, M. Maw, H. Masuzaki, H. Fukuda, K. Inuzuka, A. Fujishita, Y. Ohtani, T. Okimoto and et al. (1995). "Establishment of functional imprinting of the H19 gene in human developing placentae." Nat Genet **10**(3): 318-324.
- Johansson, A., S. Enroth and U. Gyllensten (2013). "Continuous Aging of the Human DNA Methylome Throughout the Human Lifespan." PLoS One **8**(6): e67378.
- Johnson, K. J., S. E. Carozza, E. J. Chow, E. E. Fox, S. Horel, C. C. McLaughlin, B. A. Mueller, S. E. Puumala, P. Reynolds, J. Von Behren and L. G. Spector (2009). "Parental age and risk of childhood cancer: a pooled analysis." Epidemiology **20**(4): 475-483.
- Jones, M. J., S. J. Goodman and M. S. Kobor (2015). "DNA methylation and healthy human aging." Aging Cell.
- Kahn, A. and M. F. Fraga (2009). "Epigenetics and aging: status, challenges, and needs for the future." J Gerontol A Biol Sci Med Sci **64**(2): 195-198.
- Katoh, M. and M. Katoh (2004). "Human FOX gene family (Review)." Int J Oncol **25**(5): 1495-1500.
- Kesselmeier, M., C. Putter, A. L. Volckmar, H. Baurecht, H. Grallert, T. Illig, K. Ismail, M. Ollikainen, Y. Silen, A. Keski-Rahkonen, C. M. Bulik, D. A. Collier, E. Zeggini, J. Hebebrand, A. Scherag, A. Hinney, Gcan and Wtccc (2016). "High-throughput DNA methylation analysis in anorexia nervosa confirms TNXB hypermethylation." World J Biol Psychiatry: 1-13.
- Kidd, S. A., B. Eskenazi and A. J. Wyrobek (2001). "Effects of male age on semen quality and fertility: a review of the literature." Fertil Steril **75**(2): 237-248.

- Kim, Y. S., J. D. Hwan, S. Bae, D. H. Bae and W. A. Shick (2010). "Identification of differentially expressed genes using an annealing control primer system in stage III serous ovarian carcinoma." BMC Cancer **10**: 576.
- King, M. D., C. Fountain, D. Dakhllallah and P. S. Bearman (2009). "Estimated autism risk and older reproductive age." Am J Public Health **99**(9): 1673-1679.
- Koch, L. (2014). "Epigenetics: an epigenetic twist on the missing heritability of complex traits." Nat Rev Genet **15**(4): 218.
- Komorek, J., M. Kuppuswamy, T. Subramanian, S. Vijayalingam, E. Lomonosova, L. J. Zhao, J. S. Mymryk, K. Schmitt and G. Chinnadurai (2010). "Adenovirus type 5 E1A and E6 proteins of low-risk cutaneous beta-human papillomaviruses suppress cell transformation through interaction with FOXK1/K2 transcription factors." J Virol **84**(6): 2719-2731.
- Kong, A., M. L. Frigge, G. Masson, S. Besenbacher, P. Sulem, G. Magnusson, S. A. Gudjonsson, A. Sigurdsson, A. Jonasdottir, A. Jonasdottir, W. S. Wong, G. Sigurdsson, G. B. Walters, S. Steinberg, H. Helgason, G. Thorleifsson, D. F. Gudbjartsson, A. Helgason, O. T. Magnusson, U. Thorsteinsdottir and K. Stefansson (2012). "Rate of de novo mutations and the importance of father's age to disease risk." Nature **488**(7412): 471-475.
- Krenciute, G., S. Liu, N. Yucer, Y. Shi, P. Ortiz, Q. Liu, B. J. Kim, A. O. Odejimi, M. Leng, J. Qin and Y. Wang (2013). "Nuclear BAG6-UBL4A-GET4 complex mediates DNA damage signaling and cell death." J Biol Chem **288**(28): 20547-20557.
- Kuhnert, B. and E. Nieschlag (2004). "Reproductive functions of the ageing male." Hum Reprod Update **10**(4): 327-339.
- Ladd-Acosta, C., K. D. Hansen, E. Briem, M. D. Fallin, W. E. Kaufmann and A. P. Feinberg (2014). "Common DNA methylation alterations in multiple brain regions in autism." Mol Psychiatry **19**(8): 862-871.
- Lande-Diner, L., J. Zhang, I. Ben-Porath, N. Amariglio, I. Keshet, M. Hecht, V. Azuara, A. G. Fisher, G. Rechavi and H. Cedar (2007). "Role of DNA methylation in stable gene repression." J Biol Chem **282**(16): 12194-12200.
- Lehrer, D. S., M. T. Pato, R. W. Nahhas, B. R. Miller, D. Malaspina, P. F. Buckley, J. L. Sobell, J. Walsh-Messinger, C. Genomic Psychiatry Cohort and C. N. Pato (2015). "Paternal age effect: Replication in schizophrenia with intriguing dissociation between bipolar with and without psychosis." Am J Med Genet B Neuropsychiatr Genet.
- Li, Y., V. W. Jaddoe, L. Qi, Y. He, J. Lai, J. Wang, J. Zhang, Y. Hu, E. L. Ding, X. Yang, F. B. Hu and G. Ma (2011). "Exposure to the Chinese famine in early life and the risk of hypertension in adulthood." J Hypertens **29**(6): 1085-1092.
- Lim, J., G. J. Maher, G. D. Turner, W. Dudka-Ruszkowska, S. Taylor, E. Rajpert-De Meyts, A. Goriely and A. O. Wilkie (2012). "Selfish spermatogonial selection: evidence from an immunohistochemical screen in testes of elderly men." PLoS One **7**(8): e42382.
- Lozano, R., A. Vino, C. Lozano, S. E. Fisher and P. Deriziotis (2015). "A de novo FOXP1 variant in a patient with autism, intellectual disability and severe speech and language impairment." Eur J Hum Genet **23**(12): 1702-1707.
- Lu, Y., H. Ma, J. Sullivan-Halley, K. D. Henderson, E. T. Chang, C. A. Clarke, S. L.

- Neuhausen, D. W. West, L. Bernstein and S. S. Wang (2010). "Parents' ages at birth and risk of adult-onset hematologic malignancies among female teachers in California." Am J Epidemiol **171**(12): 1262-1269.
- Lüllmann-Rauch, R. (2015). Männliche Geschlechtsorgane. Taschenlehrbuch Histologie. Stuttgart, Germany, Georg Thieme Verlag KG: 700.
- Lumey, L. H. and A. D. Stein (2009). "Transgenerational effects of prenatal exposure to the Dutch famine." BJOG **116**(6): 868; author reply 868.
- Ly, L., D. Chan and J. M. Trasler (2015). "Developmental windows of susceptibility for epigenetic inheritance through the male germline." Semin Cell Dev Biol **43**: 96-105.
- Malaspina, D., C. Gilman and T. M. Kranz (2015). "Paternal age and mental health of offspring." Fertil Steril **103**(6): 1392-1396.
- Manolio, T. A., F. S. Collins, N. J. Cox, D. B. Goldstein, L. A. Hindorff, D. J. Hunter, M. I. McCarthy, E. M. Ramos, L. R. Cardon, A. Chakravarti, J. H. Cho, A. E. Guttmacher, A. Kong, L. Kruglyak, E. Mardis, C. N. Rotimi, M. Slatkin, D. Valle, A. S. Whittemore, M. Boehnke, A. G. Clark, E. E. Eichler, G. Gibson, J. L. Haines, T. F. Mackay, S. A. McCarroll and P. M. Visscher (2009). "Finding the missing heritability of complex diseases." Nature **461**(7265): 747-753.
- Mao, J. R., G. Taylor, W. B. Dean, D. R. Wagner, V. Afzal, J. C. Lotz, E. M. Rubin and J. Bristow (2002). "Tenascin-X deficiency mimics Ehlers-Danlos syndrome in mice through alteration of collagen deposition." Nat Genet **30**(4): 421-425.
- Martino, D. J., M. K. Tulic, L. Gordon, M. Hodder, T. R. Richman, J. Metcalfe, S. L. Prescott and R. Saffery (2011). "Evidence for age-related and individual-specific changes in DNA methylation profile of mononuclear cells during early immune development in humans." Epigenetics **6**(9): 1085-1094.
- Meservy, J. L., R. G. Sargent, R. R. Iyer, F. Chan, G. J. McKenzie, R. D. Wells and J. H. Wilson (2003). "Long CTG tracts from the myotonic dystrophy gene induce deletions and rearrangements during recombination at the APRT locus in CHO cells." Mol Cell Biol **23**(9): 3152-3162.
- Milekic, M. H., Y. Xin, A. O'Donnell, K. K. Kumar, M. Bradley-Moore, D. Malaspina, H. Moore, D. Brunner, Y. Ge, J. Edwards, S. Paul, F. G. Haghighi and J. A. Gingrich (2015). "Age-related sperm DNA methylation changes are transmitted to offspring and associated with abnormal behavior and dysregulated gene expression." Mol Psychiatry **20**(8): 995-1001.
- Miller, B., E. Messias, J. Miettunen, A. Alaraisanen, M. R. Jarvelin, H. Koponen, P. Rasanen, M. Isohanni and B. Kirkpatrick (2011). "Meta-analysis of paternal age and schizophrenia risk in male versus female offspring." Schizophr Bull **37**(5): 1039-1047.
- Molaro, A., E. Hodges, F. Fang, Q. Song, W. R. McCombie, G. J. Hannon and A. D. Smith (2011). "Sperm methylation profiles reveal features of epigenetic inheritance and evolution in primates." Cell **146**(6): 1029-1041.
- Momand, J. R., G. Xu and C. A. Walter (2013). "The paternal age effect: a multifaceted phenomenon." Biol Reprod **88**(4): 108.
- Moskovtsev, S. I., J. Willis and J. B. Mullen (2006). "Age-related decline in sperm

- deoxyribonucleic acid integrity in patients evaluated for male infertility." Fertil Steril **85**(2): 496-499.
- Mutter, G. L., C. L. Stewart, M. L. Chaponot and R. J. Pomponio (1993). "Oppositely imprinted genes H19 and insulin-like growth factor 2 are coexpressed in human androgenetic trophoblast." Am J Hum Genet **53**(5): 1096-1102.
- Nardone, S., D. S. Sams, E. Reuveni, D. Getselter, O. Oron, M. Karpuj and E. Elliott (2014). "DNA methylation analysis of the autistic brain reveals multiple dysregulated biological pathways." Transl Psychiatry **4**: e433.
- Naserbakht, M., H. R. Ahmadkhaniha, B. Mokri and C. L. Smith (2011). "Advanced paternal age is a risk factor for schizophrenia in Iranians." Ann Gen Psychiatry **10**: 15.
- Niederberger, C. (2014). "Re: paternal aging and associated intraindividual alterations of global sperm 5-methylcytosine and 5-hydroxymethylcytosine levels." J Urol **191**(5): 1356.
- Njajou, O. T., R. M. Cawthon, C. M. Damcott, S. H. Wu, S. Ott, M. J. Garant, E. H. Blackburn, B. D. Mitchell, A. R. Shuldiner and W. C. Hsueh (2007). "Telomere length is paternally inherited and is associated with parental lifespan." Proc Natl Acad Sci U S A **104**(29): 12135-12139.
- Oakes, C. C., S. La Salle, D. J. Smiraglia, B. Robaire and J. M. Trasler (2007). "Developmental acquisition of genome-wide DNA methylation occurs prior to meiosis in male germ cells." Dev Biol **307**(2): 368-379.
- Oberholte, R., J. Ratzliff, P. A. Baecker, D. V. Daniels, P. Zuppan, K. Jarnagin and E. R. Shelton (1997). "Multiple splice variants of phosphodiesterase PDE4C cloned from human lung and testis." Biochim Biophys Acta **1353**(3): 287-297.
- Paul, C. and B. Robaire (2013). "Ageing of the male germ line." Nat Rev Urol **10**(4): 227-234.
- Penner, M.R., Roth, T.L., Barnes, C., Sweatt, D., 2010. An epigenetic hypothesis of aging related cognitive dysfunction. *Frontiers in Aging Neuroscience* 2.
- Perez-Torres, S., X. Miro, J. M. Palacios, R. Cortes, P. Puigdomenech and G. Mengod (2000). "Phosphodiesterase type 4 isozymes expression in human brain examined by in situ hybridization histochemistry and [3H]rolipram binding autoradiography. Comparison with monkey and rat brain." J Chem Neuroanat **20**(3-4): 349-374.
- Peterson, B. D., M. Pirritano, L. Tucker and C. Lampic (2012). "Fertility awareness and parenting attitudes among American male and female undergraduate university students." Hum Reprod **27**(5): 1375-1382.
- Ravelli, A. C., J. H. van Der Meulen, C. Osmond, D. J. Barker and O. P. Bleker (1999). "Obesity at the age of 50 y in men and women exposed to famine prenatally." Am J Clin Nutr **70**(5): 811-816.
- Reik, W., W. Dean and J. Walter (2001). "Epigenetic reprogramming in mammalian development." Science **293**(5532): 1089-1093.
- Ricarte, F., R. Menjivar, S. Chhun, T. Soreta, L. Oliveira, T. Hsueh, M. Serranilla and E. Gharakhanian (2011). "A genome-wide immunodetection screen in *S. cerevisiae* uncovers novel genes involved in lysosomal vacuole function and morphology." PLoS One **6**(8): e23696.

- Robert, L. and J. Labat-Robert (2015). "Longevity and aging: role of genes and of the extracellular matrix." Biogerontology **16**(1): 125-129.
- Rome, M. E., U. S. Chio, M. Rao, H. Gristick and S. O. Shan (2014). "Differential gradients of interaction affinities drive efficient targeting and recycling in the GET pathway." Proc Natl Acad Sci U S A **111**(46): E4929-4935.
- Sadee, W., K. Hartmann, M. Seweryn, M. Pietrzak, S. K. Handelman and G. A. Rempala (2014). "Missing heritability of common diseases and treatments outside the protein-coding exome." Hum Genet **133**(10): 1199-1215.
- Sakkas, D., E. Mariethoz, G. Manicardi, D. Bizzaro, P. G. Bianchi and U. Bianchi (1999). "Origin of DNA damage in ejaculated human spermatozoa." Rev Reprod **4**(1): 31-37.
- Sartorius, G. A. and E. Nieschlag (2010). "Paternal age and reproduction." Hum Reprod Update **16**(1): 65-79.
- Schmidt, L., T. Sobotka, J. G. Bentzen, A. Nyboe Andersen, E. Reproduction and F. Society Task (2012). "Demographic and medical consequences of the postponement of parenthood." Hum Reprod Update **18**(1): 29-43.
- Schneider, E., M. Dittrich, J. Bock, I. Nanda, T. Muller, L. Seidmann, T. Tralau, D. Galetzka, N. El Hajj and T. Haaf (2016). "CpG sites with continuously increasing or decreasing methylation from early to late human fetal brain development." Gene **592**(1): 110-118.
- Sharma, R., A. Agarwal, V. K. Rohra, M. Assidi, M. Abu-Elmagd and R. F. Turki (2015). "Effects of increased paternal age on sperm quality, reproductive outcome and associated epigenetic risks to offspring." Reprod Biol Endocrinol **13**: 35.
- Shi, X. and D. J. Garry (2012). "Sin3 interacts with Foxk1 and regulates myogenic progenitors." Mol Cell Biochem **366**(1-2): 251-258.
- Sipos, A., F. Rasmussen, G. Harrison, P. Tynelius, G. Lewis, D. A. Leon and D. Gunnell (2004). "Paternal age and schizophrenia: a population based cohort study." BMJ **329**(7474): 1070.
- Skoog Svanberg, A., C. Lampic, P. O. Karlstrom and T. Tyden (2006). "Attitudes toward parenthood and awareness of fertility among postgraduate students in Sweden." Gend Med **3**(3): 187-195.
- Smith, K. R. (2015). "Paternal age bioethics." J Med Ethics **41**(9): 775-779.
- Spiers, H., E. Hannon, L. C. Schalkwyk, R. Smith, C. C. Wong, M. C. O'Donovan, N. J. Bray and J. Mill (2015). "Methylomic trajectories across human fetal brain development." Genome Res **25**(3): 338-352.
- Spiers, H., E. Hannon, S. Wells, B. Williams, C. Fernandes and J. Mill (2016). "Age-associated changes in DNA methylation across multiple tissues in an inbred mouse model." Mech Ageing Dev **154**: 20-23.
- Stein, A. D., H. S. Kahn, A. Rundle, P. A. Zybert, K. van der Pal-de Bruin and L. H. Lumey (2007). "Anthropometric measures in middle age after exposure to famine during gestation: evidence from the Dutch famine." Am J Clin Nutr **85**(3): 869-876.
- Stobbe, G., Y. Liu, R. Wu, L. H. Hudgings, O. Thompson and F. M. Hisama (2014). "Diagnostic yield of array comparative genomic hybridization in adults with autism spectrum disorders." Genet Med **16**(1): 70-77.

- Suetake, I., F. Shinozaki, J. Miyagawa, H. Takeshima and S. Tajima (2004). "DNMT3L stimulates the DNA methylation activity of Dnmt3a and Dnmt3b through a direct interaction." J Biol Chem **279**(26): 27816-27823.
- Suh, Y. J., S. A. Cho, J. H. Shim, Y. J. Yook, K. H. Yoo, J. H. Kim, E. Y. Park, J. Y. Noh, S. H. Lee, M. H. Yang, H. S. Jeong and J. H. Park (2008). "Gene discovery analysis from mouse embryonic stem cells based on time course microarray data." Mol Cells **26**(4): 338-343.
- Sun, T., H. Wang, Q. Li, Z. Qian and C. Shen (2016). "Forkhead box protein k1 recruits TET1 to act as a tumor suppressor and is associated with MRI detection." Jpn J Clin Oncol **46**(3): 209-221.
- Susser, E. B., A. Brown and T. D. Matte (1999). "Prenatal factors and adult mental and physical health." Can J Psychiatry **44**(4): 326-334.
- Szyf, M. (2015). "Nongenetic inheritance and transgenerational epigenetics." Trends Mol Med **21**(2): 134-144.
- Tahiliani, M., K. P. Koh, Y. Shen, W. A. Pastor, H. Bandukwala, Y. Brudno, S. Agarwal, L. M. Iyer, D. R. Liu, L. Aravind and A. Rao (2009). "Conversion of 5-methylcytosine to 5-hydroxymethylcytosine in mammalian DNA by MLL partner TET1." Science **324**(5929): 930-935.
- Tang, H. F., J. Q. Chen, Q. M. Xie, X. Y. Zheng, Y. L. Zhu, I. Adcock and X. Wang (2006). "The role of PDE4 in pulmonary inflammation and goblet cell hyperplasia in allergic rats." Biochim Biophys Acta **1762**(5): 525-532.
- Tapscott, S. J., T. R. Klesert, R. J. Widrow, R. Stoger and C. D. Laird (1998). "Fragile-X syndrome and myotonic dystrophy: parallels and paradoxes." Curr Opin Genet Dev **8**(2): 245-253.
- Templado, C., A. Donate, J. Giraldo, M. Bosch and A. Estop (2011). "Advanced age increases chromosome structural abnormalities in human spermatozoa." Eur J Hum Genet **19**(2): 145-151.
- Tochigi, M., X. Zhang, J. Ohashi, H. Hibino, T. Otowa, M. Rogers, T. Kato, Y. Okazaki, N. Kato, K. Tokunaga and T. Sasaki (2007). "Association study between the TNXB locus and schizophrenia in a Japanese population." Am J Med Genet B Neuropsychiatr Genet **144B**(3): 305-309.
- Trerotola, M., V. Relli, P. Simeone and S. Alberti (2015). "Epigenetic inheritance and the missing heritability." Hum Genomics **9**: 17.
- Tripaldi, R., L. Stuppia and S. Alberti (2013). "Human height genes and cancer." Biochim Biophys Acta **1836**(1): 27-41.
- Unryn, B. M., L. S. Cook and K. T. Riabowol (2005). "Paternal age is positively linked to telomere length of children." Aging Cell **4**(2): 97-101.
- Walsh, C., S. J. Miller, F. Flam, R. A. Fisher and R. Ohlsson (1995). "Paternally derived H19 is differentially expressed in malignant and nonmalignant trophoblast." Cancer Res **55**(5): 1111-1116.
- Wang, J., S. Sun, L. Zhang, Z. Wang, L. Ye, L. Liu, N. Wu, H. Li, X. Zhang and J. Wu (2011). "Further study of genetic association between the TNXB locus and schizophrenia." Psychiatr Genet **21**(4): 216.
- Wei, J. and G. P. Hemmings (2004). "TNXB locus may be a candidate gene predisposing to schizophrenia." Am J Med Genet B Neuropsychiatr Genet **125B**(1): 43-49.

- Wei, Y., H. Schatten and Q. Y. Sun (2015). "Environmental epigenetic inheritance through gametes and implications for human reproduction." Hum Reprod Update **21**(2): 194-208.
- Weidner, C. I., Q. Lin, C. M. Koch, L. Eisele, F. Beier, P. Ziegler, D. O. Bauerschlag, K. H. Jockel, R. Erbel, T. W. Muhleisen, M. Zenke, T. H. Brummendorf and W. Wagner (2014). "Aging of blood can be tracked by DNA methylation changes at just three CpG sites." Genome Biol **15**(2): R24.
- Wijchers, P. J., M. F. Hoekman, J. P. Burbach and M. P. Smidt (2006). "Identification of forkhead transcription factors in cortical and dopaminergic areas of the adult murine brain." Brain Res **1068**(1): 23-33.
- Wolffe, A. P., et al. (1999). "DNA demethylation." Proc Natl Acad Sci U S A **96**(11): 5894-5896.
- Wu, Y., Y. Peng, M. Wu, W. Zhang, M. Zhang, R. Xie, P. Zhang, Y. Bai, J. Zhao, A. Li, Q. Nan, Y. Chen, Y. Ren, S. Liu and J. Wang (2016). "Oncogene FOXC1 enhances invasion of colorectal carcinoma by inducing epithelial-mesenchymal transition." Oncotarget.
- Yauk, C., A. Polyzos, A. Rowan-Carroll, C. M. Somers, R. W. Godschalk, F. J. Van Schooten, M. L. Berndt, I. P. Pogribny, I. Koturbash, A. Williams, G. R. Douglas and O. Kovalchuk (2008). "Germ-line mutations, DNA damage, and global hypermethylation in mice exposed to particulate air pollution in an urban/industrial location." Proc Natl Acad Sci U S A **105**(2): 605-610.
- Yuan, Y., D. A. Nymoer, H. T. Stavnes, A. K. Rosnes, O. Bjorang, C. Wu, J. M. Nesland and B. Davidson (2009). "Tenascin-X is a novel diagnostic marker of malignant mesothelioma." Am J Surg Pathol **33**(11): 1673-1682.

XII. ACKNOWLEDGEMENT

At this point I would like to express my sincere gratitude to my advisor Prof. Dr. med. Thomas Haaf for giving me the opportunity to perform this research project in his laboratory and for providing me his continuous professional support and knowledge.

Special thanks go to my supervisor Dr. Nady El Hajj for his endless help and knowledge, his positive attitude and encouragement and especially for his patient support. His guidance and great supervision made this work possible and helped me to perform this project with pleasure and motivation.

I would like to thank Stefanie Atsem for the great collaboration, her endless support and for the nice days we spent together in the lab. The same also applies to my fellow labmate Ramya Potabatulla for the stimulating discussions, all the funny moments and for the friendship that developed from working together.

Thanks to Lara Haertle, Julia Böck and Cordula Neuner for answering any question with patience and pleasure, for providing me their experience and knowledge and especially for making my time in the lab enjoyable. The members of the team of Prof. Dr. Haaf – Dr. Eberhard Schneider, Dr. Babara Vona, Dr. Indrajit Nanda, Felix Mattern, Anna Maierhofer, Julia Flunkert, Michaela Hofrichter, Caroline Lekszas – I would like to thank for their inspiring comments on my research during the lab-meetings.

Finally, I would like to thank my greatest supporters: my parents for their infinite love and support, Myriam for her great assistance, Susi for listening to my problems, Andreas and Thea for the good distraction and Vincenzo for being endlessly interested and being close to me from far away.

XIII. CURRICULUM VITAE

Persönliche Daten

geboren am 17.09.1991 in München
Familienstand Ledig

Ausbildung

2002 – 2011 Franz-Marc-Gymnasium Markt Schwaben
02.05.2011 Allgemeine Hochschulreife
10/2011 – 04/2012 Studium der Molekularen Biotechnologie an der Technischen Universität München [unabgeschlossen, Wechsel zum Studium der Humanmedizin]
04/2012 – 11/2018 Studium der Humanmedizin an der Julius-Maximilian-Universität Würzburg
16.11.2018 Ärztliche Prüfung
18.12.2018 Approbation als Ärztin

Berufserfahrung

seit 18.02.2019 Assistenzärztin an der Klinik und Poliklinik für Frauenheilkunde und Geburtshilfe, Klinikum der Universität München LMU, Campus Großhadern

Praktisches Jahr

07/2018 – 10/2018 Tertian Innere Medizin
Klinikum Rechts der Isar der Technischen Universität München
03/2018 – 06/2018 Tertian Gynäkologie und Geburtshilfe
Campus Virchow-Klinikum, Charité Universitätsmedizin Berlin
11/2017 – 03/2018 Tertian Chirurgie
Hospital das Clínicas, Universidade Estadual Paulista „Júlio de Mesquita Filho“ UNESP, Botucatu, São Paulo, Brasilien

Famulaturen

05/2017 Institute for Indian Mother and Child, Kalkutta, Indien
08/2016 Anästhesie und Intensivmedizin
Sultan Qaboos Universitätsklinikum, Muscat, Oman
03/2016 Allgemeinmedizin
Hausärztliches Zentrum Poing b. München
03/2015 Gynäkologie und Geburtshilfe
National Cheng Kung Universitätsklinikum, Tainan, Taiwan
09/2014 Chirurgie und Notfallambulanz

08/2013	Juliusspital Würzburg Forschungspraktikum am Labor für Mikrobiologie, Medizinische Fakultät von São José do Rio Preto, Brasilien
Studentische Hilfskraft	
01/2017 – 07/2017	Sitzwache am Universitätsklinikum Würzburg
09/2014 – 06/2015	Studentische Hilfskraft im Studienreferenzzentrum für Neuroradiologie des Universitätsklinikums Würzburg
10/2013 – 02/2014	Tutorin für das Anatomische Institut der Universität Würzburg

München, Januar 2020

✓ Juliane Reichenbach